eman ta zabal zazu

Universidad del País Vasco

Euskal Herriko Unibertsitatea

Lignin as a source of phenolic compounds: from lignin extraction to its transformation by different routes

A dissertation presented by

Javier Fernández Rodríguez

In Fulfillment of the Requirements for the Degree
Doctor of Philosophy in Renewable Materials Engineering
by the University of the Basque Country UPV/EHU

Under the supervision of

Dr. Jalel Labidi

Dr. María González Alriols

Chemical and Environmental Engineering Department
Engineering School of Gipuzkoa

Donostia-San Sebastián
2020

“Dalli qui nu canta, verdi qui nu livanta”

Summary

In the last decades, considerable interest has been put in using lignocellulosic streams, which have been traditionally considered as wastes, to be converted into value-added products, such as fuel, chemicals and biomaterials, which are currently obtained from fossil sources.

Lignin, the most plenty polymer as an aromatic source in nature has been traditionally considered as a by-product or side stream from pulp and paper process, although lignin commercialization as a source of phenolic compounds has gained more and more relevance lately. However, several drawbacks have to be still overcome, such as the high polydispersity and high content in impurities of the obtained lignin samples, which lead to generate a recalcitrant behavior that hinders its transformation processes into high value-added chemical compounds. Lignin-based products must be competitive with their petroleum-derived counterparts. Hence, it is very important to design energetically efficient processes for lignin extraction and purification. For this purpose, lignin-based products have to be assumed as a section of an integrated biorefinery where multiple products are obtained and in this line being able to compete in a realistic scenario.

In this work, the identification of different routes to extract lignin and its further conversion into small phenolic compounds has been developed. All approached scenarios were proposed to build up robust processes capable to reduce the high variability of the lignocellulosic process designed to obtain chemicals or building blocks.

Lignin samples from different lignocellulosic sources (blue agave plant, almond shell and olive tree pruning), delignification processes (soda or organosolv) and process stages (lignin from bleaching stages) were extracted and characterized physico-chemically to define the best alternatives for obtaining different products. Thereafter, several strategies were considered to depolymerize the lignin molecule into small phenolic monomers, such as catechol and its derivatives compounds, cresols, syringol, guaiacol, etc. These depolymerization reactions were applied to the obtained lignin samples collected from the extraction processes. Moreover, an innovative alternative to break down lignin directly from the black liquors obtained during the lignocellulosic biomass delignification process was also approached.

Finally, the techno-economic analysis of the lignin extraction and depolymerization processes was conducted to select the most suitable routes in terms of product yields, environmental wastes, energy demands, and economic balance.

Javier FERNÁNDEZ

Content

Aim and Scope

Aim and scope

The main target of this study has been the identification of different routes to extract lignin and its further conversion by robust processes that could manage the huge sensitiveness of the lignocellulosic-base processes.

An introduction to the lignocellulosic biomass valorization technologies by integrated biorefineries strategies is presented in Chapter 1. In addition, the lignin definition, potential uses and main strategies to be converted into high value-added products by its breaking down are described in this section as well.

In Chapter 2, several agricultural waste streams have been evaluated as potential lignin sources. Lignin was extracted from those materials developing a wide range of approaches that were compared to identify the most suitable strategy: (i) from delignification and bleaching stages; (ii) including or not a pretreatment; (iii) and by different delignification methods. Once lignin was obtained by those different routes, physico-chemical characterization of the generated products as well as an evaluation of the extraction yields was addressed to assess all the proposed routes.

Thereafter, in Chapter 3, lignin depolymerization reactions were studied using several lignin sources: (i) solid lignin or (ii) black liquors. The aim has been to establish relationships between the composition, properties and the yields of the obtained products depending on the used lignin source or the applied reaction mechanism.

Chapter 4 has been devoted to the simulation of the biorefinery processes based on previously carried out experimental analyses. For this purpose, Aspen Plus® simulation software was used in order to define different biorefinery scenarios and to establish the corresponding mass balances, and energy duties to estimate the potential costs of the different routes approached in the experimental section. The obtained results were compared to identify the better combinations.

Finally, the summary of the final remarks and the identification of further feasible works to widen the present study have been included in the last section of this work.

I) Introduction

1.1. Background

The threat of an imminent depletion of fossil reservoirs has been looming over the developed economies and their industrial system. However, the discovering of new reserves as well as the advances in extraction technologies have modified that apocalyptical vision that clamored for the use of alternative sources in a rush. The predictions from experts have been not fulfilled, as it can be seen in Figure 1.1, where it can be seen that the estimation of the oil production established by Hubbert has been deeply overstepped by real production in the USA [1]. This fact has been used by some skeptics about renewable resources who consider that fossil resources are and will be always the main resources of our planet.

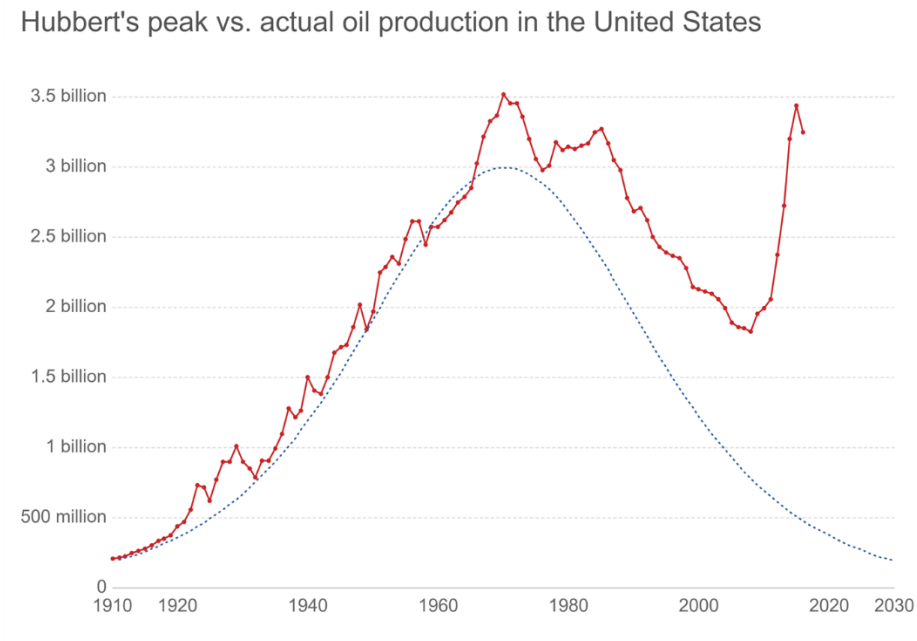

Figure 1.1. Current oil production in the USA against Hubbert's estimation, both measured in barrels per year (Source: Our World in Data).

Nevertheless, the huge impact that fossil resources have provoked over last centuries on the natural environment cannot be dismissed, specifically in the release of greenhouse gases, with more than half of world current CO_2 emissions caused by burning fossil fuels [2]. Therefore, although the idea of an absolutely necessity to replace fossil resouorces cannot be sold in the short-term without risking the supply to our growing world population, the development of more sustainable processes for energy and product obtaining is compulsory to guaranty the wellness for our further generations.

Although the global consumption is growing implying the growth of the use of fossil resources, it can be observed how the share of renewable resources is continuously increasing, gaining more and more prominence in the last years, and it is thought that this increase will continue in the next decades as it can be seen in Figure 1.2. As a clear example, the Renewable Energy Directive of the European Union (EU), officially coded as 2009/28/EC, defined the strategy to increase the share of renewable energy over the total energy needs up to 20% for 2020 [3]; and it was recently followed by the new commitment of EU for 2030, when a 27% share of renewable energy consumption and the reduction of 40% in greenhouse gas emissions compared to 1990 levels have to be reached by the country members, as it was agreed in the EU Council of October 24th, 2014 [4].

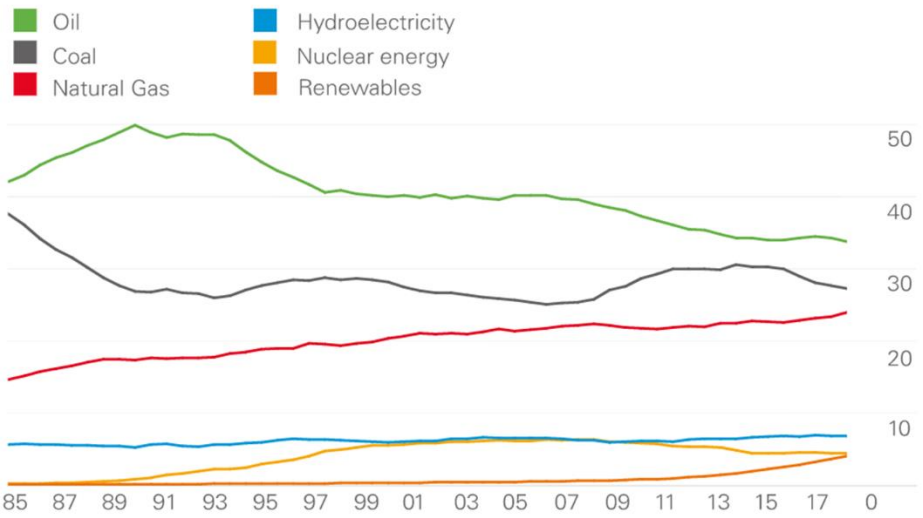

Figure 1.2. Shares of primary energy per percentage (Source: BP)

Even though it can be said that the change has already started, it is still a long way to go before having a complete switch from fossil to renewable resources for energy and product manufacturing. Nevertheless, the trend is promising. In this line, the scientific community has to continue supporting the big challenge of this transformation as it has been accomplished during the last decades, with a noticeable increase in the number of publications in renewable resources, specifically more than 6,000 publications (source: Scopus).

1.2. Biorefineries

The definition of the biorefinery concept was originated at the end of the 1990s, due to the increasing trend to use biomass for the production of non-food products that traditionally came from fossil resources after a classic refinery process. In 1997, biorefineries were

defined by Kamm et al. [5] as a complex (to fully integrated) system of sustainable and environmentally friendly technologies for the comprehensive utilization of biological raw materials in the form of green and residual biomass from a targeted sustainable regional land utilization. Several definitions have been proposed for this concept, sometimes generating strong debates about these propositions but there is a general consensus about including in the definition the following statement: "the integration of biomass conversion processes to produce a range of fuels, power, materials, and chemicals" [6].

In the last decades, the development of biorefineries has emerged with great potential due to the crude oil crisis at the beginning of the XXI century [7]. However, as it was mentioned before, making biorefineries feasible just based on the fear of the oil depletion is not valid anymore. In any case, there are several reasons that have encouraged not only to the research community but also to the industry sector to boost strategies to implement the biorefinery concept at commercial levels [8]. In terms of economic factors, the stronger points of the biorefinery concept are: (i) the feedstock cost, which is thought to be low and overall steady; (ii) the possibility to create new markets using biomass sources instead of crude oil, (iii) and tax incentives that are thought to be reached by refineries because of their environmental advantages in comparison with traditional refineries. In terms of social interest, the great advantages are: (i) the sustainable resource supply to reduce greenhouse emissions and to stop the production from resources that can be depleted in a relatively close future; (ii) the energetic stability, by reducing the dependency from the lobby's countries that control the fossil resource markets; (iii) and the rural economic development by the creation of a large scale energy crops in specific areas where agricultural actions are the current economic engine of the regions [9]. In any case, the pathway is not easy and, despite the huge number of efforts adopted in the recent years, there is still a gap between both types of industries (traditional refineries and biorefineries) that has to be reduced more and more.

The quantification of the current industrial biorefineries can be variable based on the wide definition of biorefineries. Indeed, conventional biofuels production processes and pulp mills could be considered as simple biorefineries. Thus, the number of biorefineries would be immense. However, if only the advanced biorefineries are considered, with a higher degree of integration to produce a wider range of products, the number of industrial plants is much more limited. In any case, 35 biorefinery plants were already implanted or in the construction phase at the beginning of 2018 in Europe, which is a figure that shows the trend of the European countries to change their feedstocks source to biomass [10]. The products that can be obtained from these facilities are very variable too, from biofuels (mainly bioethanol and renewable diesel production plants); bio-based chemical building blocks (levulinic acid, glycerol, succinic acid, polylactic acid, etc.) and biomaterial driven

biorefineries (cellulose, lignin, tall-oil). In this last group, the main example is the bioproduct mill of Äänekosky, which have been developed by Metsa Fiber company, with the highest production volume: 1.3M t of several products, such as cellulosic pulp, lignin, tall-oil, sulfuric acid, turpentine and biogas [11].

1.2.1. Biorefineries classification

Biorefineries can be classified depending on several factors. In general, classification can be divided into four big groups, based on the used feedstock, the employed processes, platforms and obtained products.

The main classification of biorefineries was established by Kamm [5], according to the different feedstock used:

- Lignocellulosic Feedstock Biorefinery (LCF-BR). In these types of plants, different compounds (cellulose, lignin, and hemicelluloses mainly) are extracted from cereals, reed, forest biomass using chemical or biological methods [12].

- Whole Crop Biorefinery (WC-BR). In these biorefineries, different parts from raw materials, such as the grain, meal, and straw can be used to obtain a wider range of bioproducts [13]. Chemical, biological or physical processes are conducted to extract intermediate products as sugars or lignin for further conversions.

- Green Biorefinery (GBR). In this group, green biomass, which is composed of grass, lucerne, clover, and immature cereals, is used as feedstock to obtain feed, fuels, chemical and materials [14].

- Two-platform Concept (2PC), which includes a combination of sugar and syngas platforms. The sugar platform is focused on the conversion of feedstock (composed basically of carbohydrates) into biofuels and materials by biochemical processes, mainly based on the fermentation of sugars. On the other hand, the syngas platform is based on the thermochemical conversion of biomass feedstock and by-products to obtain syngas by different processes, such as gasification, pyrolysis, or thermolysis [15].

The lignocellulosic feedstock biorefinery is nowadays the most relevant group of biorefineries due to the great availability and accessibility of the raw material that employs and the good position in the market of the products that are obtained. In this type of biorefinery, non-food materials (agricultural and forest residues, energy crops) are transformed into products/energy. The feedstock is mainly integrated by the residues

generated from agricultural-forestry activities (straw, shrubs, pruning, and trimmings) and thereof derived industries [16].

1.3. Lignocellulosic biomass

Within the previously mentioned global scenario, lignocellulosic biomass has emerged as a good alternative to address such challenges, as it is considered to be the most abundant terrestrial biomass on the planet. In the last decades, several studies have demonstrated the high potential for the sustainable conversion of lignocellulosic biomass into energy, biofuels, and chemicals [17]. Lignocellulosic feedstock includes a wide range of materials, such as agricultural wastes, forestry residues and woody materials which are the major structural components of plants [18]. They are formed mainly by three major macro-components: cellulose (40-60%), hemicelluloses (10-40%), and lignin (15-30%). Together they constitute the structural components of plants and, along with the non-structural compounds, form the plant cell wall [19]. Figure 1.3 shows a schematic representation of the chemical composition of lignocellulosic biomass. Non-structural components, such as inorganic materials, extractives and proteins, generally represent about 5-10% of the total composition. The distribution of these compounds depends on the source, plant tissue, age, and growth conditions. Typical percentages of those components according to the type of lignocellulosic biomass are presented in Table 1.1.

Table 1.1. Composition of macromolecular components of different lignocellulosic biomass sources [20].

Species	Cellulose (%)	Hemicellulose (%)	Lignin (%)
Hardwood	40-55	15-35	15-25
Softwood	40-50	10-30	25-35
Agricultural wastes	25-40	15-35	5-20
Annual plants	25-40	25-50	10-30

Cellulose is the main component of these materials, being considered as the most plenty and renewable organic polymer in the biosphere. It is a polysaccharide composed exclusively by cellobiose units, which are formed by two glucose molecules linked by β-(1-4) glycosidic bonds. The cellobiose chains are organized in fibrous cells with a degree of polymerization around 10,000 [21]. The high number of hydroxyl groups enables the formation of intra- and inter-molecular hydrogen bonds that are responsible for the rigidity of the cellulosic chain and the structure of the microfibrils respectively. The cellulosic fibers, composed by the union of these microfibrils, form aggregates that constitute the cell wall. Regarding its macromolecular structure, the cellulose fibers are organized by crystalline

and amorphous areas [22]. The inter-molecular hydrogen bonds are responsible for that crystalline region, a uniform structure entailing with a high degree of crystallinity. The amorphous zones present higher reactivity due to the easier accessibility to the hydroxyl groups [23].

Hemicelluloses are considered one of the most abundant polysaccharides found in nature beyond cellulose. Its main function is to act as a bonding agent between cellulose and lignin molecules by covalent and non-covalent linkages [24]. It is composed of a group of heterogeneous polymers that can be formed by several monomers of both hexoses and pentose sugars; the C6 sugars are mainly glucose, mannose and galactose, and the C5 monomers xylose and arabinose. Their distribution depends mainly on the source of biomass. For example, the most abundant carbohydrate type in hardwood species and grasses is xylose whereas in softwood and annual plants mannose is the main monomer [25]. Hemicelluloses are organized in branched structures with an amorphous distribution and a typical degree of polymerization around 200-300, which makes them easier to solubilize than cellulose as they do not present crystalline areas. This characteristic is exploited by many deconstruction strategies as they can be removed from the original or delignified tissue by its extraction with aqueous alkali or even water [26].

Lignin, the third major component of lignocellulosic biomass and the target product of this work will be defined in more detail in the next section.

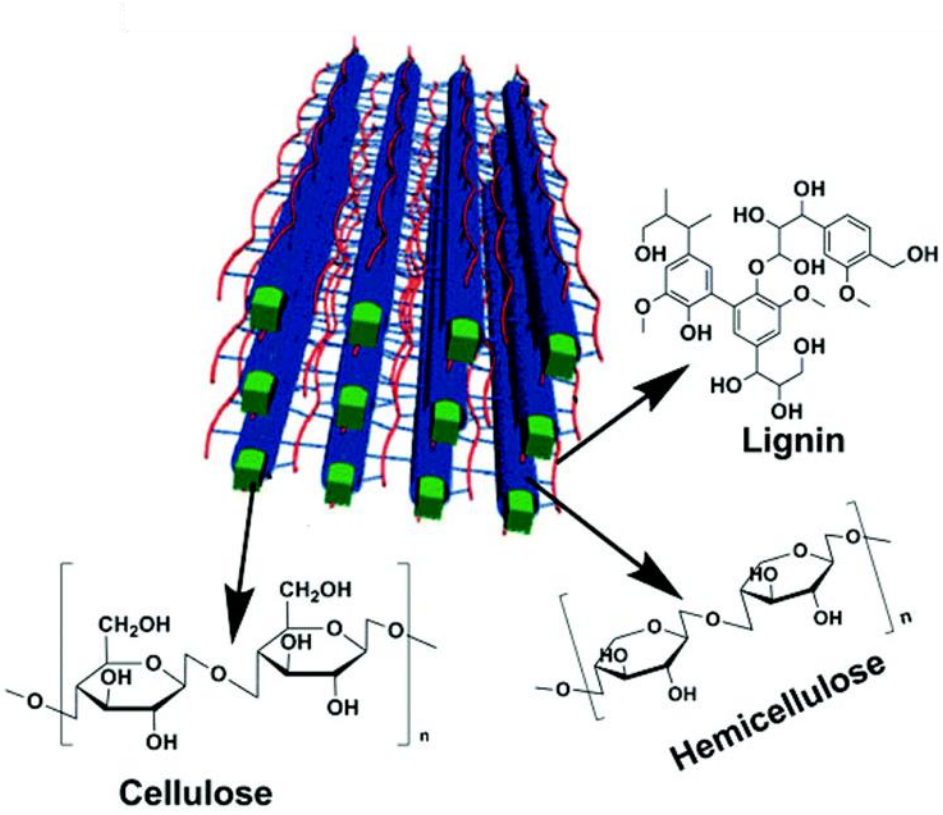

Figure 1.3. Schematic representation of structural compounds of plan cell wall [27].

Among the minority components of biomass, "extractives" are quite interesting due to the heterogeneous chemical composition that they present, mainly consisting of low molecular weight carbohydrates, terpenes, tannins, steroids, waxes, aliphatic acids, etc. These components can be easily obtained from biomass by their extraction with organic solvents [28].

Proteins compounds could represent around 5-10% of the dry weight of the primary cell wall, although its relative abundance is variable [16]. Proteins are essential in controlling the cell wall extensibility and its structure modification, the cell wall metabolism, the responses to abiotic and biotic stresses and many other physiological responses [29,30]. They also play an important role in the release of signal molecules, such as peptides or oligosaccharides [31].

Finally, inorganic compounds can be also found in cell walls, having their origin in the components of the soils where the plants are growing. These inorganic compounds are simple salts as silicates, phosphates, calcium and potassium among many others [32].

Their quantity in biomass varies considerably depending on the species but also on the different parts of the plant, usually higher at the bark and foliage tissues [33].

1.4. Lignin chemistry

The term lignin is derived from the Latin word *lignum* which means wood. Lignin is among the most abundant biopolymers on earth and the most abundant source of aromatic compounds in nature [34]. The availability of lignin in the biosphere exceeds 300 billion tons and increases by about 20 billion tons every year [35]. Most of the lignin molecules are located in the middle lamella, where they serve as a cementing agent that keep the fibers together strengthening the plant cell walls [22]. Lignin is present in the secondary wall too, where it interpenetrates and encrusts the cellulose microfibrils and the hemicelluloses providing resistance against microbial attack and playing a crucial part in the water transport by reducing the cell wall permeability [36].

The lignin chemical structure is difficult to define since its structure and properties are heavily related to the process by which it has been extracted and/or its source. Thus, it is not possible to establish its molecular weight with precision, although it is estimated to present a range from 1000 to 20,000 Da. It is constituted by a heterogeneous biopolymer formed by three different phenylpropanoid units (monolignols) with a large number of polar functional groups, generating a tridimensional amorphous structure. The monolignol precursors are synapyl alcohol (S), coniferyl alcohol (G), and *p*-coumaryl alcohol (H). The molecular structure of these compounds is represented in Figure 1.4, where the main difference between these structures is the number of methoxy groups linked to the aromatic ring [37].

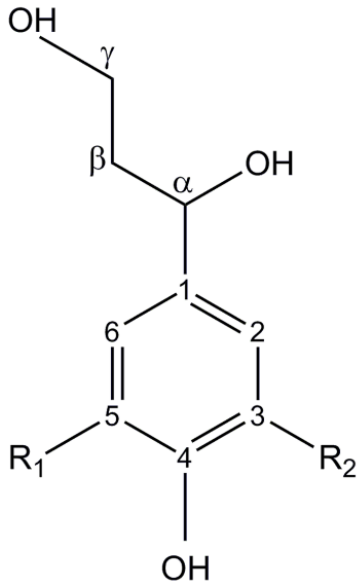

- Sinapyl alcohol: R1&R2=OMe
- Coniferyl alcohol: R1=H; R2=OMe
- *p*-coumaryl alcohol: R1&R2=H

Figure 1.4. Chemical structure of lignin precursors.

These units are randomly connected by different ether and C-C linkages in a distribution that differs regarding the source of lignin. In Table 1.1 the percentage of lignin linkages by feedstock source is shown.

Lignification is initiated by the dehydrogenation reaction of monolignols promoted by peroxidases and laccases and consists in the removal of the phenolic hydrogen atom from the precursors leading to phenoxyl radicals [38]. The most abundant linkage in the lignin molecule is the β-O-4 ether, which is the bond that can be more easily cleaved and, therefore, it is considered as the main target of the lignin depolymerization methods [36,39]. In terms of monolignols distribution, hardwood species present similar percentages of guaiacyl and syringil units, whereas, in softwood species, the guaiacyl units could reach around 90% of the total monolignol units [40]. In the case of grasses, balanced ratios of guaiacyl-syringyl units are present in the lignin molecules but also significant amounts of compounds derived from *p*-coumaryl alcohol.

Table 1.2. Different linkages proportions and bond dissociation enthalpies in lignin molecules [41,42].

Linkage type	Softwoods (%)	Hardwoods (%)	BDE (kcal/mol)
Ether linkages			
β-O-4	43-50	50-65	53.9-72.3
α-O-4	6-8	4-8	48.31-57.3
4-O-5	4	6-7	77.7-82.5
C-C linkages			
β-5'	9-12	4-6	125.2-127.6
5-5'	10-25	4-10	114.9-118.4
β-1'	3-7	5-7	64.7-165.8
β-β'	2-4	3-7	68.0-81.0
Others	16	7-8	--

Lignin molecules contain a great variation in functional groups which have a significant impact on its further reactivity [43]. Methoxyl groups are the most common functional groups of lignin, followed by aliphatic and phenolic hydroxyl groups and other ones in smaller quantities, such as carbonyl and carboxyl groups [44]. The dispersion of these groups is deeply influenced by the lignin source as well as its isolation method. In addition, due to the polar functional groups of lignin, it is also possible to find linkages with carbohydrates from hemicelluloses portions, forming lignin-carbohydrate complex (LCC) that reduces the percentage of aromatic entities in the lignin molecule [45].

Even though several studies have approached the challenge of describing the lignin molecule, big differences can be observed in the presented models due to the variable factors that influence on lignin chemical composition. Figure 1.5 presents an example of a hardwood lignin chemical composition.

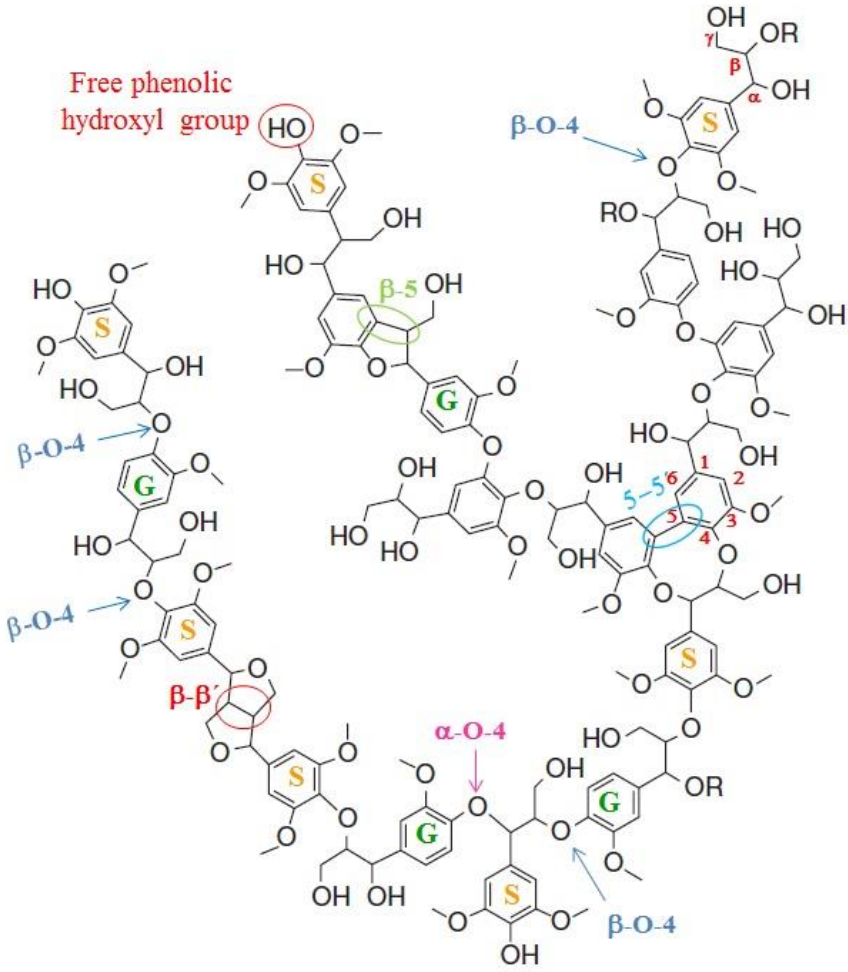

Figure 1.5. Example of hardwood lignin molecule adapted from Macfarlane et al. [43] *and its most representative linkages [20].*

In terms of properties, lignin is frequently commercialized as solid powder, with great variations in its molecular weight due to its transformation during the extraction process. As a common point, softwood lignin samples trend to present higher molecular weight than hardwood lignin [46], although the extraction process plays a significant role as it will be depicted below. Softwood lignin, composed mainly by G monolignol units, are more prone to create C-C linkages (5-5' and β-5') than S units due to the vacant space in the C_5 position of the aromatic ring that is covered by a methoxy group in the case of S units [47]. Additionally, lignin presents high values of polydispersity in comparison with other biopolymers, which hinders its further conversion.

The condensed structure of lignin and its strong intermolecular hydrogen bonding, restrict the thermal mobility of the lignin structure resulting in a high glass transition temperature (T_g). As a consequence, it is considered a rigid and brittle polymer with poor film-formability, which hinders considerably its direct use as a macro-component for composite materials [48].

Besides the most popular uses of lignin, such as dispersant and blending agent, it can be intended for other interesting high-value applications, such as antioxidant and antimicrobial agent, based on the high content in alcoholic functional groups, both from the phenolic or aliphatic origin [49].

1.5. Lignin source

Lignin is mainly obtained as a byproduct of the pulp and paper industry (P&P) as Kraft lignin and lignosulfonates. Nevertheless, although lignin is produced worldwide in amounts close to 70 million tones, only 1%–2% is used as a precursor for chemicals and materials production. The rest is used for energy generation in the same industrial process in which is generated as a byproduct [50].

The lignin isolation method is contemplated as one of the most exigent steps of the biomass fraction processes due to the complexity caused by the heterogeneity of lignin and its different wide range of types of linkages. The different processes approached for this purpose can be divided into two groups according to the route of the lignin fractionation: (i) processes in which lignin is solubilized from the lignocellulosic biomass and it is removed by separating the solid residue from the spent liquor, and (ii) processes where polysaccharides are selectively hydrolyzed leaving lignin along with some condensed carbohydrate deconstruction products as a solid residue. Therefore, the selection of the method is driven by the desired final application. For example, in the case of P&P industry where the focus is on the carbohydrate platform, methods from the group (i) would be the chosen ones, such as sulfite, Kraft, alkaline or organosolv methods. The methods for the second group are intended to reduce the carbohydrate components (cellulose and hemicelluloses) to its monomeric form to have then the sugars transformed into value-added chemicals. In this case, lignin is mostly isolated in the form of an insoluble lignin residue or as a precipitated [40,51].

1.5.1. Sulfite process

The origin of sulfite process dates from 1867, when B. C. Tilghman, a Philadelphia chemist patented a process in which the decomposition of wood with sulfurous acid and calcium was used to obtain fibrous pulp without problems of discoloration. This novel process

allowed the use of this pulp for paper manufacturing processes. However, it was not until 1874 when the Swedish chemist Carl Daniel Ekman commercialized the first sulfite pulp. Almost simultaneously to Ekman, Alexander Mitscherlich worked on the sulfite cooking process of wood in Germany and, in 1880, he started a sulfite pulp mill in Zell in south Germany [52]. Since 1890, the calcium sulfite process was rapidly extended worldwide, being the most important process in pulp industry until the 1950's decade when Kraft process overstepped the former one, mainly due to the possibility of using wider variety of wood species (calcium sulfite process could not accept softwood species). Additionally, the need to recover the waste liquor and pulping chemicals that emerged for environmental reasons, provoked the movement to the Kraft process where liquors where easier to be managed for chemicals and energy recovery [52,53].

The sulfite process was initially developed around the acid calcium bisulfite process but, nowadays, it is more flexible. It is usually accomplished under acid or neutral conditions, sulfur dioxide and/or bisulfite ions react with lignin to produce water-soluble sulfonated lignin, named lignosulfonates, which are degraded in large pressure vessels called digesters [54]. The employed salts are either sulfites (SO_3^{2-}) or bisulfites (HSO_3-) and even sulfur dioxide (SO_2) or sulfuric acid (H_2SO_4) could be employed. The content of these species varies depending mostly of the base cation used in the process, as the sulfite pulping can be conducted in a wide range of pH. The most common used salts are sodium, calcium, potassium, magnesium or ammonium sulfites. As a result, a pulp with high cellulose content is reached with lower lignin and hemicelluloses percentages than the one produced by the Kraft process. The residual lignin that still remains in the pulp is relatively easy to be removed by bleaching processes [54]. As an example, the unique Spanish mill using the sulfite process uses Total Chlorine Free (TCF) bleaching method [55].

Lignosulfonates are defined as hydrophobic poly-electrolytes, whose solubility depends on the cation used in the digestion stage. Thus, the calcium sulfite process generates the lower soluble lignosulfonates and sodium sulfites, the easiest ones to be solubilized in water [56]. In some cases, impurities can reachl 30% of dry weight, mainly composed of inorganic salts and carbohydrate fractions [57]. This type of lignin usually presents a very high average molecular weight, even higher than Kraft lignin, as sulfonate groups are added to lignosulfonate lignin during the pulping process [58]. As a consequence of the incorporation of these groups, the catalytic transformation of lignosulfonates is more difficult [59]. Moreover, in the sulfite pulping processes ether bonds are cleaved, methoxyl groups are destroyed and new carbon-carbon bonds are formed [60]. Although its production is much lower than in the Kraft process, around 1 million t/y of lignosulfonates are produced on dry basis [50].

Regarding other possible uses of lignosulfonates, they presents big potential to be used in colloidal applications, such as dispersants in concrete industry (plasticizers), surfactants or flocculants [61]. As an advanced application, they can be also converted into vanillin for food applications by its depolymerization [62].

1.5.2. Kraft process

The Kraft process (so called because of the greater strength of the resulting paper, from the German word *Kraft* for "strength") was patented by Carl F. Dahl in 1879 [63], although it was not industrially employed until 1890 in Sweden. The Kraft process became the most important paper process in the 1930s due to the invention of the recovery boiler developed by G. H. Tomlinson [64]. This stage allowed recovering the inorganic compounds used in the white liquor and generating energy that it was reutilized in the wood digestion process [22]. Based on that achievements, the Kraft process is still the main pulping process with an estimated global production of 130 Mt/y of pulp, representing around 90% of total chemical pulp. Its predominance in the P&P industry is caused by the high quality of its resulting pulp, the possibility to recover pulping chemicals, as well as the self-sufficiency of the process in terms of energy duties [65,66]. As a consequence, it is the most important process to generate lignin with a production about 50-55 million metric tons of black liquor [46,67]. Currently, 75,000 tons are estimated to be isolated from Kraft process, mainly the by LignoBoost® process.

Kraft pulping consists in the solubilization of lignin using aqueous "white liquor" composed by sodium sulfide and sodium hydroxide. During the cooking reaction at elevated temperature (145-170 ºC) and pressure, the pulp is delignified and lignin depolymerized without concurrently accelerating carbohydrate solubilization or damage [68].

After this stage, the pulp is washed and the black liquor filtrated to be concentrated to around 65% solids in direct-contact evaporators, by bringing the liquor into contact with the outlet gases from recovery boiler. After that, the strong black liquor is typically burned in the recovery boiler for energy production and the recovery of chemicals for the white liquor preparation [69].

The high quantity of steam produced in this step makes the black liquor the fifth most important fuel in the world [70]. However, the energy generated by burning the black liquor is greater than the process demand and, and the "bottleneck" stage of the pulping process, which limits the pulp production volume [71]. Hence, the valorization of lignin as a chemical precursor could be an option of sorting out this problem and obtaining and extra revenue in the process. However, the structural changes that lignin undergoes during the reaction comprise the addition of thiol groups, the cleavage of inter-unit ether linkages and the

increment of recalcitrant C–C bonds and phenolic hydroxyl groups [57,72]. As a result, Kraft lignin presents a highly condensed molecule with low amount of residual β-O-4 bonds, which together with its sulfur content, hinders possible downstream valorization processes [73]. These drawbacks are the reason why only around 2% of the total produced lignin is intended as a precursor for chemicals and materials [74]. Nevertheless, Kraft lignin is considered as a plenty source of aromatic chemical precursors that could be directly used as dispersants, emulsifiers or adhesives; but also to many other applications by its molecular reduction to smaller entities, such cosmetic or pharmaceutical preparations [75,76].

The isolation of lignin from the spent black liquor is industrially carried out mainly by the LignoBoost® process. This method was initiated in 1996 by a joint project among Innventia and Chalmers University of Technology. After years of modifications, in 2005, Öhman et al. [77] presented the final LignoBoost® process. Its methodology is based on the change in the solubility that lignin presents in function of the pH level of the dissolution. The pH of the black liquor is dropped using CO_2 recycled from the boiling stage. The precipitated lignin is dewatered using a filter press. This method overcomes the conventional filtering and sodium separation problems by re-dissolving the lignin in spent wash water and acid. The resulting slurry is once again dewatered and washed with acidified wash water, to produce virtually pure lignin cakes. The filtrated streams are recycled to different stages of the black liquor evaporation plant [78]. The main advantage of this method is its low cost, simplicity and the obtained lignin presents lower impurities of ash and carbohydrate content [79].

More recently, a team from FPInnovation developed a new process, called the LignoForce System™ process which consists in the oxidation of the black liquor using oxygen before the acidification step. The oxidation improves the filterability of the acid-precipitated lignin by providing suitable conditions with respect to pH (leads to a lower pH) and temperature (increase temperature) for lignin colloid agglomeration. In addition, it minimizes or eliminates total reduced sulfur (TRS) compounds, thereby the problematic odorous emissions during this step is hugely reduced [80].

1.5.3. Alkaline process

Alkaline pulping is the third most important pulping process with a global production of 5% of the total chemical pulp [68]. In this group, different alkali agents apart from NaOH are considered, such as KOH, $Ca(OH)_2$, anhydrous ammonia, etc [81]. The main difference with the Kraft process is that it does not use sodium sulfide as a reagent, which generates less efficient lignin depolymerization due to the lack of a strong nucleophile [82]. In this case, competing reactions take place generating the degradation of carbohydrates, known

as “peeling”. The addition of catalytic quantities of anthraquinone (AQ) has a noticeable effect on the stabilization of carbohydrates and the dissolution of lignin. However, the rate of the lignin removal is still lower, compared to the one of the Kraft process [83]. As a consequence, a poorer quality pulp is obtained. This fact explains that the soda pulping is only employed for non-woody biomass (straw, miscanthus, sugar cane bagasse, etc.) as feedstock [82] since it has lower lignin content and a more open structure, that is more prone to be solubilized by this alkaline medium.

The lignin obtained from this process is usually considered relatively free of impurities but with low β-O-4 bonds and they can present a high amount of ash due to the addition of soda [84]. Nevertheless, in comparison with lignosulfonates and Kraft lignin, it is sulfur-free lignin, that could be suitable for higher added value applications [85]. The revalorization of this lignin is the key point for producing small aromatic building blocks in order to satisfy the enormous and diverse industrial demand for these types of chemicals. Lignin catalytic transformations provide routes to obtain cresols, catechols, resorcinols, quinones, vanillin, guaiacols and many others; which are considered as potential chemicals that can be utilized in the food industry [86].

From a research point of view, alkaline treatments have significantly received attention due to the promise of becoming more important in the near future as the main lignin sulfur-free manufacturing process. Moreover, the employed reagents are both low cost and easily recoverable. Nevertheless, the lack of selectivity that drives to non-desirable reactions has hindered its implementation in huge levels for the moment.

1.5.4. Organosolv process

The organosolv pulping process has been suggested as an alternative pulping route to standard processes using organic solvents or their aqueous solutions to dissolve lignin from the lignocellulosic feedstock. The studies of this process began when Kleinert and Tayanthal discovered, in 1931, that wood could be delignified using a mixture of water and ethanol at elevated temperature and pressure [53]. Throughout the history of this method, a wide range of solvents has been proposed: alcohols, such as methanol and methanol; organic acids, such as formic and acetic acids, ketones, phenols, ethylene glycol; and mixed organic solvent-inorganic chemicals [87–89]. The intrinsic advantage of organosolv systems over Kraft pulping processes is related to the concept of recovering the solvent by using simple distillation, which also minimizes the main drawback of the process caused by the high price of these solvents. This is the reason why methanol and ethanol are the most commonly used solvents due to their lower boiling points and low cost [90].

Organosolv delignification processes are developed in a wide range of temperatures (100-250 ºC) and under pressure values that can reach up to 250 bar, depending on the used solvent [91]. The organic solvents enable the solubilization of lignin without altering its chemical structure to a high degree, which has positioned these processes into the more attractive ones to preserve the native structure of lignin during the extraction [92]. However, some lignin internal bonds are cleaved along with lignin-hemicelluloses bonds depending on the severity of the reaction, since a reduction of the β-O-4 linkages inside lignin molecule is undergone and, as a consequence, lower average molecular weight lignin is obtained [51]. Although in the organosolv processes the obtained extraction yields are traditionally lower than the ones from other processes, they could be enhanced using inorganic acids or alkali as catalysts to increase the industrial interest. The drawback of this strategy is caused by the formation of a ternary azeotrope with the solvent that would hinder the distillation stage [93].

The high purity of the obtained lignin by these methods, together with the lack of sulfur in its molecular structure, allows lignin to be employed as a source of aromatic structures for the production of high added-value chemicals that can be used for the production of glue, binders, in polymer substitutions or as phenolic precursor [94,95].

Thanks to all these advantages, the formation of separate cellulose, hemicelluloses and lignin streams and the growing concern about the environmental impact of traditional pulping processes, it is expected that the organosolv methods may awaken more interest in the future for biomass fractionation [83]. The challenge of organosolv pulping methods will be, then, to identify solvents with better selectivity towards lignin compared to those available today which simultaneously allow simple, but efficient, recovery [53].

1.5.5. Innovative processes

There exist other minority processes where lignin can be extracted from biomass with a significant difference in comparison with previously mentioned methods. As common point, these methods are still in the development phase at a research level. So far, they are considered expensive methods, but they are capable to offer significant improvements to tune the properties of the final product, which makes them attractive to be used on small scale for high value-added applications.

The ionosolv method, a process consisting in the dissolution of lignin and/or hemicelluloses by means of using ionic liquids (IL) as solvents has emerged in last years as a promising technology to obtain a pure cellulosic pulp at lower temperatures than for example organosolv process (<160 ºC). By its definition, IL are mixtures of cations and anions that do not pack well among them and that remain liquid at low to moderate temperatures. The

low melting points, below 100 ºC, are often achieved by incorporating bulky asymmetric cations into the structure, together with weakly coordinating anion. Typically, the cation is an organic compound with low symmetry, whereas the anion can be organic or inorganic [96].

The quality of lignin, which is isolated by precipitation from the pulping liquor [97] is connected to the IL employed during the reaction, as well as to the severity of the reaction conditions [98]. However, there are still some limitations to be overcome in further investigations, such as the IL cost, toxicity, and recuperation [99].

In this group, the novel methods that provoke the dissolution of lignin using deep eutectic solvents (DES) could be included as well. They have gained interest as potential green solvents for several chemical and biological applications [100,101]. Generally, DES is composed of a mixture of two or more organic compounds with a final melting point much lower than the individual components which act as either hydrogen-bond donors or acceptors [102]. During the reaction, the DES are able to generate a mild acid-base catalysis mechanism that leads to the controlled cleavage of ether linkages. As a result, extremely low molecular weight lignin, with narrower distribution than commercial technical lignins, can be obtained while maintaining most of the properties and activity of native lignin [103]. However, the cellulosic biomass pretreatment using DES is still in a nascent stage and needs detailed experimental investigation at a much greater pace to guarantee its economic feasibility.

1.6. Lignin depolymerization

Once lignin is obtained, it can be furtherly transformed into value-added products by several processes that aim the cleavage of lignin to its most elementary structure in the form of phenolic monomers or aliphatic compounds[104]. In this sense, the lignin value can be noticeably increased by its breakdown in its elemental compounds, as it is depicted in Figure 1.5. These processes are divided into two big groups: (1) thermochemical and (2) biochemical processes.

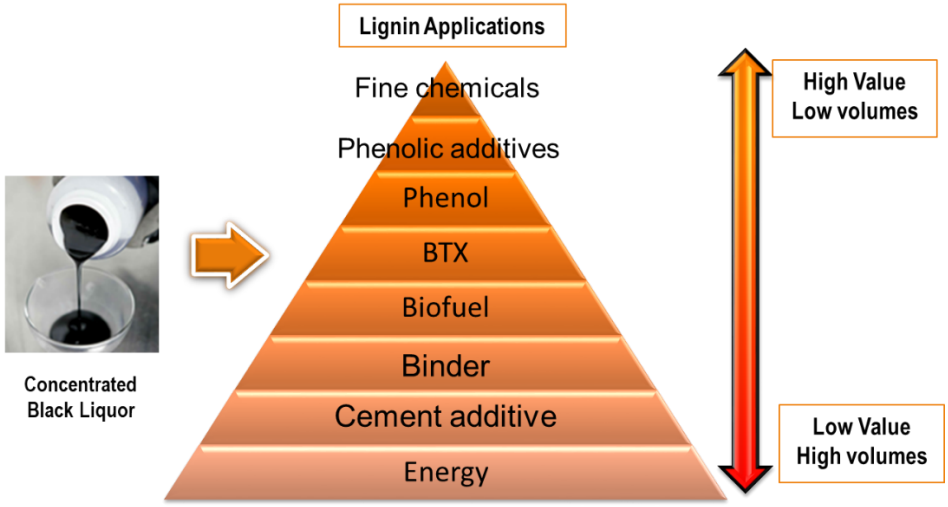

Figure 1.6. Classification of possible lignin applications.

The lignin depolymerization is an important research topic, which has resulted in a large number of published studies with emerging importance, as it can be seen in Figure 1.6, where the number of publications related to lignin depolymerization by year is represented. These figures highlight the relatively low interest that this topic awakened until the last decade and the high increase of publications in the last years. This fact remarks the relevance of biomass use in the search of alternatives to fossil resources, which has been curiously boosted after the economic crisis of 2008, indicating that the importance of the use of lignocellulosic biomass to produce fine chemicals has been promoted not only based on their environmental advantages, but also to reduce the economic dependency from countries that monopolize fossil resources, which is a common problem for European countries, and subsequently to Spain. A similar trend can be observed in the status of patent publications, since in the last few years the patent application number has strongly increased, with approximately 80% of patent applications made within the last 10 years [105].

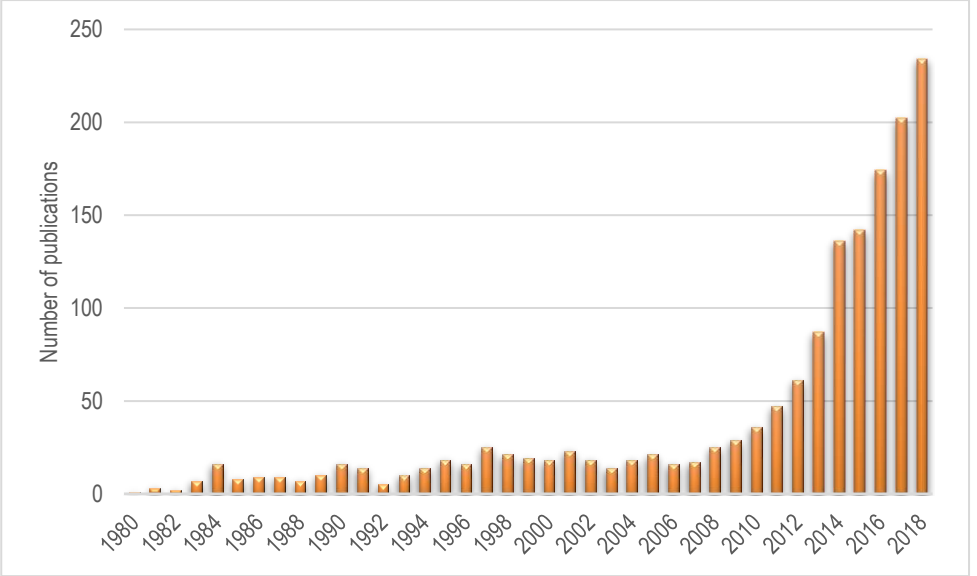

Figure 1.7. Annual evolution of publications with "lignin" and "depolymerization" as keywords (Source: Scopus).

The thermochemical processes are considered to be the most important group of routes used for the lignin depolymerization, since biochemical processes are still limited to a research level as the lignin breakdown by microbial or enzymatic degradation present high costs and long reaction times compared with the ones of thermochemical processes. However, they could reach a significant level of product selectivity, which makes them interesting for high value-added applications [44].

The thermochemical processes gather a wide range of methods that can be divided into several sub-groups [51]: (i) Base- or acid-catalyzed, (ii) solvolytic and thermal depolymerization, (iii) reductive depolymerization, and (iv) oxidative depolymerization.

1.6.1. Base- or acid-catalyzed depolymerization

Base catalyzed depolymerization (BCD) is the most studied method from this category of thermochemical processes with plenty of publications since the last two decades [106]. Several experiments have been performed at high temperatures (250-350 ºC) and pressure (150-300 bar), in presence of a soluble (mostly NaOH) or solid base (MgO or CaO as examples) [51]. The used solvent in this method is usually water, although some organic solvents have been used on some occasions too. Three main fractions are formed during the reaction: liquid oil; oligomers, often called tar fraction; and highly condensed lignin species called char. The product distribution changes accordingly to the temperature

used during the reaction. When the temperature is lower 300 ºC, methoxyphenols are the main monomers obtained within the liquid oil [107,108]. However, when the reaction temperature is above 300 ºC, the selectivity switches to catechol and catechol derivatives, such as methylcatechol, ethylcatechol, etc [109–111]. In general, the used solvent has a strong impact on product yields and selectivity. The yield of monomers is generally below 10%, and around 20% for liquid oils because of the competing and undesirable reactions that are experimented during the lignin depolymerization. Under either acid or alkaline medium, primary products derived from lignin readily undergo facile addition and condensation reactions, forming high molecular weight products. As a result, a substantial amount of solid residue is produced which restricts the liquid oil yield [112]. In some cases, this yield can be enhanced using organic solvents, such as methanol, ethanol or an ethanol/water mixture [113]. For example, ethanol not only acts as a hydrogen-donor solvent to stabilize primary intermediates that are prone to condensate in high molecular structures forming char, but also forms O-alkylation of Ar-OH groups preventing repolymerization reactions [114]. As a consequence, monomeric yields can be improved over 10% [113].

In the case of acid-catalyzed depolymerization (ACD), the applied temperatures are generally above 250 ºC, which makes considering them as high-temperature reactions. A great variety of soluble Lewis acids [115–117], soluble and solid Brønsted acids have been applied to catalyze this type of reaction [118–120]. The distribution of reported monomer yields from these surveys is deeply wide, from 2 wt.% to 60 wt.% but monomer yields are also hampered by undesirable condensation reactions undergone by reactive intermediates [51]. The reaction in ethanol and other alcohols, such as methanol and butanol, enables much higher monomer yields compared to the reaction in water. This fact has been attributed to the higher solubility of the lignin products in alcohol solvents as well as to the stabilization of intermediate unstable products, avoiding repolymerization reactions, as it was described before. The prevailing products in water were phenols and catechols, while the reaction in ethanol produced phenols and guaiacols mainly [51].

1.6.2. Reductive catalytic depolymerization

The reductive catalytic depolymerization (RCD) of lignin is carried out using a redox catalyst and a reducing agent, which is almost reduced to hydrogen. This hydrogen can be either contributed to the system using hydrogen gas (hydro-processing) or derived from hydrogen donating species, which generally are provided by the solvent or even the lignin itself (liquid-phase reforming). The obtained products are typically deoxygenated species. The degree of deoxygenation reached by these techniques depends mostly on the catalyst and the temperature, being more severe when the temperature is raised. In fact, different

approaches can be divided into mild and harsh conditions depending on the temperature employed for the depolymerization reaction [51,121].

In mild hydrocracking, the temperature is below 300 ºC and the relatively soft conditions allow to preserve monomers in methoxyphenol compounds and their substituted forms [122]. This type of reaction can be applied in aqueous, organic solvents, or a mixture of both of them over a noble metal (Pd, Pt, Rh, Ru) or base metal catalyst (Ni, Cu, WP/C, $Cu_2Cr_2O_5$, etc.) [123]. As common data values presented in the literature, monomers yields are below 25 wt.%, although much higher yields have been already reported, which depends also on the lignin sources, the lower β-O-4 linkage density is presented by lignin, the lower will be the final monomer yield [105]. The effect of catalysts can be observed by the possibility to reduce temperature to cleavage C-O bonds in lignin. As an example, Galkin et al. [124] developed a model that used Pd/C and formic acid as reducing agent under very mild conditions (80 ºC in air). Although monomer yield was almost negligible, lower molecular weight species were detected by GPC analysis.

When harsh conditions are applied to the decomposition of lignin, the reaction is typically carried out without using solvent and in extreme conditions, commonly with temperatures above 320 ºC and hydrogen pressures over 35 bar; i. e., the reaction is accomplished only between the solid catalyst and the substrate in the presence of hydrogen [125,126]. In such conditions, methoxy groups are removed from monomer products, resulting in methylated phenols (cresols, xylenols, etc.) and phenols with longer alkyl chains. Furthermore, some mono- and polycyclic deoxygenated aromatics, alkanes, catechols and methoxyphenols can be produced too. In terms of monomer yields, most common results are below 20 wt.% [127–129], but some exceptions can be also found with monomer yield of 35 wt.% [126].

In this group of RCD, bifunctional hydro-processing is also included. The process consists in the conversion of lignin into cycloalkanes by a bifunctional catalyst system which contains both acid and metal active sites [130]. In this technique, the catalyst plays a double role; the acid sites are responsible to provoke hydrolysis (if water is present) and dehydration reactions, whereas the metal sites enable hydrogenolysis and hydrogenation reactions. Therefore, lignin undergoes its depolymerization and its subsequent transformation into a complex mixture of oxygenated compounds, formed by a small set of alkanes and cycloalkanes [51]. The reductive metal catalysts employed by this technique are solid or noble metals, such as Ni, Cu, Ru or Pd; while the supporting materials can vary from acidic oxides (ZrO_2, MgO, Al_2O_3, SiO_2), acid zeolites and carbon, among others [131]. In this sense, noble metals catalyst (Pd/C, Pt/C, etc.) can reach conversions around 40 wt.% monomers, which remarks the great impact of catalytic systems. However, the high price of these components and the difficulties to recover them after the reaction to be recycled are still the main drawbacks of these processes.

The other type of RCD reaction mentioned before is the liquid-phase reforming, which is conducted without using a specific stream to add hydrogen. In this case, the solvent acts as hydrogen-donor to the system instead. As an example of these solvents tetralin, isopropanol and formic acid are the most employed substances. Several noble metals (Pt, Pd and Ru) and base metal (MoC, MgO, etc.) catalysts have been investigated for this reaction [121]. The selectivity of the process is not as high as in hydro-cracking reactions, with a wide range of products that can be obtained, such as methoxyphenols or deoxygenated aromatics and cycloalkanes. Yields of monomers reported by literature works are quite variable, but frequently close to 20 wt.%, although there can be found works achieving higher yields. For example, when the temperature is raised to 380 ºC, the monomer yield can be increased up to 60 wt.% with deoxygenated aromatics and cycloalkanes as predominant species [132].

A novel process has emerged lately by using hydrosilanes as an alternative to hydrogen as a reductant compound [133]. With an excess of Et3SiH in CH_2Cl_2 in presence of $B(C_6F_5)_3$ as a Lewis acid catalyst a range of monomer yields between 10-40 wt.%, was obtained using organosolv hardwood lignin as feedstock; and 7-17 wt.% from organosolv softwood lignin [133]. The selectivity of monomers was noticeably increased towards the formation of either propyl- or propanol-substituted compounds.

1.6.3. Oxidative depolymerization of lignin

In this case, the oxidative lignin depolymerization involves the conversion of lignin in the presence of an oxidizing agent. Specifically, the most commonly used oxidizing agents for this purpose are oxygen, hydrogen peroxide, but others can be found, such as nitrobenzene and CuO [92]. The depolymerization under strong oxidative conditions could reach the cleavage of not only side-chains, generating phenolic compounds, such as aldehydes (vanillin and syringic) and acids (vanillin and syringic); but also the breaking of the aromatic rings, which leads to generate aliphatic carboxylic acid compounds [134,135].

The possibility to obtain an aromatic flavoring product such as vanillin from alkaline lignin by oxidation methods has awakened a huge interest in the research community. Vanillin is a high demanded product in the market, due to the high value-added applications it presents, such as a flavor agent, antioxidant or due to its antimicrobial capacity [136]. The only industrial producer of vanillin from lignin is a Norwegian company, called Børregaard, who used lignosulfonates as feedstock [35]. The reduction of the sulfite pulp production around the world, as well as the legislations from E.U. and U.S. that forbid the use of chemically synthesized flavor chemicals for the production of natural flavors, have led to a decrease in vanillin production up to 15% of the market today [137,138]. This process is carried out using oxygen as oxidant agent in concentrated alkaline medium (NaOH 0.5-2

M). When pH is elevated by the alkaline medium, the free phenolic hydroxyl groups of lignin are ionized, which enables the oxidation reaction, and retards the consecutive degradation of the aromatic aldehydes. The used reaction conditions are 120-190 ºC, using oxygen or air to create the oxidant atmosphere. The increase of temperature or oxygen pressure provoke the acceleration of the vanillin formation but also its degradation, which shortens the optimum timeframe to obtain the maximum vanillin yield [139,140].

The lignin oxidation under an aerobic atmosphere can be also conducted in acid or neutral conditions, using inorganic acids mainly. Vanillin and methyl vanillate can be obtained by acidic oxidation from different sources of lignin as well [141]. However, by using only continuous reactors with high temperatures and low residence times it is possible to be close to the obtained yields, similar to the ones obtained by the alkaline oxidation [142].

Finally, as it was advanced before, some surveys have been focused on the lignin oxidation to the generation of non-phenolic carboxylic acids by the cleavage of the aromatic ring. Therefore, instead of minimizing the degradation of the phenolic monomers, this process aims the full conversion. This is possible using harsh conditions throughout high temperatures, stronger oxidant agents as hydrogen peroxide, and long reaction times. The monomer yields can be increased, with values above 50 wt.% [143]. Nevertheless, the selectivity of the obtained products is not high and, additionally, the aromatic singularity of lignin is not being leveraged since these products can be also manufactured from the carbohydrate platform of lignocellulosic biomass [23].

1.6.4. Solvolytic and thermal depolymerization

Solvolytic depolymerization involves the combination of a solvent together with a heating action. The solvent can be water, an organic solvent or a mixture of them. Hydrogen-donating solvents are commonly utilized for this aim as well, like tetralin or isopropanol [112,144]. The reaction temperatures can vary from 250 ºC to 450 ºC. The decomposition of lignin by its thermal solvolysis generates a wide range of monomer products, whose composition depends mainly on the solvent and temperature selected. When water or a mixture of water/organic solvent is used, the product selectivity tunes to unsubstituted and alkyl-substituted compounds in comparison to using only pure organic solvents. In addition, during the degradation of lignin at high temperatures, methoxyphenols, such as guaiacol or syringol are converted to catechol, cresols, and phenol [145,146]. In the case of hydrogen-donor solvents like isopropanol, the monomers selectivity switches to methoxyphenols with alkyl side-chains [112]. On the other hand, at relatively low temperatures (<300 ºC), unsaturated and oxygenated side-chains are more likely to be obtained, whereas when the temperature is increased above 300 ºC, unsubstituted and alkyl-substituted compounds predominate as resultant products [147,148].

In terms of monomer yields that can be reached, the solvolytic depolymerization is not able to achieve as great yields as other catalytic processes (acid, base or reductive), because of the benefits from the catalytic technology that this type of reaction has not implemented. In general, monomer yields are below 10 wt.%, although there can appear some exceptions with higher yields [149].

Fast pyrolysis is also considered a thermal lignin depolymerization process, which consists of burning lignin in the absence of oxygen between 300-600 ºC. As a result, a liquid oil is produced with a wide range of monophenols (phenol, guaiacol, syringol and catechol among many others), solid char and a gaseous fraction (mainly composed by CO_2 and CH_4). The proportions of these streams depend on the reaction parameters [46]. Even though most of the studies presented monomer yields below 10 wt.%, yields up to 20 wt.% are frequently reported [150,151]. This technology also presents the drawback of product repolymerization during the reaction. In this case, when products are condensed, they also undergo undesirable repolymerization reactions [152]. In line with solvolysis processes, the range of monomer products is noticeably increased in comparison with catalyzed methods. Faix and Meier [153] demonstrated that fast pyrolysis generates a more complex product mixture than mild hydro-processing and BCD, highlighting the poor product selectivity of this method. Moreover, the trend of lignin to agglomerate when is highly heated causes the plugging of the feeder and de-fluidization of the reactor bed, which makes easier to use raw biomass to fed the pyrolysis than pure lignin [154], although some strategies to overcome this problem has been developed recently, such as the pretreatment of lignin with $Ca(OH)_2$ to neutralize the lignin melting point among many others [155].

The catalytic pyrolysis is conducted when fast pyrolysis is accomplished in presence of a catalyst, which can be mixed with biomass in the reactor *in situ* or placed after the reactor, contacting only with the vapors that are generated at the reactor (*ex-situ*). The selectivity of monomer products is remarkably increased by the use of the catalyst. Concretely, deoxygenated aromatic compounds, such as benzene, toluene, xylene, and naphthalene are the most abundant products obtained by this technique, but also short-chain olefins and alkanes can be generated [156,157]. As catalyst possibilities, acidic zeolites, mesoporous silica, oxides, and metal-supported catalysts are the most studied compounds [158]. The catalytic entities play a double role in this process: avoiding repolymerization reaction and coke formation by the stabilization of intermediates as well as the transformation of depolymerized products into aimed products. In terms of reported yields, they are typically below 20 wt.% [159].

II) Lignin extraction and characterization

2.1. Motivation and objectives

Spain is considered one of the main countries in terms of biomass availability within the European Union [160]. In terms of forest reserves, Spain is the third country in volume generation, only behind Sweden and Finland. Additionally, there are other lignocellulosic waste streams more difficult to quantify but it is considered that there could be another 25 Mt/y that could be used according to current valorization strategies [161]. Most of these wastes are deposited in landfills, which creates problems of pollution, fire risk, and poor soil productivity. Nowadays, big interest has been placed on the use of these residual sources although most of them are, for the moment, intended only for energy generation. As an example, Ence company, the most important group in terms of energy generation from biomass in Spain, is planning to install a total capacity of 270 MW generation from biomass for 2023 [161]. However, it is thought that these streams present a promising potential to be further valorized based on their chemical structure. The interest in obtaining these chemicals from biomass is hugely increasing based on three main points: green principle of manufacturing chemicals from natural resources reducing the environmental impact in the common synthesis process, the higher ratio of O/C that exists in biomass compared to hydrocarbons and recent improvements in catalyst design, which is able to boost reaction yields as well as selectivity to target products [162].

In this chapter, selected agricultural waste streams were analyzed in terms of their physico-chemical composition to evaluate their potential as lignin source. After the characterization, some different lignin extraction processes were proposed. The experimental methods were defined from a sustainable perspective; using sulfur-free solvents that could lead to widen the further valorization possibilities of lignin. Furthermore, the idea of designing a versatile and adaptable extraction process capable of admitting different biomass sources without altering the main characteristics of the obtained products was evaluated in this chapter. For this purpose, the introduction of an autohydrolysis pre-stage was proposed and assessed. In addition, besides the design of lignin extraction processes from the pulping step, other processes were proposed to use the lignin from delignification and bleaching units. Finally, the influence of different sulfur-free delignification methods was evaluated by comparing the product yields as well as the chemical composition of the obtained lignins.

2.2.1. Blue agave bagasse

Blue agave (*agave tequilana*) is one of the most abundant agricultural products in Mexico, since tequila spirit is produced from this plant [163]. The National Regulator Council for Tequila Industry (CRT) had registered around 235 million plants on Mexican soil for 2011,

while the plant consumption for tequila production has reached the historical record in 2018, with more than 1,100 thousands of tones consumed [164].

The dimensions of the plant vary depending on the soil, age and climatic environment during the growth of the plant, although the weight is estimated to be around 18-35 kg. The core could represent up to 54% of the blue agave plant [165]. Traditionally agave leaves are pruned to enable the growth of the core and left in the field [165]. A picture of the harvesting process is presented in Figure 2.1. The easiest compounds to be extracted by hot water are mainly sugars from hemicellulose fraction and small aromatic compounds, which are separated from bagasse in the tequila manufacturing process. Therefore, a solid part enriched in cellulose and lignin is left as waste. Recently, the number of scientific publications based on using blue agave as feedstock has shown a noticeable increase[166,167]. However, these publications are mainly developed in agricultural and biological fields, with a low number of manuscripts in the engineering field of knowledge. Additionally, in this field, most of the publications are focused on the cellulose platform, such as nanocelluloses entities [168,169] without considering lignin as an important fraction to be valorized.

Figure 2.1. Blue agave harvesting: leaves are removed to extract the plant core used for tequila manufacturing.

Hence, the inclusion of the lignin platform to obtain value-added products is entailed as a crucial approach to integrate and improve the sustainability in the use of this species, which is also weighed as the economic engine of many rural areas in Mexico. In this line, the production of value-added materials from these streams could lead to cost reductions in feedstock, widening the range of the obtained products by approaching a multiproduct integrated biorefinery.

2.2.2. Almond shells

Almonds from the almond tree (*prunus amigdalus*) are one of the most common type of tree nuts and rank number one in the tree nut production [170]. They are typically used as snack foods and as ingredients in a variety of processed foods, especially in bakery and confectionary products. The almond production is located mainly in countries with Mediterranean climates such as, Italy, Spain, and California. After the U.S.A., with 80% of the global production share, and Australia (7%), Spain is the third almond producer worldwide (4%). However, the production and efficiency are not necessarily related since Spain is the largest country in terms of harvested surface (661,000 ha). Most of the cultivation in Spain is of dry-type whereas the irrigation crop was limited to 14% of the total surface in 2017 [171]. Hence, the great production of almond lead to a huge waste biomass generation that could be used as feedstock for different biorefinery approaches.

Among the more than 100 different varieties produced in Spain, only three of them are botanically native: *Marcona*, *Larqueta* and *Planeta*. The kernel is covered by a ligneous material called almond shell. This shell, which can be observed in Figure 2.2, has been considered as a lignocellulosic waste stream that has been traditionally intended for energy generation due to its high calorific power [172]. In the last years, almond shells have awakened certain interest in the research field because of their high lignin content, from 30-50%, [109,173]. Several research projects have addressed the valorization of almond shell for activated carbon generation [174], xyl-oligosaccharides obtaining [175] or the production of biodegradable composites [176], among many others.

Figure 2.2. Picture of almond fruits which are covered by the described lignocellulosic shell.

2.2.3. Olive tree pruning

The variety of olive trees growing in Spain today is the O*lea europeae*, one of the oldest tree species of the Mediterranean basin, where it remains the most important crop of edible

fruit and oil. Spain is the world leader harvester of olive. Around 2.4 million hectares are covered by olive crops, followed by Italy and Greece, with 1.4 and 0.7 million hectares respectively. In terms of annual production, the volume generated in Spain reaches more than 600,000 t per year, whereas Italy and Greece produce more than 300,000 and 200,000 t respectively. It has to be considered that trees in Italy and Greece have a slightly better yield than those located in Spain [177].

The olive tree trunk can measure up to 15 meters height, the bark is finely fissured with grey or silver tones. Two botanical varieties have been typically recognized for the Euro-Mediterranean olive (*O. europaea L. ssp*. *europaea*): the cultivated europaea (var. *sativa*) and wild oleaster (var. *sylvestris*) [178].

The crop of wild *Olea Europaea L*. has been enhanced and diversified since antiquity for natural and artificial selection by man [179], and it is one of the oldest cultivated species in the world. This fact, along with the facility of vegetative propagation, plant selection by olive growers, cross-pollination, mutation and clonal selection, have contributed to the high number of varieties of this species in the world. Nowadays, around 2000 of olive tree autochthonous varieties can be found all over the world [180].

The pruning of olive trees is performed before the following harvest, generating a huge amount of lignocellulosic biomass that has been traditionally burned in the fields for its removal, without extracting any economic profit from it. In fact, the pruning deposition at the landfills is forbidden to avoid the propagation of diseases. Recently, some trend to collect these wastes to obtain energy for electricity generation has arisen. However, the possibility of using these residues for obtaining chemical intermediates based on their lignocellulosic content has been also demonstrated [181,182], which broadens the opportunities to create value-added products from waste streams whose potential profitability for energy generation is considered as limited.

Figure 2.3. Image of waste olive pruning landfilling on the ground.

2.3. Lignin extraction from bleaching stages (Publication I)

The extraction of lignin is mainly accomplished during the pulping process, but also in the subsequent bleaching stages, in order to obtain fiber with a high cellulose content (>98%). In the bleaching stage, the Elemental Chlorine Free (ECF) process has been the most widely used method at industrial level in European countries, which use ClO_2 or $NaClO_2$ as reagents in the main step of the bleaching. However, environmentally friendlier methods are possible to be used for this purpose avoiding chlorinated compounds. This group of processes is known as Total Chlorine Free (TCF), where ozone or peracids are employed as bleaching agents. The first approach was to complete the replacement of all ECF processes by TCF. Nevertheless, the use of those reagents tend to deteriorate the pulp quality providing weaker fibers [183]. Moreover, it is difficult to obtain pulps with the same level of whiteness and brightness obtained with the use of chlorinated compounds due to the lower delignification power of hydrogen peroxide, owing to a higher residual lignin content. However, there are niche products where TCF can be successfully used , as in the case of easily refining pulps or for the production of nanofibers [184,185]. In any case, by 2001, TCF pulp production remained constant, maintaining a small niche market at just over 5% of the world bleached chemical pulp production [186].

Despite the Kraft process is, by far, the most widely used method for biomass delignification, organosolv method was used in this section due to its suitability for the obtaining of highly homogeneous and sulfur-free lignin which enables its further valorization into value-added products. In addition, this process could enable the solvent recovery by distillation, allowing its reuse as fresh liquor [187].

Agave bagasse (AB) and Agave Leaves (AL) were selected for this work due to its availability at the BioRP Laboratory, since a project focused on the use of the cellulose

fraction was being carried out without considering the lignin platform contained in these lignocellulosic materials. In this sense, lignin samples from AB and AL were extracted and physico-chemically characterized at different stages of the process developed by Robles et al., [188]. Hence, by isolating not only the cellulose, but also the lignin contained in the blue agave, the integral valorization of this biomass waste was conducted [189], boosting the concept of the "Integrated Waste Biomass Biorefinery". A brief description of the processes approached in this section is represented in Figure 2.4.

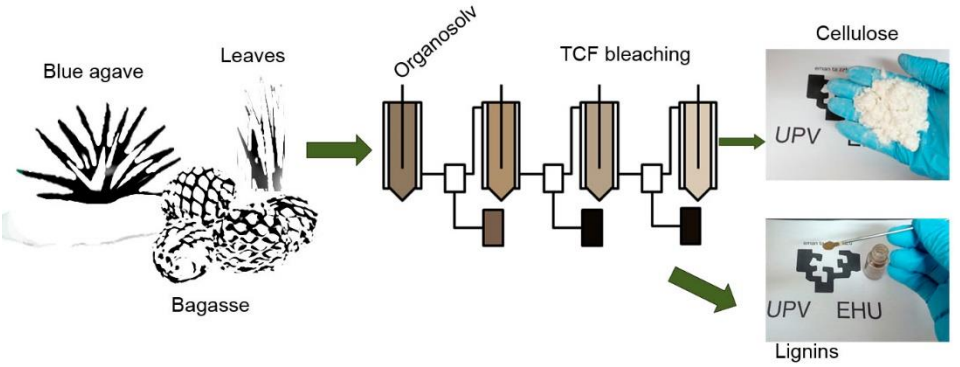

Figure 2.4. The valorization process approached for blue agave bagasse and leaves [190].

2.3.1. Experimental procedure

Blue agave bagasse and leaves were subjected to an organosolv delignification reaction, which was performed using a mixture of ethanol/water (70:30 v/v) as a solvent, at 200 ºC during 90 min and fiber to liquid ratio of 1:15 (w/v). These conditions were the ones established by Gordobil et al. [191] with slight modifications, mainly in the solid/liquid ratio because of the low density of agave bagasse and leaves. The liquid fraction was separated via filtration and the solid fraction was washed several times until driving the remaining fibers to a neutral pH level. Fibers were dried and separated for subsequent treatments.

The bleaching stages were conducted approaching an industrial method based on an O-O-PQ-PO sequence. At first, two oxygen steps with alkali (O-O) were performed, followed by a peroxide stage (P) with secondary chelating reaction (Q) and alkaline peroxide stage (PO) as a final step. The black liquors were extracted from the double oxygen stage, in which water was set at a pH of 11 using NaOH and 0.2 wt.% $MgSO_4$ to neutralize the remaining metals. This experiment was performed under a 6 bar oxygen atmosphere at 98 ºC for 60 min each time. After these stages, the pulp followed several peroxy stages from which no relevant liquor was obtained and, thus, it was discarded for this work, Figure 2.5 shows a graphical description of the delignification and bleaching stages as well as the lignin samples recovered from each stage of the global process.

The lignin isolation methods by precipitation varied depending on the stage in which the lignin samples were obtained from. Organosolv lignin samples (ABO and ALO) were isolated adding 2 volumes of acidified water (pH = 2), i. e., changing the polarity of the solvent agent; whereas, in bleaching liquors, the precipitation was provoked by the change in their alkalinity, adding H_2SO_4 until dropping the pH to 2. Afterward, the precipitated lignin samples were filtrated with polyamide filters (0.2 µm pore), washed with acidified water and dried at 50 ºC for 24 h. The isolated lignin was quantified to calculate the total extraction yield and chemically characterized by the analytical methods described in Appendix 1.

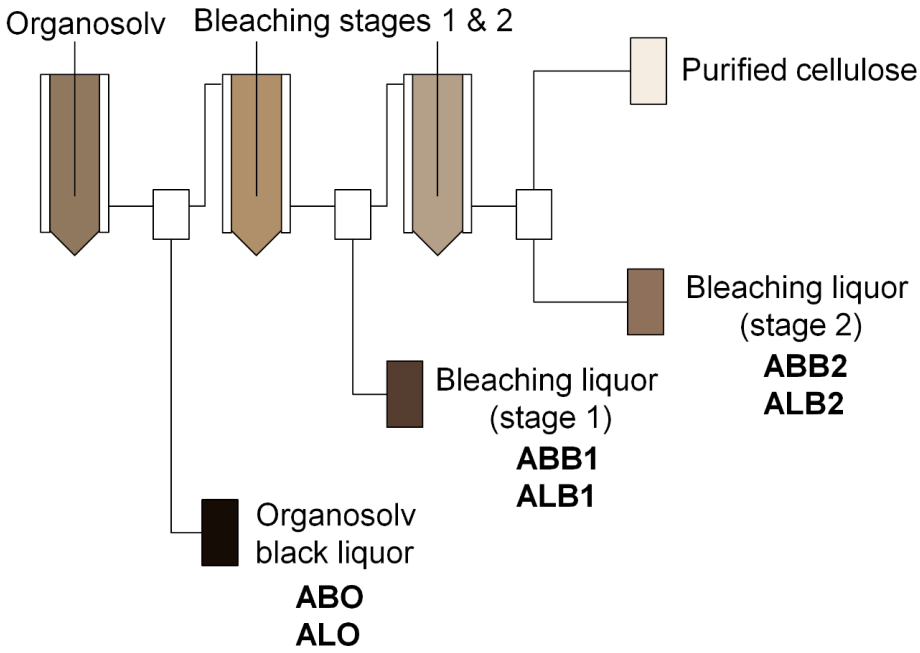

Figure 2.5. Description of the developed flowsheet as well as the lignin samples collected from each stage [190].

2.3.2. Raw materials characterization

The chemical compositions of the feedstock used in these experiments are detailed in Table 2.1. It was remarkable the high cellulose content of both biomass sources, which indicates the potential of their use for producing cellulose nanoparticles. Moreover, the lignin content, which was higher than 10%, could be considered enough to try to valorize it within an integrated biorefinery approach. The hemicelluloses content was lower than other similar biomass types because some of the hemicellulosic sugars were solubilized during the tequila production process. The ash content was found to be higher for AB, constituting

a more recalcitrant feedstock, whereas the extractives composition was bigger in AL, remarking its higher content flavors for instance.

Table 2.1. The original composition of Agave Bagasse (AB) and Agave Leaves (AL) feedstock.

Sample	Cellulose (%)	Hemicelluloses (%)	Lignin (%)	Ashes (%)	Extractives (%)
AB	54.60 ± 1.70	13.95 ± 0.28	16.20 ± 0.48	4.50 ± 0.33	5.42 ± 0.23
AL	63.10 ± 0.75	15.50 ± 1.71	12.40 ± 0.36	1.20 ± 0.56	7.30 ± 0.98

2.3.2.1. Physico-chemical characterization of lignin samples

After the delignification stage and the subsequent bleaching stages, different lignin samples were extracted and physico-chemically characterized in order to evaluate the quality of the bleaching stages. In the case of AL, after the second oxygenated bleaching (ALB2), no significant amount of lignin was precipitated from the liquor. Therefore, this sample was not furtherly considered.

The chemical composition of the isolated lignin samples, together with molecular weight parameters are shown in Table 2.2. Techniques used for these analyses were described in Appendix C. The purity of all lignin samples, expressed as the acid-insoluble content (AIL) plus the acid-soluble content (ASL), was above 75%, which is considered a relatively high value, even higher than some others reported in the literature from waste biomass sources [191,192]. Nevertheless, the stage which the lignin samples were collected from had a big influence on these properties, since lignin samples from bleaching stages presented, in all cases, lower purity (75-85%) than the samples from the organosolv delignification process (85-90%). With regard to the feedstock, bagasse lignin samples presented, in all the cases, higher purity values than the lignin samples obtained from leaves (submitted to similar processes). Hence, bagasse lignin samples presented the highest lignin content and higher purity as well. The reason could be based on the link between lignin and carbohydrates forming lignin carbohydrate complexes, which can be measured by the quantity of sugars on the lignin samples [193,194]. The highest content in sugar impurities in the lignin samples from leaves was in concordance with the highest carbohydrate content in the initial feedstock. In addition, the lignin samples from bleaching stages showed the greatest sugar content (around 10% or more). This fact indicates that the purest lignins were extracted in the first step, during the delignification process. The ash or inorganic content was similar for all recovered lignin samples.

Different behavior in terms of variation of molecular weight (M_w) and molecular weight distribution (M_w/M_n), was observed depending on the feedstock. In the case of AB, lignin

samples from bleaching stages (ABB1 and ABB2) showed a bigger size than ABO; i. e., the bigger molecules of lignin were more difficult to be extracted from the feedstock. Furthermore, this was countersigned by the determined M_w/M_n values, which were higher for lignin samples obtained from bleaching stages than for organosolv lignin samples. In the case of AL, the size of ALO was bigger than ALB1, making easier to extract larger lignin molecules in the earlier stage. This fact remarks the variability of the final lignin depending on the raw material source, even when it came from the same species but different part of the plant.

Table 2.2. Composition of the different lignin samples collected along the cellulose nanoparticles production process. (AIL: Acid Insoluble Lignin; ASL; Acid Soluble Lignin).

Sample	AIL (%)	ASL (%)	Sugars (%)	Ashes (%)	M_w	M_w/M_n
ABO	89.63 ± 2.73	2.85 ± 0.92	2.67 ± 1.32	4.95 ± 0.48	2933	3.61
ABB1	84.79 ± 2.68	1.87 ± 0.07	8.97 ± 2.75	4.25 ± 0.78	7414	5.79
ABB2	79.99 ± 1.87	2.16 ± 0.29	12.32 ± 2.34	5.86 ± 1.29	6741	5.26
ALO	85.19 ± 0.88	2.51 ± 0.51	6.03 ± 0.32	4.13 ± 0.39	4904	4.09
ALB1	74.29 ± 1.34	2.83 ± 0.74	11.67 ± 2.11	5.36 ± 0.97	3942	3.39

The chemical functionality of the lignin samples was evaluated by Fourier Transform Infrared (FT-IR) spectroscopy whose spectra are shown in Figure 2.6. The presence of –OH groups was detected for all lignin samples by a wide absorption band around 3400 cm^{-1}, with greater pronunciation for ALO and ALB1 lignin samples. The absorption bands from 2930 to 2840 cm^{-1} can be assigned to C-H stretching in $–CH_2-$ and $-CH_3$ groups [195]. Smaller bands were noticed at 1710 cm^{-1}, which indicated the presence of non-conjugated carboxylic acids in the observed samples [195]. Signals between 1400 and 1700 cm^{-1} were attributed to the aromatic skeletal vibrations of lignins. The peaks at 1595 and 1510 cm^{-1} were due to C-C of aromatic skeletal vibrations. The bands found at 1460 cm^{-1} and 1420 cm^{-1} were attributed to the C-H deformation in $-CH_2-$ and $-CH_3$ groups and C-H aromatic ring vibrations, respectively. In this region, no clear differences were observed between the samples. The band at 1325 cm^{-1} could be attributed to the presence of syringyl units (C-O stretch). Moreover, at 1265 cm^{-1} a small shoulder could be observed, which corresponds to the guaiacyl (C-O stretch) ring. Some characteristic bands associated with syringyl and guaiacyl units in lignin were detected at 1220, 1125 and 1030 cm^{-1}, corresponding to C-C, C-O and C=O stretching (G), aromatic C-H in-plane deformation (S) and aromatic C-H in-plane deformation (G > S) [196–198], where AL samples showed higher absorption to G units than to S ones.

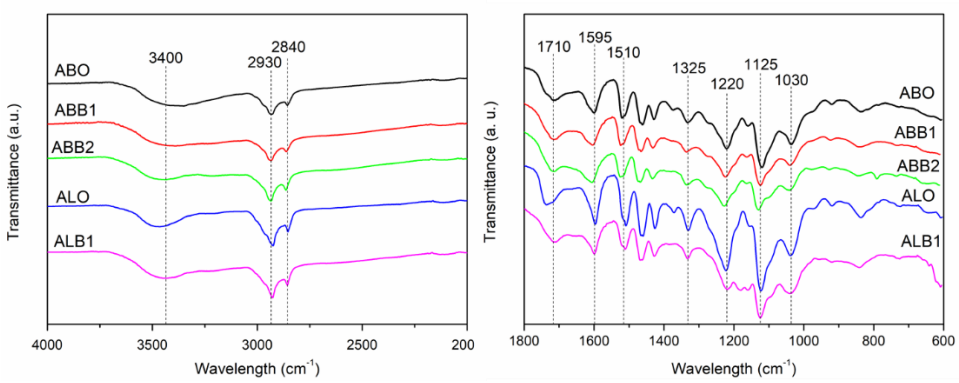

Figure 2.6. Evaluation of the functional groups of the isolated lignin samples by FT-IR analysis.

^{1}H NMR analysis of acetylated lignin samples was carried out in order to determine, for each one of them, the distribution of different proton signals per gram of lignin. The assignment of signals was based on similar literature works [199,200], following the method described in Appendix C. The obtained results, based on ^{1}H NMR spectra, are shown in Figure 2.7 and described in Table 2.3. All lignin samples presented hydrocarbon contaminant at 1.25 ppm. Signals between 6.00 and 8.00 ppm are assigned to the aromatic protons in syringyl (S), guaiacyl (G) units [201] being the resonances at 6.7 and 6.9 ppm due to the presence of aromatic protons in syringylpropane and guaiacylpropane structures, respectively. This protonated aromatic region is closely related to the degree of condensation of the lignin samples. A more condensed structure presents lower aromatic H content [202]. It could be seen that ABB2 presented the highest condensed structure, which was also sustained by its low H in methoxyl group content and high guaiacyl derivatives, which are related to the S/G ratio, showing a strong signal at ~4 ppm. In this case, the reduction of methoxyl proton signal was appreciable for lignins isolated after bleaching steps. The signals at 2.3 ppm and 2.0 ppm corresponded to the phenolic and aliphatic acetate groups, respectively. AL lignin samples presented higher content in hydroxyl groups in its structure than the ones isolated from the bagasse. On the other hand, it was possible to appreciate a decreasing in the content of total acetates (aromatic and aliphatic) decreased for both materials after bleaching stages.

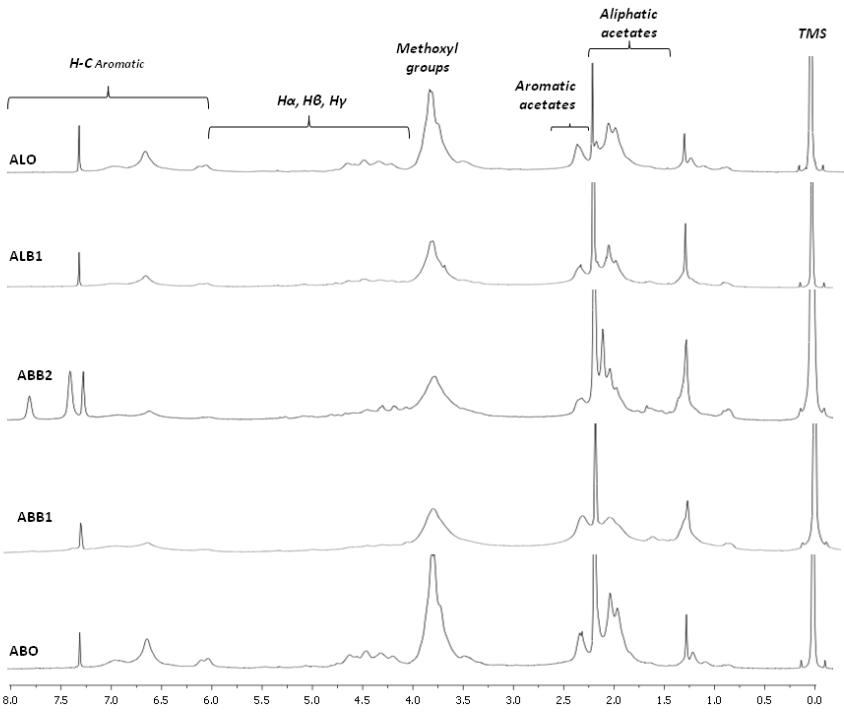

Figure 2.7. ^{1}H NMR spectra of acetylated lignin samples extracted at different stages of this process.

Table 2.3. Proton distributions per gram of acetylated lignin samples.

Assignment	ppm	ABO [mmol/g]	ABB1 [mmol/g]	ABB2 [mmol/g]	ALO [mmol/g]	ALB1 [mmol/g]
Aromatic H	8.00-6.00	1.23	1.7	0.86	1.84	1.24
Hα, Hβ, Hγ in aliphatic chains	6.00-4.00	1.21	1.54	0.77	1.75	2.11
H in methoxyl groups	4.00-3.00	3.54	2.91	1.21	6.09	3.84
Aromatic acetates	2.50-2.25	0.71	1.17	0.26	1.27	0.85
Aliphatic acetates	2.25-1.40	4.59	3.09	1.87	4.9	5.22

The chemical composition of the lignin was also characterized by Py-GC-MS, following the methodology depicted in Appendix C. The identification and relative quantification of the main compounds released during the pyrolysis are represented in Table 2.4. In addition, the total amount of the compounds classified by the elemental monomer they come from is described as summary at the bottom of the table. The identified phenolic products from pyrolysis were divided into four categories according to their aromatic structure: phenol-

type compounds (H), guaiacyl-type compounds (G), syringol-type compounds (S), and catechol-type compounds (Ca). Catechol derivatives were considered as S-type compounds following the procedure used in other studies, where it was proved that these phenolic products come from the degradation of syringyl compounds when the pyrolysis was performed at elevated temperatures [203–205]. Consequently, the syringyl/guaiacyl ratio S/G was calculated by the ratio of the sum of peak areas from syringyl units (including catechol derivatives) between the sum from the peak areas of guaiacyl derivatives.

The most plenty monomer in the lignin samples was syringol, in all the cases. Therefore, the S/G ratio was always above the unit. Similarities were found between lignin samples from organosolv treatment in comparison with lignin samples obtained after the first bleaching stage. Hence, it could be concluded that the structure of the lignin was not modified after the first bleaching stage. In the case of bagasse lignin samples, the S/G ratio even increased after the first bleaching, from 2.3 to 2.8. However, after the second bleaching stage, this ratio decreased to 1.1, which it is considered a deep variation. The more guaiacyl units, the more condensed structure the lignin presents because it is believed that more steric space is available in the C_5 position of the aromatic ring to create C-C linkages that generate condensed structures. Thus, this reduction in S/G ratio is thought to be caused by the more condensed structure of the lignin that remained in the solid after the organosolv and the first bleaching stages. This fact leads to the conclusion that lignin samples from the second bleaching stage had a more recalcitrant structure that would hinder its further conversion. In the case of lignin samples from leaves, there was no big difference between samples recovered after the organosolv process or after the first bleaching stage. However, both values were low, close to the unit (1.6 and 1.4 respectively). Hence, leaves not only presented lower lignin amount to be extracted, but also a more condensed lignin structure, which could be the consequence for not extracting enough material in the second bleaching stage to be characterized. Finally, very low amounts of compounds whose main monomer was H were detected.

Table 2.4. Py-GC-MS results described by peak detected at pyrograms, given by the m/z index as well as the relative intensity of detected monomers by each lignin sample.

Compound	m/z	Monomer*	ABO (%)	ABB1 (%)	ABB2 (%)	ALO (%)	ALB1 (%)
Phenol	94/66/65	H	0.06	-	0.52	0.04	0.43
3-Methylphenol	108/107/79	H	0.03	-	0.13	0.02	0.08
4-Methylphenol	108/108/77	H	0.07	-	0.69	0.07	0.25
Guaiacol	109/124/81	G	0.45	-	2.77	0.61	0.35
4-Ethyl-phenol	107/122/77	H	0.14	-	0.15	0.07	0.13
4-Methyl-guaiacol	138/123/95	G	0.64	0.07	2.30	1.47	1.07
3-Methoxycatechol	140/125/97	Ca	0.17	0.02	2.51	0.52	0.11
4-Ethyl-guaiacol	137/152/122	G	0.27	0.09	1.21	0.65	0.17
4-Vinylguaiacol	150/135/107	G	0.97	0.22	3.40	1.07	0.43
Syringol	154/139/111/96	S	2.39	0.22	8.74	3.57	0.94
Eugenol	164/149/131/77	G	0.60	0.09	0.41	0.31	0.22
3,4-Dimethoxyphenol	154/139/151/111	S	0.11	0.06	0.52	0.23	0.10
4-Propylguaiacol	137/166/122	G	0.10	0.11	0.36	0.19	0.39
Vanillin	151/152/81	G	1.25	0.75	0.54	0.87	0.55
cis-Isoeugenol	164/149/77/131	G	0.41	0.11	0.32	0.30	0.26
trans-Isoeugenol	164/149/77	G	0.27	0.57	-	-	-
4-methyl-syringol	168/153/125	S	5.86	0.57	8.59	8.59	0.42
4-Propylguaiacol	137/166/122	G	0.27	0.10	0.12	0.35	1.53
Propenylguaiacol	162/147/91	G	0.09	0.06	0.22	0.09	-
Acetoguaiacone	151/166/123	G	0.41	0.11	0.71	0.35	0.25
4-Ethylsyringol	167/182/168/77	S	1.24	0.11	2.86	2.48	0.35
Guaiacyl acetone	137/180/122	G	0.52	0.13	1.05	0.51	0.90
4-Vinylsyringol	180/165/137/73	S	3.71	0.77	6.49	3.80	2.46
Propioguaiacone	151/180/123	G	0.57	-	0.27	0.46	0.56
4-Allylsyringol	194/91/119	S	3.27	0.25	1.46	2.00	0.20
4-Propylsyringol	167/196/168/123	S	0.83	0.36	0.58	0.95	0.16
4-Allylsyringol	194/91/179	S	2.56	0.04	1.13	1.57	0.86
Syringaldehyde	182/181/111/167	S	4.27	2.51	1.36	2.95	0.29
Propenylsyringol	192/177/131	S	0.88	0.25	0.59	0.60	0.19
4-Allenylsyringol	192/177/131	S	0.51	0.14	0.38	0.35	0.63
Allylsyringol	194/91/179	S	14.5	3.46	6.10	8.48	0.39
Acetosyringone	181/196/153	S	1.14	0.31	1.52	1.10	0.45
Syringyl acetone	167/210/168	S	1.35	0.44	2.29	1.30	2.45
Propiosyringone	181/182/210	S	0.87	0.13	0.65	0.61	0.82
Total *p*-Coumaryl derivatives			**0.75**	**-**	**4.25**	**0.81**	**1.23**
Total Guaicyl derivatives			**20.5**	**4.14**	**43.6**	**26.5**	**11.2**
Total Siryngyl derivatives			**48.0**	**11.6**	**47.3**	**42.0**	**15.4**
S/G ratio			**2.35**	**2.81**	**1.08**	**1.59**	**1.37**

**H: Phenol; G: 2-methoxyphenol (guaiacyl); S: 2.6-dimethoxyphenol (syringyl); Ca: 1.2-benzediol (catechol); C: carbohydrate*

The thermal behavior of lignin is an important issue that could define its use on further applications, for example for composite manufacturing as it was depicted by Gordobil et al. [206]. Differential Scanning Calorimetry (DSC) and Thermogravimetric Analysis (TGA) techniques were used for this assessment according to the methodology indicated in Appendix C. The DSC curves of the lignin samples are presented in Figure 2.8. Although, DSC is the most accepted technique to determine the glass transition temperature (T_g) of lignin samples, it is often difficult to detect due to its complex structure, heterogeneity, as well as to its broad molecular weight distributions. The glass transition temperature of lignin depends on its molecular weight properties among other factors although, in general, for non-derivatized lignin samples. The range in which T_g could be found in lignin samples is between 90-180 ºC [195,207,208].

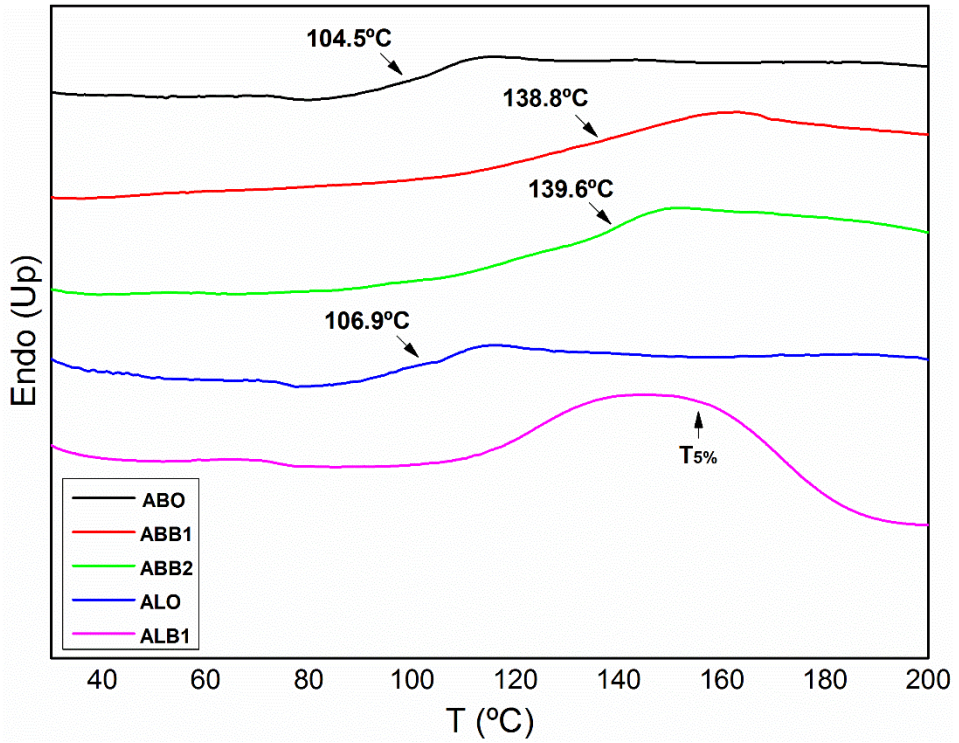

Figure 2.8. DSC thermogram of isolated lignin samples.

ABO lignin presented lower T_g (104.5 ºC) than ABB1 and ABB2 (around 140 ºC) samples, which demonstrated the lower molecular weight of organosolv lignin samples (ABO) in comparison to those ones from the bleaching side streams (ABB1 and ABB2). This fact supports the values shown in Table 2.2. This low T_g could have an influence on its softening point. On the other hand, the T_g of ALB1 was difficult to determine as its glass transition temperature was close to the initial thermal degradation temperature ($T_{5\%}$), as it can be

seen in Table 2.5. The higher T_g point for bleaching lignin samples, indicated a higher condensate structure than the ones obtained from organosolv pulping. Although the sugar content was higher, thus generating a lower value for the initial thermal degradation temperature for ALB1 sample, the lignin fraction presented a highly condensed structure. Comparing samples from different sources, the higher T_g of ALO (106.9 ºC) against ABO justifies the lower molecular weight of the last one.

The thermogravimetric analysis (TGA) and first derivative curves (DTG) of isolated lignin samples under nitrogen atmosphere are presented in Figure 2.9. The initial degradation temperature ($T_{5\%}$), the maximum weight loss temperature, and the char residue are reported (T_{max}) in Table 2.5. All lignin samples had a small weight loss (1-4%) below 100 ºC due to gradual evaporation of moisture. The main weight loss for all lignin samples occurred in the temperature range between 300 and 600 ºC [209], and is centered around 350-370 ºC. The principal stage is associated with the fragmentation of inter-unit linkages, such as cleavage of typical ether linkages among the aromatic units. Then, the cracking of aliphatic side-chains and the cleavage of functional groups occurs [74,210,211].

According to the DTG curves, the decomposition of all lignin samples was presented as a wide peak due to its high polydispersity. Moreover, a small weight loss around 200 ºC could be observed, due to the carbohydrate contamination. Lignin samples from bleaching stages presented lower initial degradation temperature (both below 200 ºC), which was related to the higher carbohydrate content in their structure. Although ABB2 samples had the highest sugar content, the same trend was not observed, as the structure of the lignin was different and it had a more condensed structure. Concerning the maximum degradation temperature, a small decrease could be observed in all the bagasse lignins (5-7 ºC) On the other hand, for leaves lignin samples, a slight increase was observed. Organosolv lignin samples from either bagasse or leaves had around 32% of char residue. However, as the bleaching sequence goes by, the char residue increased. This trend was more evident in the case of ABB1 and ABB2.

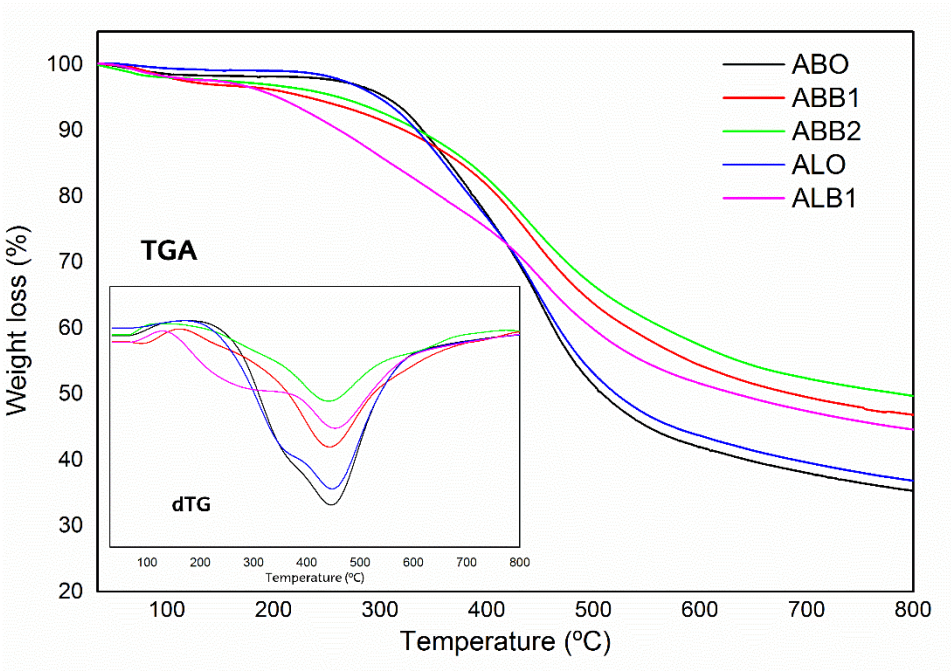

Figure 2.9. TG and dTG curves of isolated lignins.

Table 2.5. Temperatures and char residue values for the evaluated lignin samples.

Lignin sample	$T_{5\%}$ (ºC)	T_{max} (ºC)	Residue at 800 ºC (%)
ABO	244.3	359.9	31.9
ABB1	186.1	354.1	43.5
ABB2	210.6	352.3	45.7
ALO	238.4	359.8	32.8
ALB1	163.6	361.1	34.8

2.3.2.2. Lignin extraction yields

The assessment of the performance for every lignin extraction stage was accomplished by gravimetric analysis. In addition, the average yields after each stage and overall yield (Y_T) are presented in Table 2.6. This value was obtained as the sum of the total lignin yields with regard to the total fed material, and the relative yield (Y_L) was calculated as the lignin extraction yield, but referred to the original lignin contained in the feedstock.

Table 2.6. Evaluation of lignin yields obtained at the different stages of the tested processes (Y_O: Lignin extraction yield for organosolv stage with regard to initial biomass; Y_{B1}: Lignin extraction yield from first bleaching stage; Y_{B2}: Lignin extraction yield from second bleaching stage; Y_T: Total lignin extraction yield, referred to the initial biomass; Y_L: Total lignin extraction yield with regard to the initial lignin in the different used feedstock).

Feedstock	Y_O (%)	Y_{B1} (%)	Y_{B2} (%)	Y_T (%)	Y_L (%)
AB	9.49 ± 1.37	3.64 ± 0.84	1.95 ± 0.53	14.48	89.4
AL	7.46 ± 1.29	1.74 ± 0.77	-	9.07	73.12

As it was expected, the largest amount of lignin was extracted during the organosolv treatment (Y_O). The recovery of lignin after the pulping and bleaching processes for cellulose products production resulted in a high amount of this byproduct, obtaining total yield values (Y_L) referred to initial lignin existing in the raw biomass, around 90% for AB and more than 70% for AL. The reduction of the extraction yields for subsequent stages in the process is typically experimented in cascade separation processes, because of the higher complexity to remove a fraction that is in minor concentration at the next stages. As a consequence, the yields were dropped in the last stages. The minor yields obtained for leaves could be due to the higher difficulty of extraction when less quantity of a component exists in the initial mass, highlighting the concept of the cascade separation process.

2.4. Influence of pretreatment on lignin composition

In this section, the influence of a pretreatment stage on the final lignin properties was studied in order to determine the importance of introducing the pretreatment stage in the lignin extraction process. The different routes designed in this section for the lignin extraction are described in Figure 2.10. Following the previous section, AB and AL were used as feedstock sources. Two options were considered: (i) direct delignification stage using a sulfur-free method, such as organosolv process; or (ii) including a pretreatment, which consisted in a hot-water extraction, named autohydrolysis method, to reduce the hemicelluloses content in the solid which would be fed to the delignification stage, carried out in equal conditions as in the first option.

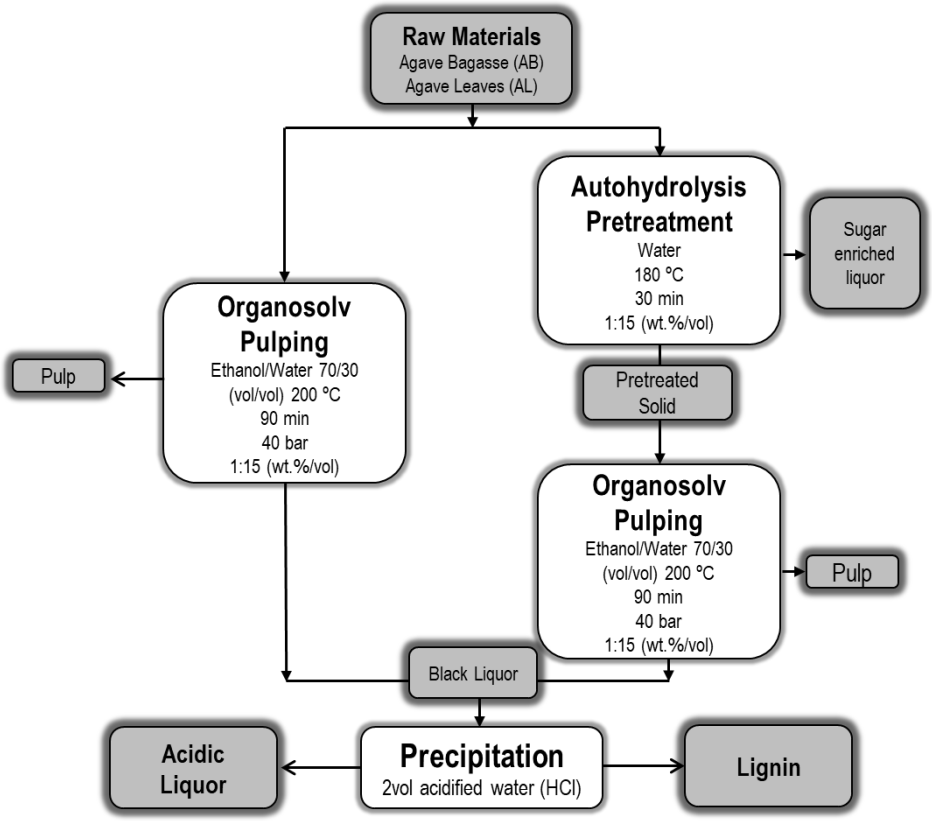

Figure 2.10. Scheme of the lignin extraction processes approached in this section.

The pretreatment step was carried out using only water as reagent at 180 ºC, for 30 min in a solid/liquid ratio of 1:15, following a similar methodology designed in a previous work developed by the BioRP research group [212] whereas the delignification stage by organosolv process was accomplished following the same method described in the previous section. After the delignification stage, regardless the taken route, lignin was precipitated by adding 2 volumes of acidified water. The final isolated lignin samples were quantified in order to calculate the total extraction yield and physico-chemically characterized.

2.4.1. Physico-chemical characterization of lignin samples

The compositions of the isolated lignin samples are detailed in Table 2.7, where one can see the increase in the total lignin content (AIL+ASL) for the lignin samples obtained after using a pretreatment before the delignification stage. This increment was only 1.8% for bagasse, but higher for leaves (5.6%). The sugar content in the lignin samples was consequently reduced for lignin samples obtained throughout a previous pretreatment,

both for bagasse and leaves samples. The ash content was slightly reduced when the pretreatment was performed. In terms of molecular weight and molecular weight distribution, the inclusion of the pretreatment led to a standardization of the obtained lignin samples, regardless the source (PBO and PLO), the final obtained value was similar, while there was a noticeable difference between BO and LO samples when delignification stage was accomplished directly. This importance of this fact is based on the traditional high variability of biomass products, which hinders its commercialization. Hence, the design of a process capable of providing uniform samples, where the influence of the feedstock on the final lignin properties is reduced, is very interesting.

Table 2.7. Composition of the different lignin samples collected from the two evaluated processes (BO: Bagasse Organosolv lignin; PBO: Pretreated Bagasse Organosolv lignin; LO: Leaves Organosolv lignin; and PLO: Pretreated Leaves Organosolv lignin).

Sample	AIL (%)	ASL (%)	Sugars (%)	Ashes (%)	M_w	M_w/M_n
BO	89.6 ± 2.7	2.9 ± 0.9	2.7 ± 1.3	5.0 ± 0.5	2933	3.61
PBO	92.1 ± 1.9	2.1 ± 0.5	1.8 ± 0.3	3.2 ± 1.6	4215	3.97
LO	85.2 ± 0.9	2.5 ± 0.5	6.0 ± 0.3	4.1 ± 0.4	4904	4.09
PLO	90.3 ± 2.3	2.8 ± 0.4	2.4 ± 0.7	2.3 ± 0.3	4575	4.09

Moreover, lignin samples were evaluated by FT-IR analysis. The spectra are presented in Figure 2.11. High absorptions can be observed in –OH band at 3400 cm^{-1} for all lignin samples. Absorption bands from 2930 to 2840 cm^{-1} are assigned to C-H stretching in $–CH_2-$ and $–CH_3$ groups. High similarity existed between all the samples in the range of 1400 to 1700 cm^{-1} bands, signals attributed to the aromatic skeletal vibrations of lignin. Finally, at 1325 and 1265 cm^{-1} bands can be related to syringyl and guaiacyl (C-O stretch) ring respectively. In general, all samples were very similar according to their chemical functional groups. Thus, no clear differences could be established by this technique.

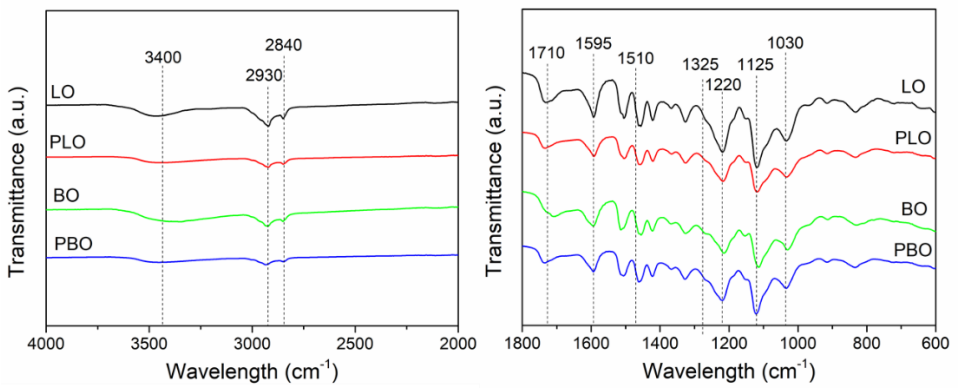

Figure 2.11. Evaluation of the functional groups of the isolated lignin samples by FT-IR analysis.

2.4.2. Lignin extraction yields evaluation

The inclusion of a new stage in a process cannot be only evaluated by the quality or composition of the final product, but also by the influence on the extraction yields too. These extraction yields are detailed in Table 2.8. Around 20% of the original biomass was removed by the autohydrolysis pretreatment, mostly composed of sugars and acids from the hemicellulosic platform, although the concentration in the autohydrolysis liquor was really low based on the high solid/liquid ration used at the reactor. In the case of bagasse, the total lignin extraction yield in the solid fraction decreased by ~45%, i. e., the inclusion of the pretreatment made the yield of lignin extracted after the organosolv process considerably lower. However, the opposite case was experienced with leaves. In this case, the lignin extraction after the organosolv treatment increased. This fact could be considered as illogical, since some lignin should be extracted in the autohydrolysis pretreatment. Nevertheless, the low lignin content existing in the original leaves as well as the difficulties to be extracted, could drive to the conclusion that the solid was physically more prone to be impregnated by the organosolv liquor after the pretreatment than before, which drove to obtain higher lignin extraction yields.

Table 2.8. Evaluation of lignin yields obtained by the two routes compared in this section (Y_P: total extraction yield from initial biomass in pretreatment stage; Y_T: Lignin extraction yield for whole process, referred to initial biomass; Y_L: Lignin extraction yield for whole process with regard to initial lignin existing in the different biomass used).

Feedstock/Route	Y_P (%)	Y_T (%)	Y_L (%)
BO	-	9.5	58.6
PBO	21.1	5.3	32.6
LO	-	7.5	60.2
PLO	19.4	9.7	77.9

2.5. Influence of the delignification method and the lignin isolation process on the lignin characteristics (Publications II and III)

Two lignocellulosic wastes: almond shells (A) and olive tree pruning (O), were used for the study of the influence of the delignification method and the lignin isolation process on the lignin properties. These materials were selected due to their abundance, availability as well as their high lignin content, greater than agave bagasse or leaves, which were used in previous sections. A pretreatment stage, consisting of an autohydrolysis step similar to the process employed before, was conducted for the hemicellulose content reduction to avoid lignin contamination with sugars.

Besides the organosolv delignification method, the soda process was also used to be compared as an alternative sulfur-free delignification method. In this line, the reduction of some environmental problems caused by the sulfur used in Kraft and sulfite cooking liquors was addressed. In addition, the obtaining of lignin samples free of sulfur traces could enable their further conversion or widening of their potential applications [109].

Lignin samples from alkaline processes (Kraft or soda) are commonly isolated by precipitation with the acidification of the liquor, filtration, and washing, being the LignoBoost® process the most currently used method for this purpose [213]. However, the commercial precipitated lignin presents high heterogeneity that hinders its further transformation [214]. Hence, more selective technologies for lignin isolation have been proposed to enhance the purity of the final lignin [215]. In this sense, selective precipitation could play an important role in the fractionation of lignin. On the other hand, the isolation of the organosolv lignin is carried out by the addition of an antisolvent that reduces the solubility of the lignin in the liquor. The most common method is based on the addition of water, which caused the precipitation due to the high hydrophobicity of the organosolv

lignin samples. In addition, the simplicity and low-cost of this method are very appreciated [216].

2.5.1. Process description

Both raw materials were firstly pretreated by means of the autohydrolysis process, which uses water as a unique reagent at high temperature and pressure. This process aims to remove a high percentage of the hemicelluloses present in the original composition, fact that could reduce the sugar impurities in the further lignin samples as it was explained in the previous section. The reaction conditions were similar to the ones used before (180 ºC, 30 min), but a solid:liquid ratio of 1:8, following the optimization of previous work [212]. After the autohydrolysis step, the liquid fractions were filtered and separated from the solid fraction, which was chemically characterized prior to be sent to the delignification stage. The yield of this stage was gravimetrically determined.

The solid fractions derived from the autohydrolysis process were subjected to the delignification processes. The organosolv process was accomplished at 200 ºC, 90 min; using a mixture of ethanol:water of 70:30 (v/v) as solvent reagent, and a solid:liquid ratio of 1:6; conditions optimized by Toledano et al. [217]. On the other hand, the applied conditions in the soda process were selected from the work of Urruzola et al. [218]: NaOH 7.5 wt.% was used as solvent at 121 ºC, during 90 min with a solid:liquid ratio of 1:6. After finishing the pulping processes, the obtained solid fractions were washed until neutral pH and then chemically characterized, whereas the black liquors were kept to be further treated for lignin precipitation.

Organosolv lignin was isolated in three fractions by adding different amounts of acidified water (HCl 37% to reach pH 2) in order to decrease the solubility of lignin in the black liquor. Specifically, ratios of 1 volume, 2 volumes, and 4 volumes of acidified water were added to one volume of the black liquor. On the other hand, soda lignin was precipitated by dropping the pH level of the black liquor by means of the addition of sulfuric acid (96 wt.%). Three fractions of different pH levels (6, 4 and 2) were obtained. Hence, 12 different lignin samples were obtained and physico-chemically characterized to identify the best routes to extract lignin in higher amounts and better quality to its further conversion into high value-added compounds. The abbreviations to identify the 12 lignin samples are detailed in Table 2.9.

Table 2.9. Abbreviation list for the different obtained lignin samples.

Symbol	Definition
AS	Almond shell soda lignins
AO	Almond shell organosolv lignins
OS	Olive tree pruning soda lignins
OO	Olive tree pruning organosolv lignins
AS pH=6	Almond shell-Soda lignin precipitated at pH=6
AS pH=4	Almond shell-Soda lignin precipitated at pH=4
As pH=2	Almond shell-Soda lignin precipitated at pH=2
AO 1vol	Almond shell-Organosolv lignin precipitated adding 1 volume of water
AO 2vol	Almond shell-Organosolv lignin precipitated adding 2 volumes of water
AO 4vol	Almond shell-Organosolv lignin precipitated adding 4 volumes of water
AS pH=6	Olive tree pruning-Soda lignin precipitated at pH=6
AS pH=4	Olive tree pruning-Soda lignin precipitated at pH=4
AS pH=2	Olive tree pruning-Soda lignin precipitated at pH=2
OO 1vol	Olive tree pruning-Organosolv lignin precipitated with 1 volume of water
OO 2vol	Olive tree pruning-Organosolv lignin precipitated with 2 volumes of water
OO 4vol	Olive tree pruning-Organosolv lignin precipitated with 4 volumes of water

A schematic description of the whole process followed in this section is presented in Figure 2.12.

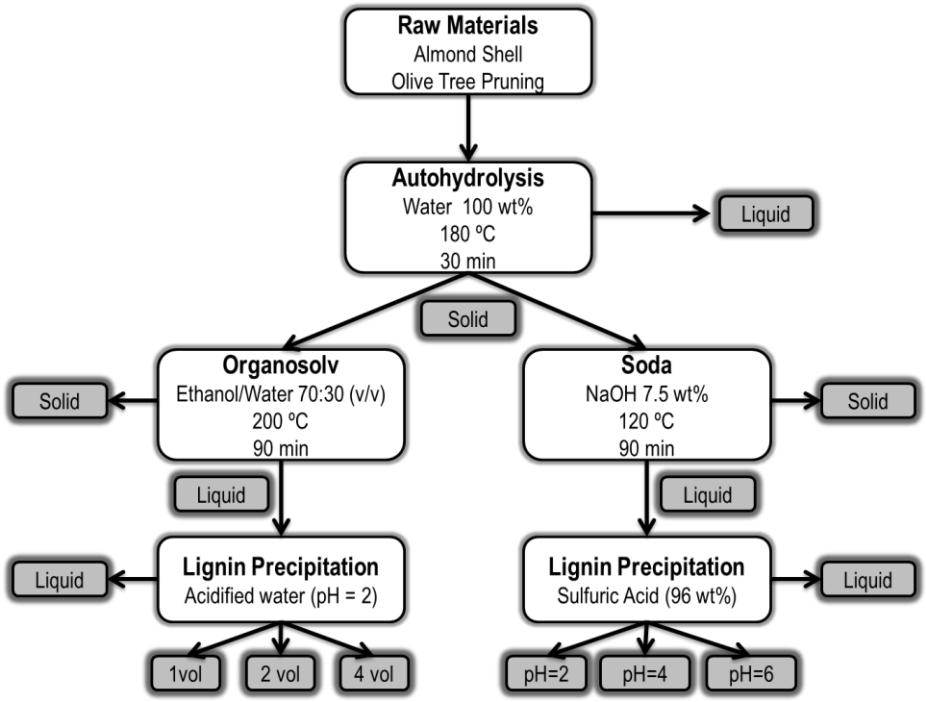

Figure 2.12. Scheme of the lignin extraction processes by the different routes approached in this section.

2.5.2. Influence of the pretreatment stage in the solid fraction

At first, an evaluation of the macro-components obtained in the solid fractions in each of the different stages of the proposed flowsheets was addressed. The obtained results are presented in Figure 2.13.

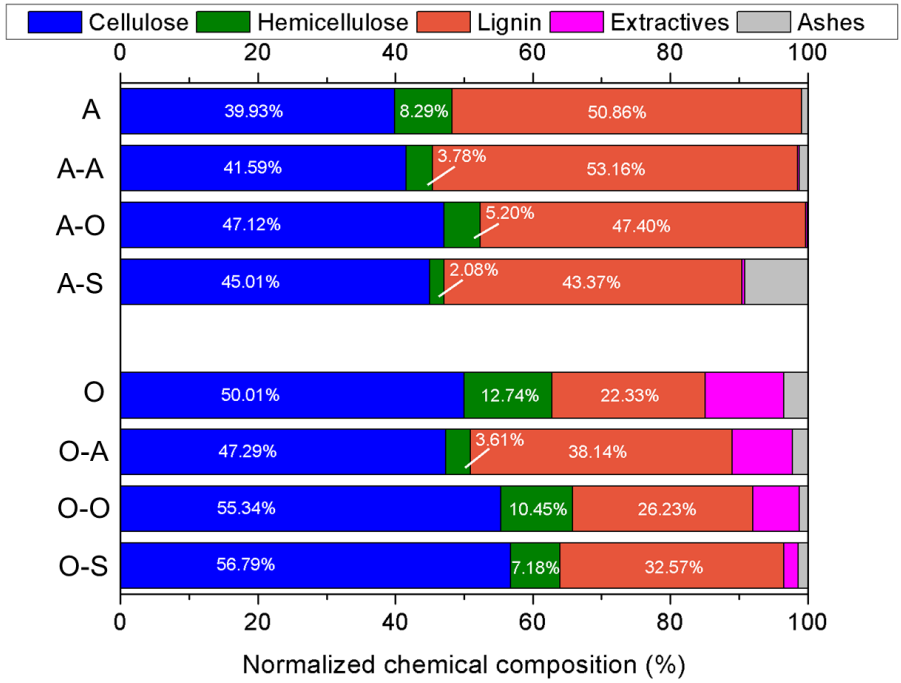

Figure 2.13. Macro-components compositions of solid fractions after each stage (A: Almond shell; A-A: Almond shell post-autohydrolysis; A-O: Almond shell post-organosolv; A-S: Almond shell post-soda; O: Olive; O-A: Olive post-autohydrolysis; O-O: Olive post-olive; O-S: Olive post-soda).

Regarding the comparison between the raw materials, the most remarkable aspect was the high content of lignin in A (~50%) while O presented less than a 25%; i. e. more than the double quantity of lignin is available from A than O. On the contrary, the contents in cellulose, hemicellulose and extractives were found to be significantly bigger for O than in A. Hence, it could be established that A is an interesting raw material for lignin-based products, whereas O could be more suitable for carbohydrate products. Nevertheless, both materials were subjected to the whole process to obtain and depolymerize lignin.

The autohydrolysis pretreatment provoked the reduction of the hemicellulose content in both materials (54% and 71% for A and O, respectively), increasing the lignin percentage in the obtained solid fraction that was sent to the delignification stage. The increase in the lignin percentage of the solid fraction for O was especially significant (70.8%), whereas it was notably lower (4.52%) for A. This fact is attributed mainly to the initial composition of the raw materials, since A presented lower hemicelluloses content and, therefore, less amount could be removed. In spite of this lower increment, the total amount of lignin per gram of material continues to be higher for A after the pretreatment, concretely 53.2% against 38.1% for O.

Both pulping processes (organosolv and soda) extracted mainly lignin from the different raw materials, as it was expected. However, depending on the feedstock, the selectivity of the pulping process towards the lignin extraction varied. In the case of A, the soda pulping was more effective with a reduction of 18.4% whereas. For the organosolv process, the reduction of the lignin content was only 10.8%. On the other hand, O feedstock presented higher level of lignin content in the final solid after each delignification process (14.6% for soda and 31.2% for organosolv).

2.5.3. Quantification and physico-chemical characterization of selectively precipitated lignin samples.

All the lignin samples collected from the different routes explained in the previous section were physico-chemically characterized. The results are summarized in Table 2.10.

Table 2.10. Lignin extraction and isolation yield, chemical composition of each purified lignin, average molecular weight (M_w) and molecular weight distribution (M_w/M_n).

Lignin Sample	AIL (%)	ASL (%)	Sugars (%)	Ash (%)	M_w (g/mol)	M_w/M_n	Yield (%)
AO 1vol	98.83±1.03	0.90±0.54	0.23±0.01	3.71	5,713	2.98	11.59
AO 2vol	99.75±1.76	0.64±0.09	0.27±0.07	3.27	4,381	3.03	17.18
AO 4vol	96.12±3.70	1.09±0.27	0.25±0.02	2.44	4,166	3.18	19.93
AS pH=2	85.76±2.72	2.64±0.57	1.11±0.11	7.55	27,322	12.33	39.31
AS pH=4	91.20±5.34	2.08±0.69	1.54±0.64	7.37	22,743	11.39	41.02
AS pH=6	94.22±4.51	2.12±0.49	1.92±0.16	9.28	33,190	15.48	37.43
OO 1vol	99.55±0.83	0.73±0.15	0.19±0.08	3.3	6,530	3.94	8.49
OO 2vol	94.70±2.30	1.20±0.13	0.19±0.04	1.96	5,164	3.89	11.16
OO 4vol	95.24±0.90	1.16±0.20	0.20±0.05	3.31	4,725	3.89	8.96
OS pH=2	88.04±1.21	2.59±0.11	0.18±0.06	4.21	20,405	12.01	41.31
OS pH=4	93.12±4.60	2.28±0.37	0.20±0.09	4.95	16,282	10.43	44.04
OS pH=6	92.23±2.41	1.90±0.30	0.17±0.03	8.76	18,151	11.53	46.92

As it was explained before, the sum of AIL and ASL fractions were considered to evaluate the purity of lignin. The inclusion of the pretreatment stage led to obtain lignin samples with purity over 88% in all the cases, which is a great value in comparison with previous studies developed in this research group [191,192,219]. In this case, the autohydrolysis stage was the sole difference with regard to other works. In fact, the most remarkable aspect was the

sugar content which was noticeably decreased in all lignin samples. The isolated lignin samples from the soda liquors presented lower purity contents, with values between 88% and 95%. The samples extracted at higher pH levels of precipitation presented lower percentages of impurities, since the addition of acid enables the precipitation of inorganic salts contaminating the lignin samples. Despite the lower purity of the soda lignin samples, these values were certainly high for the soda process [220,221].

Regarding the contamination of the lignin samples by carbohydrate compounds, it was found that the sugar content was almost negligible in every studied case. This fact justifies the use of the pretreatment stage, since, the fewer amounts of hemicelluloses in the feedstock, the fewer sugar impurities over the lignin were obtained.

In the ash content, less content was found in the lignin samples obtained from the organosolv process, whereas the soda treatment produced samples with more impurities based on the inorganic chemicals used in the white liquor as well as in the precipitation method. The lignin obtained after the organosolv treatment presented similar results at different conditions and, for both raw materials (between 1.96% and 3.71%). In the soda process, the lignin samples obtained at pH = 6 presented the highest quantity of ashes (9.28% and 8.76%), which could be caused by poor cleaning of the lignin sample, since the ash content for rest of soda samples were very similar between them.

Regarding the molecular weights and molecular weight distributions, the lignin samples obtained from AO and OO, presented very low M_w (4166 g/mol for AO 4vol as minimum value) and polydispersity index (2.98 for AO 1vol), in agreement with values published by other authors that used the organosolv method to isolate lignin from lignocellulosic biomass [222]. Nonetheless, AS and AO lignin samples presented the highest M_w and M_w/M_n (up to 33,190 g/mol and 15.48 respectively, for AS pH2). This fact is caused by the different delignification mechanisms, since the strong alkaline medium used in the soda process enables repolymerization and condensation reactions of primary products derived from lignin decomposition, forming higher molecular weight structures. More in detail, hydroxyl groups form quinone methide intermediates which easily react with other lignin fragments that lead to the generation of alkali-stable methylene linkages. As a consequence, higher lignin structures are created [223]. On the contrary, the ethanol used as solvent in the organosolv process not only acts as hydrogen-donor solvent, but also it is able to stabilize those primary intermediates, which are prone to condensate in high molecular structures, as it was explained in Section 1.6.1.

In the case of organosolv lignin samples, OA and OO showed higher M_w when adding fewer volumes of acidified water. Hence, a greater change in the solvent medium has to be carried out to precipitate the smaller lignin fractions. In the soda lignin samples there

was not found a clear trend. For AS samples, the biggest M_w value was presented by the sample precipitated at pH 6, in line with the previous statement. However, for OS, the biggest value was presented when precipitation was performed at pH 2 instead of pH 6. It was highlighted also the high M_w/M_n presented in soda samples, which indicated the presence of fractions with very different molecular weights in the soda lignin samples.

The analysis of the lignin extraction yields showed that the highest quantities of lignin were obtained with the soda treatment (up to 47% for OS pH = 6), whereas the organosolv method showed low yields of lignin extraction and isolation (between 8% and 20%). The higher yields from the soda process can be explained by the fact that the dissolution of lignin fragments is facilitated by the action of NaOH, which ionizes aliphatic hydroxyl groups as well as phenolic groups, contributing to the solubility of lignin fragments [224]. The use of O or A as raw materials did not indicate any clear trend for extraction yields. For instance, the same raw material (O) presented the highest isolation yields in soda process in comparison with the rest of samples, but also the lowest yields were obtained for O after the organosolv pulping. This fact indicates that the feedstock was not the determining variable to maximize the lignin extraction yield.

The chemical structures of these lignin samples were assessed by FT-IR analysis. Figures 2.14 to 2.17 present the spectra of the different studied lignin samples.

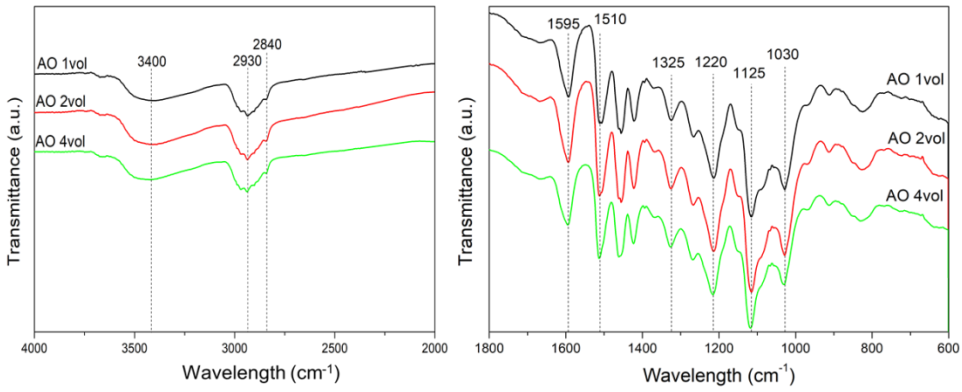

Figure 2.14. FT-IR spectra of AO lignin samples.

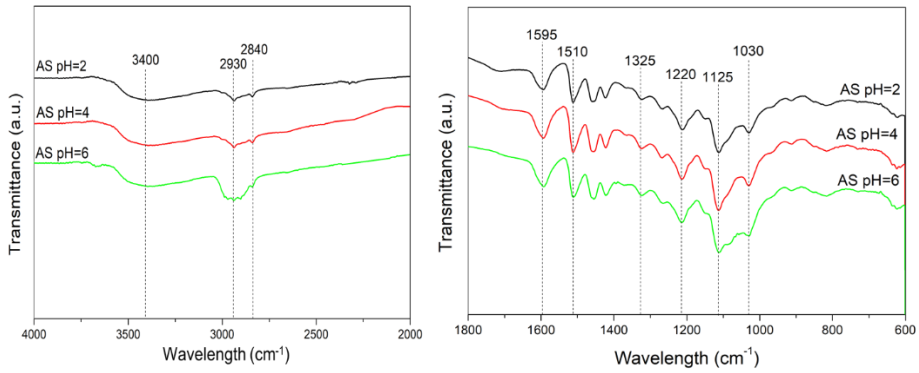

Figure 2.15. FT-IR spectra of AS lignin samples.

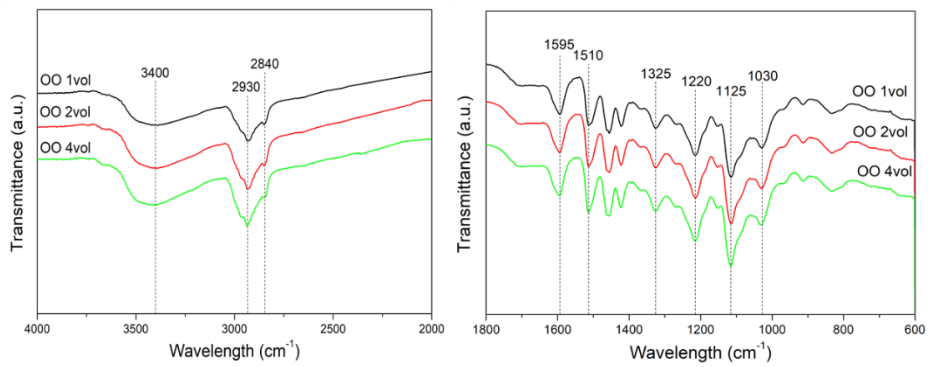

Figure 2.16. FT-IR spectra of OO lignin samples.

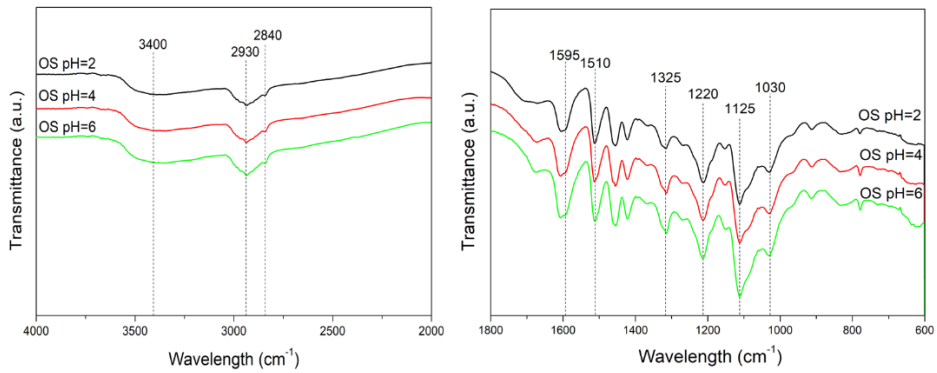

Figure 2.17. FT-IR spectra of OS lignin samples.

In all spectra, the wide signal detected 3400 cm^{-1} refers to the stretching vibration of the hydroxyl group and hydrogen bonding. The bands at 2930 cm^{-1} and 2840 cm^{-1} correspond

to C-H stretching and bending vibrations in methyl and methylene groups. Typical aromatic skeletal vibrations of the lignin were identified by the bands at 1595 cm^{-1}, 1510 cm^{-1}. The band at 1325 cm^{-1} could be attributed to the presence of syringyl units (C-O stretch). Some characteristic bands associated with syringyl and guaiacyl units in lignin were detected at 1220, 1125 and 1030 cm^{-1}, corresponding to C-C, C-O, and C=O stretching (G), aromatic C-H in-plane deformation (S) and aromatic C-H in-plane deformation (G > S). For all the analyzed spectra it was shown very high similarities among them. Hence, this technique demonstrated that the extraction method did not entail important changes in the functional group of lignin samples.

Based on these previous analyses, where selective precipitation at different levels was found to not have a clear effect on the final lignin properties, one sample from each delignification method from both raw materials was selected to perform a deeper chemical characterization with advanced techniques, such as Py-GC-MS and 2D-HSQC. From the organosolv method, only the samples precipitated by adding 2 volumes of acidified water were used, whereas, for the soda process, the ones precipitated at pH 4 were chosen.

For the Py-GC-MS technique, the same methodology mentioned in section 2.3.2.1 was followed to determine the syringyl/guaiacyl ratio (S/G). The results are listed in Table 2.11. In terms of monomeric composition, several structural differences were found between lignin samples from A and O. The chemical structure of lignins isolated from A by organosolv and alkali treatments were based on 33-36% of guaiacyl and 55-58% of syringyl (S/G: 1.58-1.77). However, lignins from O presented higher syringyl content (69-71%) and around 21-23% of guaiacyl units in their structural composition (S/G: 3.15-3.32). Hence, no significant variations between lignins from the same raw material were detected, evidencing that the monomeric composition was totally dependent on the origin and not on the extraction processes, as it was found out with agave biomass, where bagasse samples showed always higher S/G ratio regardless the process they were extracted from (except after second bleaching stage).

Table 2.11. Identification of the pyrolysis products from four lignin samples their mass fragments (AO: Almond Organosolv; AS: Almond soda; OO: Olive Organosolv; OS: Olive Soda).

Compound	m/z	Monomer*	AO (%)	AS (%)	OO (%)	OS (%)
Phenol	94/66/65	H	0.75	0.59	0.79	0.74
p-cresol	107/108/77/79/51	H	0.72	0.49	0.65	0.7
o-cresol	108/107/79/77/90	H	0.43	0.37	0.18	0.28
4-Etylphenol	107/122/121/77	H	0.43	0.45	0.27	0.36
Catechol	110/81/64	Ca	---	1.32	0.78	1.57
3-Methoxycatechol	140/125/97	Ca	5.94	4.54	7.45	6.45
4-Methylcathechol	124/123/78	Ca	1.49	---	0.87	---
Guaiacol	109/124/81/53	G	6.24	14.79	5.34	9.66
3-Methylguaiacol	123/138/77/95/67	G	0.64	0.93	---	---
4-Methylguaiacol	138/123/95	G	13.5	4.05	6.77	4.4
5-Methylguaiacol	123/138/95	G	---	0.21	---	---
4-Vinylguaiacol	150/135/107/77	G	4.09	5.05	2.74	3.41
4-Ethylguaiacol	137/152	G	2.82	2.23	2.33	1.99
Isoeugenol	164/77/149	G	0.23	---	---	---
Vanillin	151/152/109/81	G	4.79	3.17	2.42	1.45
Acetoguaiacone	151/166/123	G	1.01	1.17	0.75	0.49
Guaiacyl acetone	137/180/122	G	0.99	0.77	0.5	0.43
4-Propylguaiacol	137/166/122	G	0.85	0.2	0.63	---
Propenylguaiacol	162/147/91	G	0.27	0.26	---	---
3.4-dimetoxytoluene	152/109/137	G	0.11	0.42	0.14	0.28
Syringol	154/139/111/96	S	8.05	25.53	15.48	28.59
3.4-dimethoxyphenol	154/139/111	S	2.26	0.64	2.58	1.22
4-Methylsyringol	168/153/125	S	18.3	10.07	20.31	12.39
Acetosyringone	181/196	S	1.03	0.86	0.45	0.46
4-Vynilsyringol	180/165/137	S	4.44	4.77	6.21	5.74
4-Ethylsyringol	167/182/168/77	S	2.55	2.43	4.57	4.07
4-Propylsyringol	167/196/168/123	S	0.64	0.91	1.07	0.78
4-Propenylsyringol	194/91/151	S	0.44	0.31	0.34	0.27
Syringaldehyde	182/181/111	S	1.4	1.13	0.8	---
4-Allylsyringol	194/91/179/119	S	9.54	5.62	10.82	7.69
Syringilacetone	167/210	S	---	0.65	---	0.39
Total *p*-Coumaryl derivatives			**2.33**	**1.9**	**1.89**	**2.08**
Total Guaicyl derivatives			**35.5**	**33.2**	**21.6**	**22.1**
Total Siryngyl derivatives			**56.1**	**58.8**	**71.7**	**69.6**
S/G ratio			**1.58**	**1.77**	**3.32**	**3.15**

**H: Phenol; G: 2-methoxyphenol (guaiacyl); S: 2.6-dimethoxyphenol (syringyl); Ca: 1.2-benzediol (catechol); C: carbohydrate.*

Additionally, the 2D-HSQC analysis revealed several differences concerning the main inter-unit linkages between the elemental units of lignin samples. In this case, the 2D-HSQC methodology was selected instead ^{1}H NMR, since more information can be obtained

from it, such as the distribution of the molecular linkages. In Figure 2.18 it is shown the main substructures found in lignin samples, and Table 2.10 summarized the ^{13}C-^{1}H cross signals, which were assigned according to previously reported data [193,196,198]. These signals were divided into side-chain region (δC/δH 50-90/2.6-6) and aromatic region (δC/δH 100-150/5.5-8). With regard to aromatic region, the presence of S-unit and G-unit was observed for all lignin samples, as it is detailed in Table 2.12.

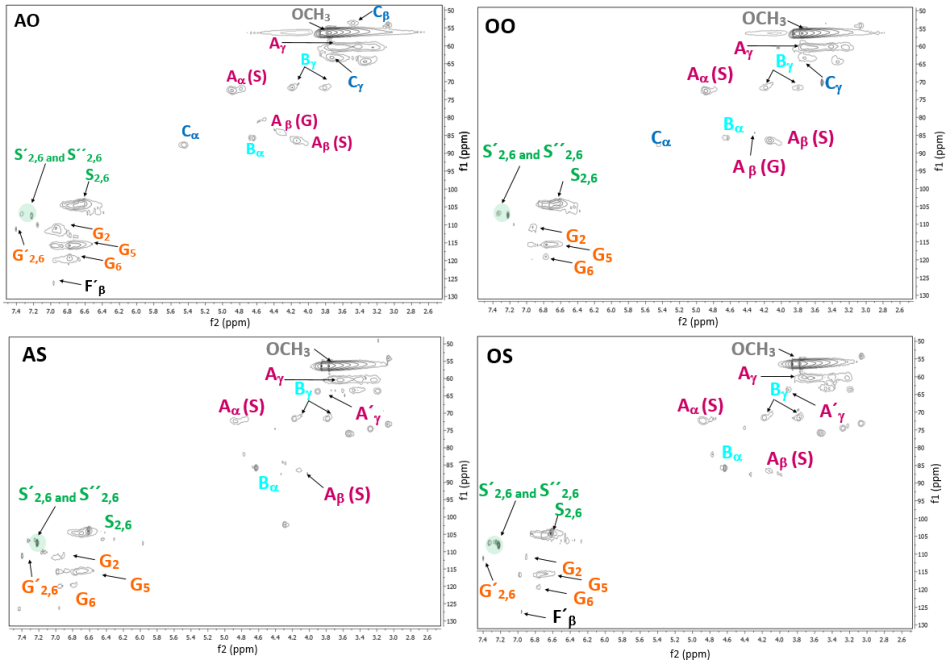

Figure 2.18. Main structures present in lignin samples.

Table 2.12. Assignments of ^{13}C-^{1}H cross signals in the HSQC spectra and their presence in lignin samples isolated from the studied black liquors and the calculated S/G ratio.

δ_X/δ_H (ppm)	Assignments	AO	AS	OO	OS
126.3/6.96	C_β–H_β of cynnamyl acetate end-groups (F´$_\beta$)	✓	×	×	✓
119.2/6.80	C_6-H_6 in guaiacyl units (G_6)	✓	✓	✓	✓
115.8/6.77	C_5-H_5 in guaiacyl units (G_5)	✓	✓	✓	✓
111.2/7.40	$C_{2,6}$-$H_{2,6}$ in oxidized (Cα=O) guaiacyl unit (G'$_2$)	✓	✓	×	✓
110.8/6.93	C_2-H_2 in guaiacyl units (G_2)	✓	✓	✓	✓
107.5/7.33 and 7.22	$C_{2,6}$-$H_{2,6}$ in oxidized (Cα=O) syringyl unit (S'$_{2,6}$ and S´´$_{2,6}$)	✓	✓	✓	✓
104.3/6.70	$C_{2,6}$-$H_{2,6}$ in syringyl unit ($S_{2,6}$)	✓	✓	✓	×
87.7/5.45	C_α–H_α in β-5´ (phenylcoumaran) substructures (C_α)	✓	×	✓	✓
86.5/4.12	C_β–H_β in β-O-4 substructures linked to S unit (A_β (S))	✓	✓	✓	✓
85.8/4.63	C_α–H_α in β-β´ (resinol) substructures (B_α)	✓	✓	✓	✓
84.2/4.32	C_β–H_β in β-O-4 substructures linked to G unit (A_β (G))	✓	×	✓	×
72.4//4.90	C_α–H_α in β-O-4 substructures linked to S unit (A_α (S))	✓	✓	✓	✓
71.6/3.81 and 4.18	C_γ–H_γ in β-β´ (resinol) substructures (B_γ)	✓	✓	✓	✓
63.7/3.90	C_γ–H_γ in γ-acetylated β-O-4 (A´$_\gamma$)	×	✓	×	✓
63.2/3.73	C_γ–H_γ in β-5´ (phenylcoumaran) substructures (C_γ)	✓	×	✓	×
60.3/3.68	C_γ–H_γ in β-O-4 substructures (A_γ)	✓	✓	✓	✓
53.6/3.48	C_β–H_β in β-5´ (phenylcoumaran) substructures (C_β)	✓	×	×	×
56.3/3.76	C-H in methoxyl groups (OCH_3)	✓	✓	✓	✓
	S/G ratio	1.3	1.5	2.9	2.6

Nevertheless, the most meaningful results were provided by the side-chain region, which demonstrated that the extraction processes had an important influence on the inter-unit linkages between the phenylpropane units. The relative distributions of the main inter-unit linkages in lignin samples are represented in Figure 2.19, which were calculated by a semi-quantitative method proposed by Wen et al. [225]. As it can be observed, lignin samples from soda delignification processes presented higher condensed structures than lignin

samples from organosolv treatments, with the presence of 41.4% and 61.0% of β-β´ bonds in resinol substructures for almond and olive soda lignins, respectively. In the case of organosolv lignins, β-β´ in resinol and β-5´ in phenylcoumaran linkages were also found. However, the most predominant linkage in both organosolv lignins, especially in the case of olive organosolv, was the β-aryl-ether linkage (β-O-4). The linkages between structural elemental units significantly affect to the depolymerization step, where the cleavage of β-O-4 bonds plays an important role in the production of phenolic monomer compounds as it will be described in further sections. The S/G ratio calculated from HSQC spectra follows the same trend as those that were obtained from the pyrolysis technique. As summary, the lignin source led to the main difference in lignin chemical structure (S/G ratio), with a slight increase in β-O-4 linkages in organosolv process, although only detected in olive samples. The higher amount of this type of inter-unit linkage in AO could be due to the lowest S/G ratio. The presence of higher content of guaiacyl units in its chemical structure, which contains reactive positions (C_5 positions) in the aromatic ring, allows the formation of condensed bonds like β-5´ [226].

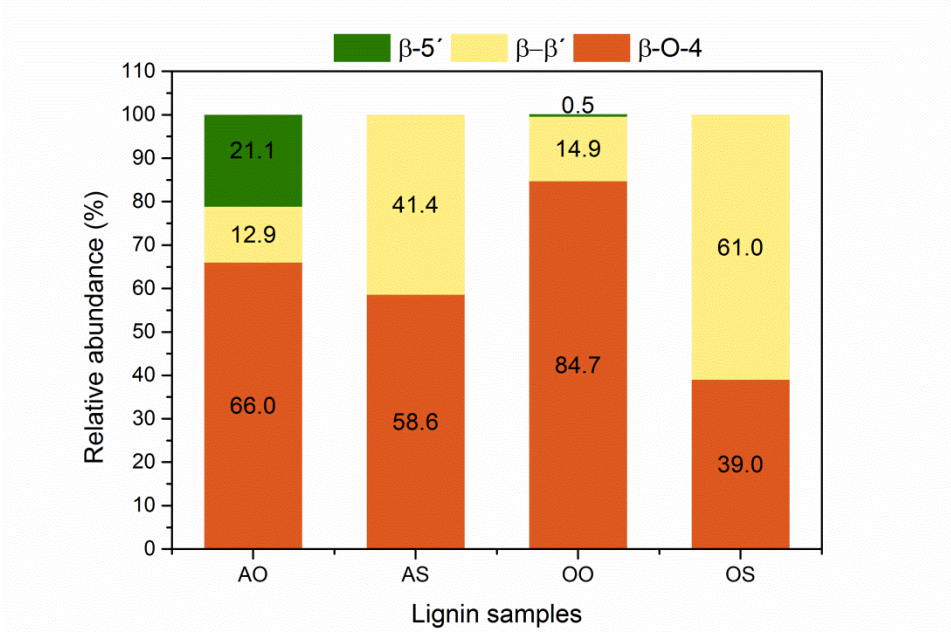

Figure 2.19. Distribution of intermolecular linkages presented in the isolated lignin samples.

2.6. General conclusions

In this chapter different routes have been proposed to obtain lignin from several sources. The extraction of lignin from side-streams generated in a global process intended for the production of cellulose nanoparticles was approached as first point, demonstrating that it

is possible to extract lignin even from the bleaching stages. However, the extraction yields, as well as the quality of the obtained lignin, were poorer in those bleaching stages.

Afterward, the influence of a pretreatment stage was evaluated by the inclusion of an autohydrolysis reaction to reduce the hemicellulosic content in the solid subjected to lignin extraction. Consequently, purer lignin samples were obtained. However, that increase was not significant and the most remarkable advantage about the inclusion of the pretreatment was the obtaining of much more homogeneous samples regardless the used raw material, which could enable the use of wide sources of biomass.

Finally, a comparison between two sulfur-free delignification methods was approached. The inclusion of the autohydrolysis step increased lignin purity. Furthermore, the organosolv method provided lignin samples with higher percentages of ether linkages that would be easier to be cleaved to generate small phenolic compounds from lignin as it will be approached in next chapter. On the other hand, the extraction yield for soda process was noticeably higher than in the organosolv method.

The influence of these parameters, both the physico-chemical composition of the obtained lignin samples and the extraction yields reached by the different routes developed in this section will relate to the lignin depolymerization reaction to identify the most suitable conditions to maximize the wished reaction products.

III) Lignin depolymerization

3.1. Motivation and objectives

The technical challenge of obtaining economically useful compounds from lignin has to overcome twofold aims: (i) the lignin polymer needs to be depolymerized; and (ii) interesting compounds have to be produced in meaningful quantities. In this frame, the purpose of this section was the development of several strategies to obtain monomeric phenolic compounds, such as guaiacol, syringol, phenol and catechol and cresol derivatives by the thermochemical depolymerization of lignin.

In terms of economic value, soda lignin and organosolv lignin are considered almost like a commodity product with values of 150-275 €/t for soda lignin and 250-475 €/t in case of organosolv lignin [226]. However, the possibility to obtain monomeric phenolic products represents a great potential to maximize the value that can be obtained from lignin.

Phenol is considered an important chemical precursor in the production of a wide range of consumer goods. The global production of phenol is estimated in almost 13 Mt/y for 2019 [227] with a proximate price of 1.4-1.6 €/kg for 2017 according to ICIS reports [228]. Its main application (49%) is the production of Bisphenol A, an intermediate compound to manufacture polycarbonates for instance, and also in the production of phenol-formaldehyde resins, a starting material in the manufacture of laminated plywood. Other phenol and phenol derivative products include adhesives, agrochemicals, dyes, insecticides, herbicides, preservatives, antioxidants and flavorings for foods, impregnating resins, antiseptics, and disinfectants, etc [229].

Catechol is synthetically obtained by the hydroxylation of phenol using hydrogen peroxide as a dominant process. Approximately 50% of its total production is used as starting material for insecticides, 35–40% for perfumes and drugs and 10–15% for polymerization inhibitors and other chemicals [230]. Catechol has also been used as an antiseptic, in photography, dyestuffs, electroplating, specialty inks, antioxidants, and light stabilizers, and in organic synthesis. The market price of catechol is estimated at around 4.0 – 5.5 €/kg [231,232] with an estimated global consumption of around 40 kt/y [233].

As pure substances, *o*- and *p*-cresol are crystalline, whereas *m*-cresol is viscous oil at room temperature. The cresols have a phenolic odor and are colorless [234]. The most implanted process to produce cresols is its recovery from coal tar and spent refinery caustics, comprising around half of the total global production, which is estimated to rise up to 180 kt/y, which would involves an estimated value of 750 M€/y [235]. However, this process is not enough to meet the rising demand. There are other industrial processes by chemical synthesis, such us the synthesis by methylation of phenol, where *o*-cresol is produced in a single step reaction in the presence of catalysts. The main applications of cresols are

depending on the isomer but it can be simplified in agrochemical and pesticides, antioxidants, dyes, chemical intermediates, electronics, etc. As estimation, its price could vary in the range 2-3 €/kg [236].

Guaiacol is a compound used as intermediate in the synthesis of flavors (e. g., in the synthesis of vanillin), fragrances and pharmaceutical substances, but also as an antioxidant additive for plastics and rubbers [237]. Petrochemical guaiacol is prepared by monomethylation of catechol using methyl halides or dimethyl sulfate. Monomethylation of catechol can also be accomplished with methanol in the presence of phosphoric acid, phosphates, or an ion exchanger [231]. However, guaiacol represents a great interest as vanillin precursor, product that can reach a market value around 12-14 €/kg. Syringol, which is present mostly in hardwood lignins is, together with guaiacol, a product of primary degradation of lignin. Syringol generates the main aroma of smoked and grilled foods, being an interesting compound to be used in synthetic smoke flavorings [238]. For both components their global consumptions are around 40 kt/y with a proximate price of 3.2-3.4 €/kg [239].

As a summary, in this section some of the isolated and characterized lignin samples were submitted to thermochemical depolymerization using different routes. At first place, BCD reactions were used to demonstrate the influence of several parameters, such as lignocellulosic source, delignification method or isolation process. The comparison of two different reaction mechanisms, BCD and solvolysis, was also accomplished in this section. Furthermore, a novel concept to carry out lignin depolymerization directly from the liquors by avoiding its precipitation stage was tested, adding an industrial liquor to check the distance between laboratory liquors and industrial ones. Finally, to reduce the generation of undesirable products some blocking agents were tested to evaluate different possibilities to maximize the product yields.

3.2. Solid lignin depolymerization by BCD (Publication II)

3.2.1. Thermochemical lignin depolymerization

As it was mentioned in Section 1.6.1., BCD is the most used method for lignin depolymerization due to its simplicity and relatively high efficiency as the main strong points. The reaction mechanism undergone by lignin molecule is breaking down into its elemental compounds triggered by the high alkaline conditions the reaction is taken place. In such environment, the formation of an alkaline phenolate (cationic ion depends on the base used) and a carbenium ion-like transition state, which is instantly neutralized by a hydroxide ion, are generated. The cationic species (Na, K, Ca, etc.) catalyze the reaction by forming cation adducts that polarize the ether bonds. This step increases the negative

partial charge of the oxygen and, consequently, the energy necessary for heterolytic bond cleavage is reduced [240]. As a result, phenolic monomers-rich oil is obtained in a quantity not higher than 20%–23%, regardless of which conditions lignin is exposed due to undesirable reactions that also undergo during the lignin breaking down. A schematic representation of the BCD reaction mechanism is presented in Figure 3.1.

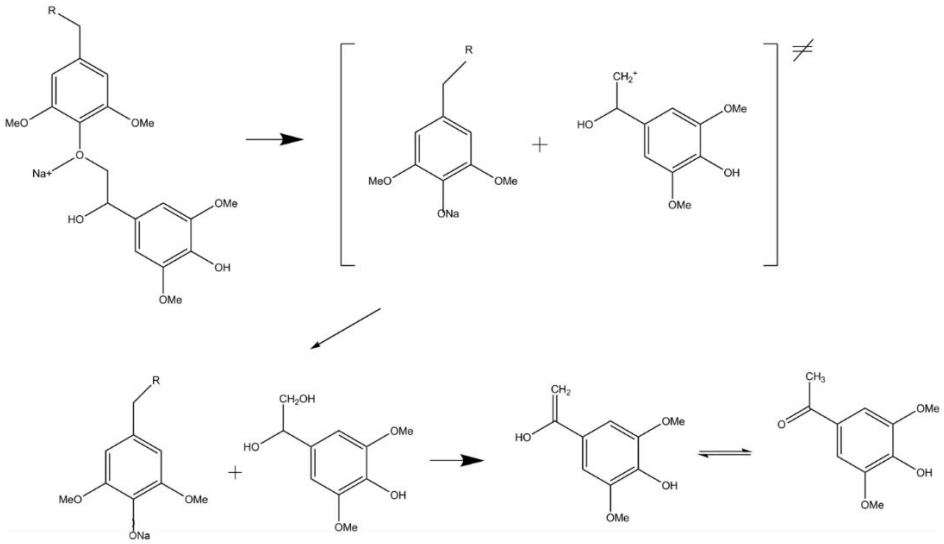

Figure 3.1. Cleavage of the b-O-4 bond and formation of syringol derivatives [241].

This phenolic oil yield is limited by the repolymerization reactions that occur during the process, when highly reactive phenolic and catechol derivative monomers undergo polymerization reactions instead of staying as monomeric products, generating residual lignin and coke as undesirable products. This reaction is happening due to a delocalization of the charge in the phenolate ions present in the alkaline media. The phenolate ion also exists as carbanion with a negative charge in *o*- or *p*- positions of the phenolic hydroxyl groups as a reason for resonance stabilization [241]. Therefore, the interaction of the carbanion species to other phenolic compounds with ketone groups will induce the facile formation of carbon–carbon bonds between these compounds, leading to the repolymerization of lignin. An example of this repolymerization mechanism is represented in Figure 3.2. Roberts et al. [107] stated that as the reaction takes place via carbenium ions, syringylic carbenium is more stable than guaiacyl carbenium since it has more methoxy substituent to disperse the positive charge. Miller et al. [242] conducted an experiment with syringol in aqueous NaOH and they observed the formation of guaiacol, catechol and other phenolic compounds. They also reported that dealkylation, demethylation and demethoxylation reactions occurred in BCD of lignin model compounds [219].

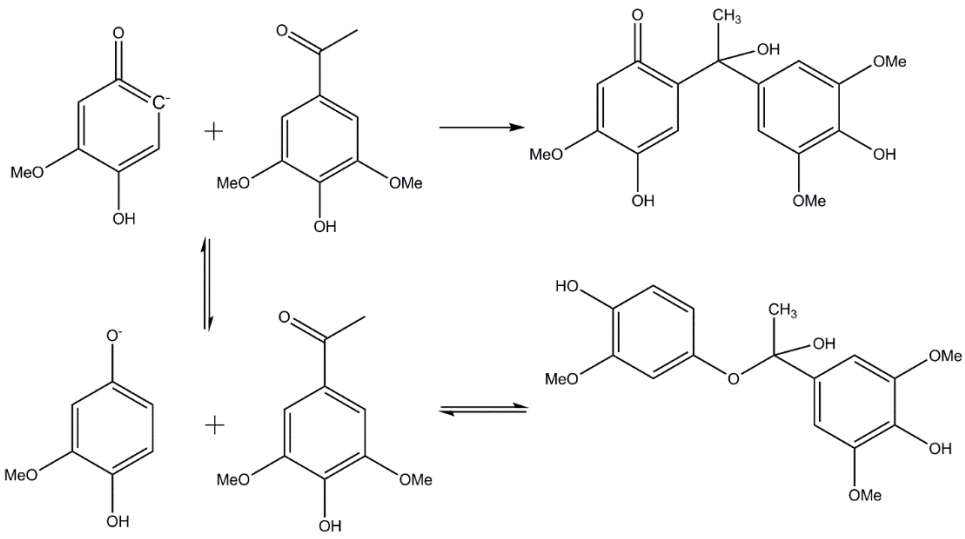

Figure 3.2. Repolymerization reaction between a phenolate and carbenium ion [241].

The Biorefinery Process group (BioRP) has positioned as one of the most productive groups in the topic of lignin depolymerization with 17 publications by early 2019, considered as the second most important group in terms of publication volume worldwide (Source: Scopus). Concretely, prior to this work, 14 publications have been published in indexed scientific journals focused on this topic. The most highlighted parameters of these works are detailed in Table 3.1.

Table 3.1. Publication of lignin depolymerization works developed by BioRP Research Group (PO: Phenolic oil; PM: Phenolic monomer; RL: Residual Lignin; C: Char).

Biomass	Extraction Process	Solvent/Catalyst	Reaction conditions	Products Yield	Ref.
Olive prunning	Ethanosolv	NaOH 4%	300 ºC, 90 bar, 40 min	PO: 5-20%; PM:3%; RL: 45%	[111]
Olive prunning	Ethanosolv	NaOH 4%	310 ºC, 105 bar, 30 min	PO: 22.5%; RL: 58,3%; C: 1%	[219]
Olive prunning	Ethanosolv	NaOH 4%	250-310 ºC, 90-30 min	PO: 22.5%; RL: 60%	[243]
Olive prunning	Ethanosolv	tetralin, isopropanol, glycerol and formic acid / Ni10%Al-SBA15	200W /200 ºC, 30 min	PO: 20-50%; PM: 1.3%; RL: 35-80%	[244]
Olive prunning	Ethanosolv	Formic acid / Ni10%-SBA15	100W /150 ºC, 30 min	PO: 25-35%; RL: 55-65%	[245]
Olive prunning	Ethanosolv	Tetralin / (Ni/Pd)-Al-SBA-15	400 W / 140 ºC, 30 min	PO: 3-17%; PM: 2.0%; RL: 30-76%	[246]
Olive prunning	Ethanosolv	NaOH 4% / (Phenol, H_3BO_4)	300 ºC, 40 min, 90 bar	PO: 45-160%; RL: 20-45%	[127]
Apple prunning	Ethanosolv	Ethanol / [Bmim][$MeSO_4$] + TiO_2	300W, 0-7 h	PO: 10-25%; PM: 4%	[247]
Willow	Ethanosolv IL	[Et_3NH][HSO_4] / TiO_2, H_2O_2	120 ºC, 1 h	PO: 7-22%	[248]
Miscanthus	IL	[HC_4im][HSO_4]-[Et_3NH][HSO_4] / H_2O_2	120 ºC, 1 h	PO: 4-19%; PM: 2%	[249]
Olive prunning	Ethanosolv	NaOH 4%	300 ºC, 20-100min	PO: 16.5-22.5%; PM: 3.5%; RL: 30-45%	[250]
Olive prunning	Acetosolv / Formosolv	NaOH 4%	300 ºC, 80 min	PO: 13-18.5%; PM:3-5%; RL:24%	[240]
Olive prunning	Acetosolv / Formosolv	Methanol, ethanol, acetone	300 ºC, 40 min	PO: 30-38%; PM 1.0-1.5%; RL: 3-5% C: 35-40%	[251]
Eucalyptus	Ethanosolv	NaOH 4%	300 ºC, 40 min	PO: 22%; PM: 0.5%; Tar: 60%	[252]

In half of these publications, the BCD mechanism has been used to break down the lignin molecule. Excepting the work of Toledano et al. [127], where the use of phenol as blocking agent to avoid lignin repolymerization led to an increase of phenolic oil (PO) yield, since this blocking agent was also collected in the oil; the rest of studied reactions showed phenolic oil yields with maximum values between 20-25%, in line with the previous comment extracted from the literature review. The total phenolic monomer yields (PM) were higher than other mechanisms (acid or solvolysis), with values above 5% [240]. The main drawback of this reaction mechanism is the harsh condition under which this reaction has to be carried out to obtain such a good performance (around 300 ºC). However, its simplicity makes BCD a feasible process to be scaled up to industrial level. On the contrary, other innovative processes studied in this group demanding lower energy, as ionic liquids [247,249] or microwave-assisted depolymerization [244,246], still present a scalability far to be reached.

3.2.1. Experimental procedure

Solid lignin samples collected from Section 2.5 were submitted to a BCD following the reaction methodology described by Erdocia et al. [250] in a batch reactor. This reaction was carried out using NaOH (4 wt.%) as an alkaline catalyst at 300 ºC for 80 min, reaching a pressure of 90 bar, and 1:20 (wt./wt.) as solid/liquid ratio.

After finishing the depolymerization process, the reaction mixture was treated to separate the different products, following the patented method depicted by Erdocia et al. [253], graphically represented in Figure 3.3. In the first stage, the mixture was acidified with HCl (37 wt.%) dropping the pH to 2 to precipitate the residual lignin formed during the reaction as an undesirable reaction product. The solid phase (residual lignin and coke) was separated from the mixture by filtration and washed with acidified water (pH = 2 with HCl as the acidic agent) to remove residual liquid. After that, the separation of the residual lignin from the coke was carried out using tetrahydrofuran (THF) as solvent, stirring the dissolution for 3 h, and filtrating again later. The non-solubilized solid (coke) remained in the filter, whereas the residual lignin goes throughout the filter due to its solubility in the THF. The solvent is finally evaporated under vacuum to recover the residual lignin.

On the other side, the liquid phase produced after the filtration of the residual lignin and coke was subjected to a liquid–liquid extraction to separate the phenolic-enriched oil from the aqueous phase using ethyl acetate as organic solvent. The residual aqueous phase was completely removed from the organic phase by an extraction process with sodium sulfate anhydrous. After a filtration step for the solid separation, the organic solvent was removed by evaporation, remaining the phenolic oil in a liquid phase. The yield of each

product was calculated gravimetrically referring to the initial lignin weight introduced in the reactor.

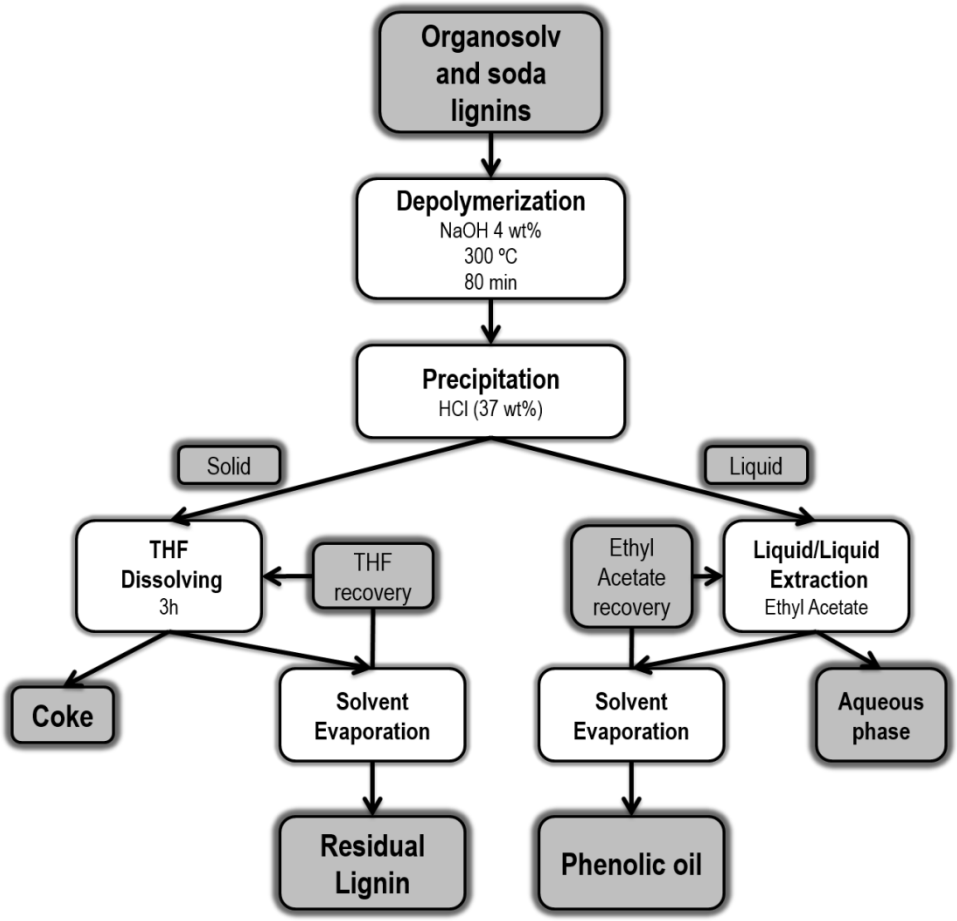

Figure 3.3. Schematic representation of the lignin depolymerization process and products separation.

3.2.2. Lignin depolymerization yields by BCD

As it was described above, three main products were obtained through the above-described method: phenolic oil, enriched in small phenolic molecules, residual lignin and coke. An aqueous stream was also produced, which was characterized using a HPLC equipment. Only small quantities of acetic acid, formed by the degradation of sugars, were found (concentration lower than 0.1%), and this stream was neglected in consequence. This fact was expected due to the low amount of sugars in the precipitated lignin samples, main precursors of these components. The yields of the rest of streams are shown in Figure 3.4.

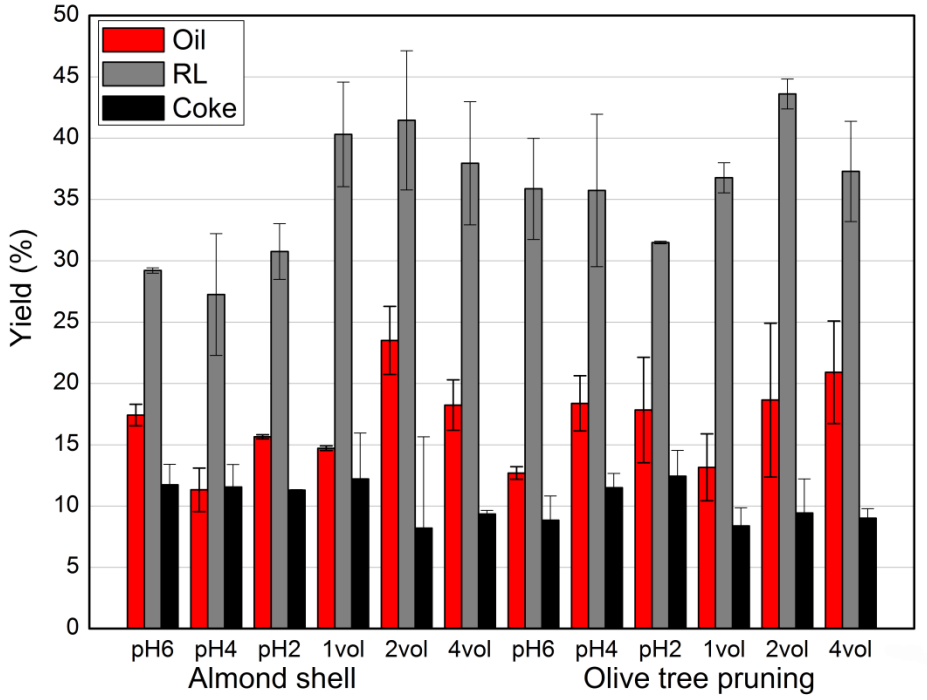

Figure 3.4. Product yield from the lignin depolymerization reaction of the three main products: phenolic oil, residual lignin (RL), and coke.

Regarding the oil production, the aimed product of the reaction, the variation of the yields did not follow a clear trend. However, it can be established that the highest yields of oil (from 18.23% up to 23.5%) were obtained from the organosolv lignin samples, excepting those precipitated using 1 volume of acidified water, whose yields were much lower (14.72% and 13.16%). In general, bigger yields of phenolic oil were obtained for organosolv samples. The lower values for AO and OO 1 vol, was in line with their bigger M_w in comparison with rest of organosolv samples. However, among almond and olive samples, there was no clear difference between them, despite the difference showed in terms of the S/G ratio shown in Table 2.9 and Table 2.11. In the case of the soda lignin samples, the trend was more complex, pointing the independency of the lignin precipitation pH value and the lignin source (almond shell or olive tree pruning) in the production of high phenolic oil yields. These results lead to the hypothesis that the repolymerization reactions have buffered the differences that were expected to be found according to the characterizations carried out in the previous chapter. In any case, the reported phenolic oil yields were in line with even best results presented in previous works of the group in comparison with the values detailed in Table 3.1.

The most abundant product of the reaction was the residual lignin (RL). The collected quantities were around the double of the phenolic oil yield. Reactions carried out using organosolv lignin samples generated higher quantities of RL. Whereas the coke, the other compound that also appears during the repolymerization reactions by the condensation and dehydration of small phenolic fractions, was lower for the organosolv samples. The structure of coke presents a lower ratio of oxygen per carbon atom, as it was demonstrated by Long et al. [128]; which makes it the most undesirable product of the reaction.

Even if RL is not the most desirable product of the reaction, it would allow its recirculation, in the case of a continuous process or its valorization as a modified lignin, as it was published by Mahmood et al. [254], who proposed to use residual lignin as feedstock for polyurethane production since this residual lignin contained more hydroxyls groups than the initial one. Therefore, residual lignin can be considered as a byproduct itself of the reaction and not a waste product. Notwithstanding, the low solubility of coke makes it a recalcitrant compound whose possibilities to be furtherly valorized are complicated.

Therefore, the delignification process should be designed in consonance with the undesirable product that would interest to produce in the lowest amount. Thus, if coke is designated as the less desirable product, and the focus is pointed out on maximizing the phenolic oil yield, it is found that the lignin samples from the organosolv process are more suitable to be depolymerized than the soda ones. On the other hand, the independence of the precipitation process was remarkable, with obtained coke yields very similar for the lignin samples that were precipitated with different methods, without observing a clear tendency that would help to determine the best conditions for this stage.

3.2.3. Products characterization

As first, the amount of the phenolic monomers obtained during the reaction, which were measured by GC-MS analysis by the methodology described in Appendix 3, are detailed in Table 3.2. All catechol and catechol derivatives (3-methylcatechol, 3-methoxycatechol, 4-methylcatechol, 4-ethylcatechol) were classified in the same group as well as cresols (*o*-*m*-, and *p*- cresol). All the product yields were represented with regard to the lignin fed to the reactor.

Table 3.2. Monomeric phenolic compounds measured in the oil fraction after the reaction.

Lignin Sample	Yield (% w/w)	Catechols (%)	Phenol (%)	Cresols (%)	Guaiacol (%)	Syringol (%)
AS pH=6	6.20 ± 0.49	5.80 ± 0.55	0.25 ± 0.05	0.13 ± 0.01	0.02 ± 0.01	-
AS pH=4	3.16 ± 0.74	2.85 ± 0.60	0.18 ± 0.06	0.11 ± 0.06	0.02 ± 0.01	-
AS pH=2	6.32 ± 2.22	5.97 ± 2.14	0.23 ± 0.05	0.11 ± 0.02	0.02 ± 0.01	-
AO 1 vol	6.44 ± 0.63	6.01 ± 0.45	0.25 ± 0.09	0.12 ± 0.04	0.04 ± 0.04	-
AO 2 vol	8.27 ± 0.62	7.78 ± 0.47	0.31 ± 0.09	0.15 ± 0.04	0.02 ± 0.01	-
AO 4 vol	6.62 ± 0.84	6.24 ± 0.73	0.24 ± 0.06	0.12 ± 0.04	0.01 ± 0.00	-
OS pH=6	3.11 ± 0.21	2.82 ± 0.17	0.16 ± 0.01	0.12 ± 0.03	0.01 ± 0.00	0.01 ± 0.00
OS pH=4	4.56 ± 0.38	4.22 ±0.34	0.19 ± 0.01	0.12 ± 0.01	0.02 ± 0.00	0.01 ± 0.00
OA pH=2	4.91 ± 0.06	4.59 ± 0.05	0.19 ± 0.01	0.12 ± 0.01	0.02 ± 0.00	-
OO 1 vol	3.84 ± 1.29	3.65 ± 1.16	0.11 ± 0.09	0.07 ± 0.04	0.01 ± 0.00	-
OO 2 vol	3.91 ± 0.39	3.61 ± 0.34	0.18 ± 0.02	0.11 ± 0.03	0.01 ± 0.00	-
OO 4 vol	6.41 ± 0.63	6.06 ± 0.65	0.22 ± 0.01	0.13 ± 0.02	0.02 ± 0.00	-

It was observed that, even if beforehand, the olive pruning lignin samples were more suitable for the depolymerization process than the almond lignin ones (higher percentage of β-O-4 linkages and higher S/G ratio), the best yields were obtained with the almond samples. On the other hand, the obtained yields for organosolv samples were in concordance with their lower M_w and their slightly higher density of ether linkages.

Regardless of the initial lignin sample used, the major components found in phenolic oil were catechol and its derivatives, followed by phenol and cresols (*o*-*m*-*p*-cresol) respectively. This fact reinforces the statement that the NaOH catalyzes, besides the depolymerization reactions, the hydrolysis of the ether bonds, which lead to syringol and guaiacol, demethoxylation, demethylation and dealkylation reactions. The mechanism of this reaction can be seen in Figure 3.5. In alkaline conditions, the hydroxyl groups in the phenolic ring react with NaOH to form a phenolate anion. After several electron migration steps, a phenolate side chain was eliminated by hydrolytic cleavage of an ether bond to form a quinone intermediate [255]. As a consequence, phenol, cresol or catechols are produced.

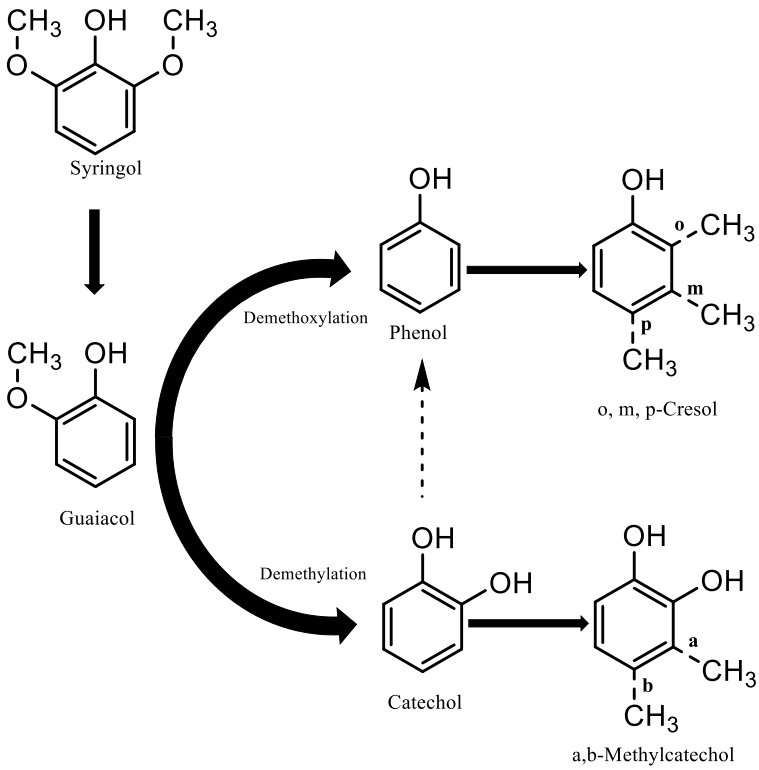

Figure 3.5. Schematic representation of the demethoxylation and demethylation reactions undergone in BCD [256].

Amongst the yields reached by each lignin samples used in the study, the almond shell lignin samples presented the highest yields, above 6% in all the cases, except for "AS pH 4". For olive tree pruning lignin samples, the total yield values were always lower than 6%, with the exception of "OO 4vol". Regarding the differences between the two lignin extraction processes, a perfect correlation was not found although organosolv lignin samples obtained the highest yields in both cases, in line with higher phenolic oil yields as well as the greater ether linkages percentage in lignin samples. Regarding, the precipitation method, it could not be found a clear tendency for the variation on the obtained yields neither. In general, despite the observed differences, the distribution of the obtained products was really similar for the 12 used samples because, which countersigned that the mechanism of BCD depolymerization followed the same patterns regardless the lignin source used.

The yields of the phenolic monomer compounds were slightly higher than the yields reported so far by the investigations accomplished by this group as it can be seen in Table 3.1. This fact was attributed to the used reaction conditions since they were selected from

an optimization survey [250]; the chosen biomass (almond shells presented better yields than olive tree pruning), as well as the inclusion of the pretreatment stage to maximize the purity of the lignin samples. Although the difference was narrow, these results reinforced the chosen strategy. The comparison of the obtained results with other works included in the literature that also used BCD for lignin depolymerization was somehow complicated, due to the different processes used, the different phenolic monomer measured, the concepts applied to differentiate products, etc. However, in some cases, where the reaction conditions were quite similar, the comparison can be established. For instance, Limarta et al. [257] presented a maximum total monomers yield of 6.1 wt.%, even using heterogeneous catalyst (Ru/C 10%+MgO/$ZrO_2$10%) during the reaction. Although many of the phenolic oil yields reported in the literature are higher than the ones presented in this work, the phenolic monomer yields were similar to the values obtained in this study, as it was the case of the work presented by Dabral et al. [258], who, despite achieving a phenolic oil yield higher than 50%, could not reach phenolic monomer yields above 5 wt.% using inorganic base catalyst, such as dimethyl carbonate (DMC). The use of organic solvents in BCD enables an increase in the monomer production, as it was demonstrated by Long et al. [259], who reached a total monomer yield of 13.2% using THF as lignin solvent with MgO as base catalyst. A phenolic monomer yield close to 25 wt.% was reached by Chaudhary and Dephe [260], using basic zeolites (NaX) in ethanol-water solvent. In general, the obtained values were located in the frame of the top values previously obtained by the BioRP group. Nevertheless, they were still below the best performances presented by other works that already used the BCD mechanism.

Regarding RL, in spite of its phenolic structure, its composition was different from the original lignin introduced to the reactor. Primarily, the molecular weight (M_w) and the polydispersity index (M_w/M_n) of these RL samples were analyzed by GPC analysis. The results are detailed in Table 3.3.

Table 3.3. Molecular weight distribution of the RL reaction.

Residual Lignin	M_w (g/mol)	M_w/M_n	Residual Lignin	M_w (g/mol)	M_w/M_n
RLAS pH=6	6253	7.14	RLOS pH=6	5103	6.89
RLAS pH=4	7892	7.54	RLOS pH=4	4844	6.64
RLAS pH=2	5031	6.07	RLOS pH=2	4819	6.85
RLAO 1 vol	7311	8.15	RLOO 1 vol	6804	8.71
RLAO 2 vol	7004	7.73	RLOO 2 vol	5910	7.44
RLAO 4 vol	6535	7.34	RLOO 4 vol	5281	7.03

The big differences in terms of M_w and M_w/M_n that was shown in Table 2.8, between soda lignin samples (with M_w above 15,000 and M_w/M_n above 10) and organosolv lignin samples (around 4000-6000 g/mol of M_w and M_w/M_n below 5); was totally reduced for RL, since very similar values for both M_w and M_w/M_n were obtained for the 12 studied samples.

This fact indicated that the mechanism of the undesirable repolymerization reaction through which RL was produced, was similar regardless of the type of lignin used as raw material. The alkaline conditions enabled the formation of phenolate carbanions from catechols and phenols mainly, which were not blocked by an extra capping or blocking agent. The consequence of undergoing the same mechanism for all reactions was that not big differences were found in the yields of RL and coke regardless the lignin sample used. The structure of this RL was also analyzed by FT-IR spectrums. In order to simplify the understanding of the analysis, only the spectra of the representative samples were represented in Figure 3.4. Indeed, there was no difference at all between the spectra of samples collected from the same raw material and delignification method, with the only difference in the isolation method.

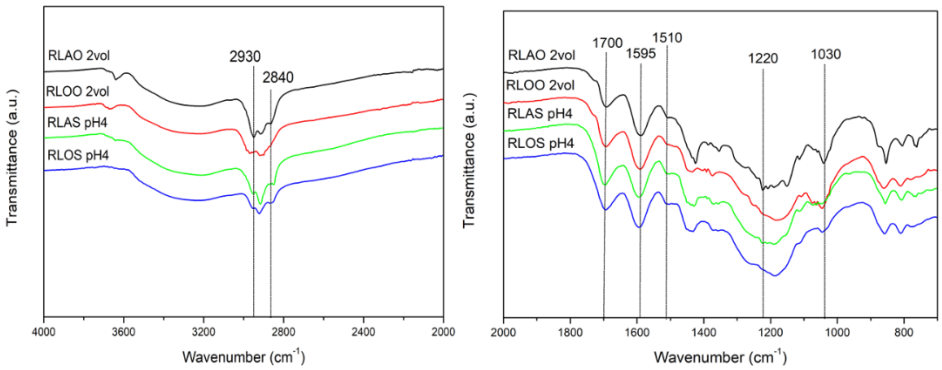

Figure 3.6. FT-IR spectra of RL.

The wide signal around 3400 cm^{-1} was very smooth for all RL. A new peak that was not detected in the lignin samples was detected at 1700 cm^{-1}. This band corresponds to the characteristic stretching frequency of the carbonyl group [128]. This could be related to the cleavage of β-O-4 ether bonds of the raw lignin during the depolymerization reactions that lead to unstable fragments that, in order to stabilize themselves, form a double bond between the carbon and the oxygen creating the carbonyl group in the RL. The peaks at 1510 cm^{-1} related to benzene structural lignin absorbance almost disappeared in the RL spectra, which suggested that RLs have lower aromatic nature than the initial lignin samples. In addition, the peak at 1220 cm^{-1} that was visible in the initial lignin samples, which is assigned to the ring breathing with C–O stretching of both the syringyl and guaiacyl structures [113]; was not visible in the RL samples. All this indicates that the so-called RL fractions have a lower quantity of syringyl and guaiacyl units which have reacted during the depolymerization reactions and have been transferred to the phenolic oil fraction. Hence, as the RL presented a different structure in comparison with the initial ones, it could be established that the conversion of all raw lignin samples was total.

3.3. Direct lignin depolymerization from black liquors (Publication III)

Another strategy to increase the lignin depolymerization yields was approached in this section. Besides all the works where solid lignin has been depolymerized by alkaline hydrolysis or employing only water and ethanol as a hydrolyzing agent, very few studies have been carried out using the liquors from the biomass delignification processes. In a previous work, developed by Erdocia et al. [261], an organosolv black liquor was submitted to a high temperature and pressure process after its conditioning, where most of the ethanol was removed. The major obtained compounds were syringol and guaiacol, but high quantity of char was undesirably produced. In another work, black liquors from alkaline

delignification of biomass employing NaOH and KOH were also treated at high temperatures in order to hydrolyze the lignin [253]. In this case, the black liquors were also concentrated, removing half of the water, prior to their treatment. In this case, the main compound obtained after the lignin hydrolysis was catechol and considerable amounts of phenol and cresols were also reported.

In this section, the black liquors were directly submitted to a hydrothermal treatment instead of precipitating lignin prior to its BCD depolymerization. In this sense, the removal of some stages of the global processes formerly presented was addressed in order to simplify and reduce the cost of the process.

3.3.1. Experimental approach

Two reaction mechanisms were approached: (i) BCD mechanism was used in the case of soda black liquor, and (ii) solvolysis for organosolv black liquors. Both treatments were applied to almond shell and olive tree pruning liquors with the aim of obtaining relevant information about the influence of the raw material. The reaction conditions were 300 ºC and 80 min with constant stirring and reaching pressure values of 90 bar, in the case of soda liquors and 110 bar, in the case of organosolv liquors. These are the same conditions used for depolymerizing solid lignin samples and were selected in order to allow the comparison of the obtained results by the two paths. The quantity of liquor introduced in each case was 20 g.

The applied downstream separation processes were similar to the ones described before for soda liquors. Nevertheless, in the case of organosolv liquors, after the cooling down, the tar (RL + char) separation from the liquid phase was carried out by adding 2 volumes of acidified water (pH = 2). The rest of the process was exactly the same as it was reported in Section 3.2.1.

3.3.2. Characterization of the black liquors

As a first step, the black liquors were physico-chemically characterized to determine the initial conditions of the material subjected to the depolymerization reactions. In Table 3.4, the most important parameters of those liquors are detailed.

Table 3.4. Physico-chemical characterization of black liquors (AOL: Almond Organosolv Liquor; ASL: Almond Soda Liquor; OOL: Olive Organosolv Liquor; OSL: Olive Soda Liquor).

Parameter	AOL	ASL	OOL	OSL
Density (%)	0.85 ± 0.01	1.07 ± 0.00	0.86 ± 0.00	1.08 ± 0.01
pH	4.11 ± 0.01	13.89 ± 0.02	4.02 ± 0.03	13.77 ± 0.02
Dry content (%)	4.90 ± 0.06	14.99 ± 0.07	5.06 ± 0.11	15.29 ± 0.08
Organic matter (%)	4.86 ± 0.06	5.39 ± 0.07	5.01 ± 0.11	5.67 ± 0.05
Inorganic matter (%)	0.04 ± 0.00	9.60 ± 0.01	0.04 ± 0.01	9.61 ± 0.04
Lignin content (%)	4.7	4.57	4.79	4.73

As it was expected, the soda liquors presented much higher inorganic matter than the organosolv liquors. This high percentage was due to the moderate quantity of sodium hydroxide introduced in the soda process while, in the organosolv process, any inorganic compound was used as a reagent. The organic matter was also higher in the case of the soda processes. This fact was associated with the higher potential of the soda process to increase the yield of the delignification stage because, besides lignin, it also solubilizes hemicelluloses as well as some parts of the cellulose. On the contrary, the organosolv process is more selective to dissolve mostly lignin. The other parameters of the black liquors were inherent to the biomass used as feedstock. The density was higher in the soda liquors as it was a mixture of water and sodium hydroxide while the organosolv black liquors had lower density as they were a mixture of water and ethanol. The measured pH was close to 14 in the case of soda black liquors because of the sodium hydroxide dissolved in the medium, and around 4 for organosolv black liquors. The acid character of these liquors was principally associated with the acetic and formic acids formed in the delignification process from the degradation of the hemicellulosic compounds.

Regarding the lignin content, the obtained values were very similar in all the characterized liquors. The delignification treatment and the raw material did not have a huge influence on the lignin concentration in the final liquor. However, the total amount of the obtained black liquor was higher for the soda processes (around 30% more liquor obtained) than in the organosolv delignification. This fact led to higher lignin extraction yields for the soda process despite the concentration was lower in the liquor. The reason for this higher extraction yield could be based on the different severity factors applied during the delignification stage process, which not only depends on the time and temperature under which the feedstock was submitted during the reaction, but also the pH the reaction took place at [262].

In spite of the lower temperature at which the soda process was accomplished, its alkaline conditions created a more severe medium that explains the greater lignin extraction yield as well as the higher M_w of the obtained lignin samples as it was already demonstrated by other works [263]. However, the organosolv process was carried out at a higher temperature, which reduced the difference to obtain similar concentrations of lignin in the black liquors. In the case of soda liquors, around 84% of the total organic content was lignin whereas in the case of organosolv liquors this amount rose up to 95%.

3.3.2. Liquor depolymerization yields

The yields of the three main products (phenolic oil, RL and coke) are shown in Figure 3.7. These yields were calculated using the percentage of organic matter contained in the black liquors as the basis since some of the products obtained after the reaction could also come from that organic compounds that were contained in the liquor but not precipitated as lignin.

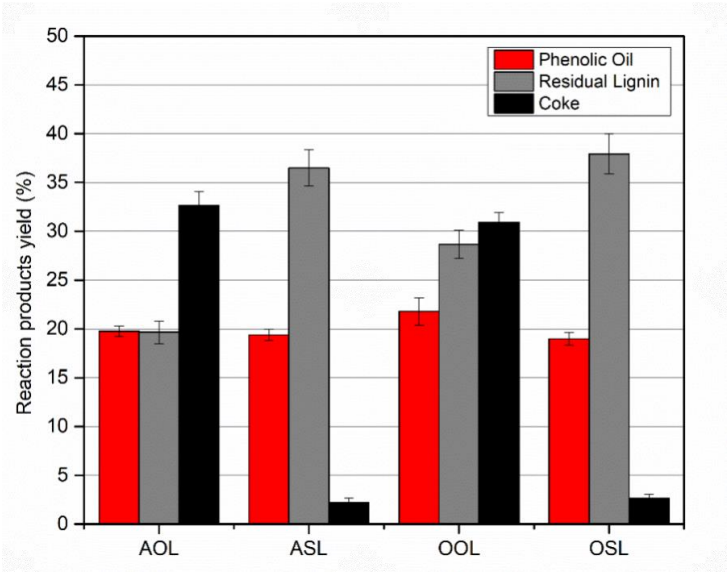

Figure 3.7. Yield of the products recovered after thermally lignin depolymerization from black liquors.

It can be observed that the yield of the phenolic oil was around 20% in all the cases. The minimum value was obtained for OSL with 18.98%, while the maximum was produced with OOL, with a yield of 21.78%. In general, the differences regarding the obtained phenolic oil yields could be considered negligible. Thus, regardless of the feedstock and the selected reaction mechanism (BCD or solvolysis), the undesirable repolymerization reactions limited the phenolic oil yields to similar values. These values were really close to those obtained when solid lignin was depolymerized in alkaline solutions under similar

operation conditions [109,240,264]. Nevertheless, it has to be highlighted that these yields were referred to the total organic content, which includes not only the lignin but also other components originated from the hemicelluloses and the cellulose platform. Therefore, it could be said that the obtained reaction yields were even higher than the ones obtained from precipitated lignin if we could have separated the exact amount of lignin at the initial black liquors, which was impossible to be achieved with accuracy. As it was pointed out before, the lignin content was almost the same in the different liquors and the treatments of these liquors led to a similar quantity of phenolic oil, remarking the independency of the raw material and the reaction mechanism when the reactions conditions are harsh.

However, a huge influence of the employed solvent was observed on the rest of the yields for RL and coke. Regarding the RL, in which the soda liquor was used, the generation of this byproduct was significantly higher than in the case of the organosolv process (from 36.5-37.9% for soda samples to 19.7-28.8% for organosolv ones), whereas the coke production performed the other way around, with higher percentages for organosolv samples (around 30-35%). On the contrary, soda samples presented a small production of char (lower than 3.0%). These results were found to be in the opposite trend than the ones obtained with the solid lignin depolymerization, where more RL and lower coke were generated from lignin obtained by the organosolv delignification method.

This behavior could be explained due to the activity of the NaOH, which could act also as a catalyst, inhibiting the formation of coke [111]. The OH^- ions of the sodium hydroxide neutralize the molecules which cause the polymerization for char formation as, for example, the carboxylic acids, which are prone to react with hydroxyl groups to form ester bonds, which are responsible for the formation of coke [265]. The lower yield was followed by an increase in the formation of RL, which leads to the conclusion that the RL was created by the polymerization reaction, and the formation of coke is one step forward in such reaction, where highly condensed structures are created, which are not possible to be solubilized even in organic solvents, such as THF. Therefore, because of the lack of these OH^- ions presented in the organosolv delignification, the depolymerization from black liquors suffered an increase in the coke formation.

3.3.2.1. Reaction streams characterizations.

According to the characterization of the products, the obtained phenolic oil was composed of a wide range of products due to the heterogeneity of lignin, even if the complete depolymerization of lignin to phenolic monomeric structures was not reached. The monomers were characterized by GC-MS and the obtained values are collected in Table 3.5.

Table 3.5. Phenolic monomer compounds analyzed by GC-MS spectra.

Compound (%)	AOL	ASL	OOL	OSL
Phenol	0.28 ± 0.02	0.66 ± 0.07	0.33 ± 0.02	1.01 ± 0.13
Cresols	0.15 ± 0.02	0.30 ± 0.01	0.27 ± 0.08	0.42 ± 0.00
Guaiacol	5.44 ± 0.34	0.03 ± 0.00	3.90 ± 0.34	0.05 ± 0.01
Catechol	0.77 ± 0.06	1.63 ± 0.13	0.45 ± 0.05	1.50 ± 0.02
3-methylcatechol	0.11 ± 0.00	0.90 ± 0.03	---	0.91 ± 0.02
3-methoxycatechol	2.64 ± 0.24	---	2.10 ± 0.25	---
4-methylcatechol	0.16 ± 0.02	1.85 ± 0.02	---	1.81 ± 0.11
Syringol	11.30 ± 0.56	----	10.25 ± 0.23	----
4-ethylcatechol	0.14 ± 0.00	0.89 ± 0.08	---	0.97 ± 0.05
Acetovanillone	0.32 ± 0.08	----	0.09 ± 0.03	---
Guaiacylacetone	0.73 ± 0.16	----	0.32 ± 0.04	----
Acetosyringone	0.19 ± 0.03	---	0.13 ± 0.04	----
Monomers concentration (%)	22.23 ± 0.9	6.26 ± 0.4	17.51 ± 1.10	6.67 ± 0.30

There was an appreciable difference between the compounds in the oil from the soda liquors and the organosolv liquors. In the organosolv liquors, the main obtained compounds were guaiacol and syringol, while these two compounds almost did not appear in the oil from the soda liquors. Therefore, the role of NaOH as catalyst to release not only the lignin cleavage, but also the demethoxylation, demethylation, and dealkylation reactions were proven.

On the other hand, in the case of organosolv black liquors, the β-O-4 ether bonds of the lignin were broken down due to the solvolysis of the reaction mixture (water/ethanol), where the hydrogen-donating medium created a lower oxidant medium that did not lead to demethoxylation, demethylation and dealkylation reactions, as in the case of the extreme alkaline medium. The cleavages of these bonds, which are the major bonds in the lignin macromolecule, led to the formation of syringol and guaiacol but did not go on to form other monomeric phenols. Indeed, all the monomers identified in noticeable amounts in the case of soda black liquors, have no methoxy groups in their molecular structures, whereas in the case of organosolv black liquors, besides guaiacol (1 methoxy group) and syringol (2 methoxy groups), high quantity of 3-methoxycatechol was recovered, and, as consequence, some catechols were quantified. In addition, acetovanillone,

guaiacylacetone, and acetosyringone, all of which have a methoxy group, did not appear in the soda black liquor, whereas they were measured in the organosolv liquors.

Comparing the concentration of the phenolic monomers in the organic oil, big differences were observed between the organosolv and the soda methods. The former presented a higher purity of this oil in terms of phenolic monomers compounds, as it was intended (around 20% for both feedstocks). On the contrary, barely 6-7% of the oil was formed by monomers using soda liquors. Therefore, the use of soda as solvent allowed the achievement of complete reactions of demethoxylation, demethylation, and dealkylation, but the total yield of monomers was found to be around three times lower than in the organosolv black liquors. It is thought that the presence of ethanol as hydrogen-donor agent stabilize the primary unstable products, such as the phenolic hydroxyl intermediates, which are prone to repolymerize to form bigger structures limiting the maximum yield of monomers that can be reached [114].

To facilitate the comparison of the phenolic monomer yields obtained by the direct depolymerization of lignin contained in the black liquors and the yields reached when precipitated lignin was submitted to the depolymerization reaction (Table 3.2), the results of the phenolic monomeric yields are presented in Table 3.6, related to the initial lignin contained in their respective liquors (Table 3.4). The phenolic monomer composition was expressed by monomer groups in the same way it was reported in Table 3.2.

Table 3.6. Phenolic monomer yields of the different samples subjected to the depolymerization reaction (Catechols: catechol, 3-methylcatechol, 3-methoxycatechol, 4-methylcatechol, and 4-ethylcatechol. Cresols: o-, p-, and m-cresol. Guaiacols: guaiacol, vanillin, acetovanillone, and 4-hidroxy-3-methoxy-phenylacetone. Syringols: syringol, syringaldehyde, and acetosyringone).

Black Liquor	Yield (% w/w)	Catechols (%)	Phenol (%)	Cresols (%)	Guaiacols (%)	Syringols (%)
AOL	4.57 ± 0.05	0.78 ± 0.05	0.06 ± 0.01	0.03 ± 0.01	1.35 ± 0.05	2.36 ± 0.06
ASL	1.44 ± 0.04	1.20 ± 0.01	0.15 ± 0.01	0.07 ± 0.01	0.01 ± 0.01	0.01 ± 0.01
OOL	4.01 ± 0.10	0.57 ± 0.06	0.08 ± 0.01	0.06 ± 0.02	0.97 ± 0.06	2.37 ± 0.08
OSL	1.52 ± 0.01	1.18 ± 0.01	0.23 ± 0.03	0.10 ± 0.02	0.01 ± 0.02	n.d.

In comparison with depolymerization from lignin precipitated samples, the obtained monomer yields were lower in most cases. Indeed, the best result obtained for isolated lignin samples (AO2vol) was almost double (8.27%) than the best results obtained with direct lignin depolymerization (AOL with 4.57%). In this sense, it could be concluded that the simplification of the whole process by the removal of the isolation stage for lignin precipitation drove to obtain poorer results in terms of phenolic monomer, which it was likely hindered by the co-existence of other compounds in the liquor, such as carbohydrates and acids mostly.

Finally, the RL samples isolated from liquors were also characterized by means of their molecular size and polydispersity as it is shown in Table 3.7.

Table 3.7. Residual Lignin (RL) analysis based on their molecular size (M_w) and polydispersity (M_w/M_n).

Residual Lignin	M_w (g/mol)	M_w/M_n
RL AOL	2433	4.50
RL ASL	2177	4.77
RL OOL	3426	4.27
RL OSL	2465	4.84

At first glimpse, the high similitude among all the RL samples collected after the reactions could be observed. Neither the raw material nor the reaction mechanism made big differences in the repolymerization reaction, as it was suggested before. Therefore, the unique difference in terms of the lignin undesirable repolymerization reactions, was the degradation level of this repolymerized lignin or RL, which, in the case of the organosolv black liquors underwent a further degradation to generate coke. In the case of soda liquors, the action of NaOH was thought to prevent this degradation to a highly condensed structure, such as coke. All the values for Mw were really low, and lower than both the Mw of the initial lignin samples, as well as the residual lignin obtained after depolymerization reaction using solid lignin samples. However, their M_w/M_n was higher than the initial organosolv lignin samples values, despite their smaller size, which leads to conclude that RL streams were composed by several fractions of different size, forming a heterogeneous compound. In comparison with RL from isolated lignin samples, both values were smaller (M_w and M_w/M_n).

The difference between the streams involved in the reaction, with the exception of coke, whose collected amount was insufficient to perform the analysis, was also shown by the spectra curves collected by the GPC technique. A quantitative analysis of the phenolic oils was not possible to be conducted since their fractions were completely at the extrapolation region of the calibration curve. Nevertheless, the qualitative differentiation by GPC spectra was significant enough. Hence, in Figure 3.8 all the spectrum curves collected from the GPC analysis of almond samples are presented, which were selected as reference to facilitate the visual interpretation.

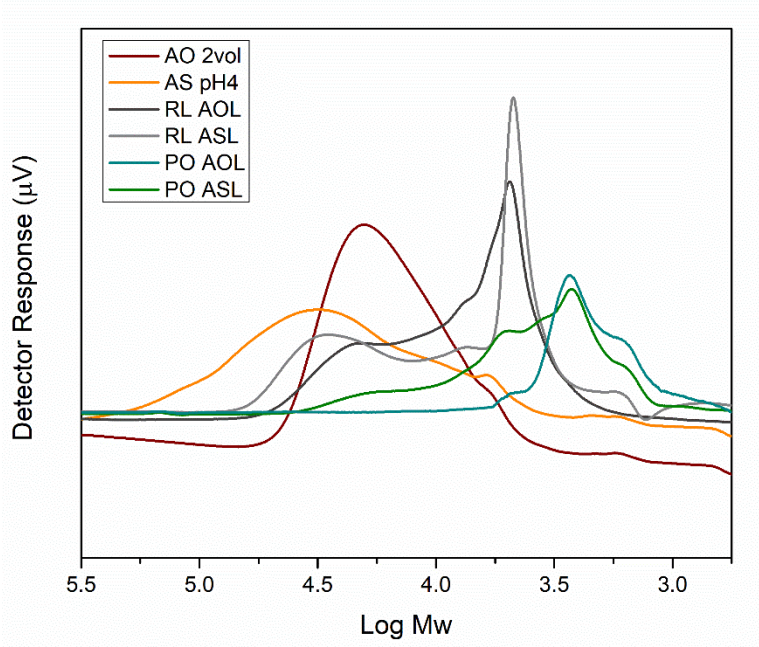

Figure 3.8. Spectrum curves of the GPC analysis (AO2vol: Almond Organosolv lignin precipitated with 2vol; ASpH4: Almond Soda lignin precipitated at pH 4; RL AOL: Residual Lignin from Almond Organosolv Liquor depolymerization; RL ASL: Residual Lignin from Almond Soda Liquor depolymerization; PO AOL: Phenolic Oil from Almond Organosolv Liquor depolymerization; and PO ASL: Phenolic Oil from Almond Soda Liquor depolymerization).

Different shapes and peak locations between samples can be observed. ASpH4 was the sample whose main peak was most displaced to the biggest M_w sizes. This peak was found to be really wide, remarking both the big average size of the sample as well as its high polydispersity, as it was reported in Table 2.8. AO2vol showed a narrower peak in comparison with other samples, with a polydispersity of 3.03. The spectra of the RL were very similar among them, with two main peaks that led to a higher polydispersity than the organosolv sample one. This similarity between curves highlighted that this component was obtained by the same mechanism during the reaction, despite the used initial lignin and solvent. The shape of the two peaks of the curve indicated that not all the fraction of the repolymerized lignin was able to reach such a big structure. Finally, the peaks of the curves corresponding to the phenolic oils were located in the lowest M_w section. Additionally, the difference among the phenolic oils was also noticeable, since the phenolic oil from the organosolv lignin presented a displaced curve to the lowest M_w area, which is in consonance with the higher percentage of monomeric compounds measured by GC-MS for such phenolic oil.

3.4. Lignin depolymerization from industrial liquor: towards maximizing depolymerization yields (Publication IV)

The different scenarios approached to obtain small phenolic compounds from lignin, either if the depolymerization reaction was accomplished using solid lignin or directly from black liquors, have experimented also negative aspects in form of repolymerization reaction, whose existence limited the phenolic monomer yields and created more recalcitrant byproducts, such as RL and coke.

The undesirable repolymerization reaction mechanism under alkaline conditions was also explained in section 3.2.1, where it was mentioned that the instability of some intermediate products leads to undergo these undesirable reactions. Several approaches have been proposed to minimize this phenomenon. Among them, the use of phenol to reduce the cross-linking reaction to form high molecular weight compounds and to avoid lignin repolymerization has been demonstrated by other experimental works [127,266]. On the other hand, as it was advanced in Chapter 1, the oxidative depolymerization of lignin can increase the lignin depolymerization yields, although non-phenolic structures could be obtained because, under severe conditions, the aromatic ring of lignin can be broken down to form carboxylic acids.

In this section, two strategies were tested to maximize the lignin depolymerization yields through the formation of phenolic oil: (i) increase the oxidative environment of the reaction by the addition of an oxidant agent, and (ii) using a capping agent that could avoid lignin repolymerization by stabilizing the reaction intermediates that are prone to undergo such reactions.

The depolymerization reaction is structured in the same way as the previous section, i. e., using the direct depolymerization approach from lignin contained in the black liquors. As liquor, instead of using streams collected after laboratory scale, industrial Kraft black liquor was utilized to check the current possibilities of an existing stream.

3.4.1. Experimental procedure

The reactions were accomplished at 300 ºC for 80 min following the same conditions of previous sections, reaching a pressure inside the reactor of 90 bar. Industrial Kraft black liquor from eucalyptus species was used as raw material.

Different catalytic agents (a capping and an oxidant) were used to increase the yield of phenolic products and to reduce the coke formation. Phenol and hydrogen peroxide were used for this purpose in a homogeneous phase reaction with a lignin/facilitating agent ratio

of 1:0.5 (wt.%). These selected ratios were in accordance with similar works consulted in literature [127,267]. After the reaction, the downstream processes were conducted following the same procedure described in the previous section for the soda black liquors.

3.4.2. Characterization of Kraft black liquor

As a first step, a characterization of the Kraft black liquor supplied directly from the mill was performed mainly to establish the concentration of lignin. The obtained values are presented in Table 3.8.

Table 3.8. Physico-chemical characterization of Kraft black liquor (KBL).

Parameter	KBL
Density (g/cm3)	1.39 ± 0.84
pH	12.9 ± 0.12
Dry content (%)	14.0 ± 0.46
Inorganic matter (%)	10.2 ± 0.06
Organic matter (%)	5.6 ± 1.89
Lignin content (g/L)	67.4 ± 5.21

Density and pH correspond with the typical values of KBL [268]. The content in organic matter was remarkably lower than in inorganic matter due to the composition of the white liquor used for the Kraft cooking, a mixture of NaOH and Na_2S. However, the lignin content represented more than 85% of this organic matter, highlighting the potential of this stream to be valorized by transforming lignin in value-added bio-products.

The lignin content and the subsequent characterization of Kraft lignin (KL) contained in the black liquor was carried out after the isolation of that lignin by its precipitation using H_2SO_4 to acidify the liquor until pH = 2. The isolated KL was analyzed by several techniques. The molecular weight (M_w) and the molecular weight distribution (M_w/M_n) were calculated by GPC analysis, whereas S/G ratio and linkage distribution values were taken from a previous work carried out in the in BioRP research group by Gordobil et al. [269] using Py-GC-MS and 2D-HSQC techniques respectively; following the same experimental procedure that was used in Section 2.5.3. The characterization values are detailed in Table 3.9.

Table 3.9. Physico-chemical characterization of Kraft lignin (KL).

Sample	M_w (g/mol)	M_w/M_n	S/G ratio	β-O-4 (%)	β-β´ (%)	β-5' (%)
KL	2418 ± 461	3.21 ± 0.32	3.8	29.7	49.4	20.9

The obtained M_w and M_w/M_n values for this KL were low in comparison with the ones of lignin obtained by other pulping methods [222]. This fact could be a positive aspect to facilitate its conversion into high depolymerization yields. A great value of S/G ratio was detected for KL from eucalyptus species, whereas the percentage of β-O-4 linkages was really low for this sample, in comparison with previously analyzed samples, with around half of this value. KL usually showed lower amount of ether linkages than lignin obtained by other processes, due to the harsh alkaline conditions the Kraft process is accomplished, which induce a severe lignin degradation and the appearance of repolymerization reactions [51].

3.4.3. Kraft black liquor depolymerization

The depolymerization reaction product yields are detailed in Table 3.10. The yields were referred to the organic matter contained in the liquor. Firstly, a blank reaction without any additive was conducted as a reference point to identify the action of the capping agent. Then, the same reaction was performed using phenol as capping agent and hydrogen peroxide as oxidant compound. The initial phenol amount was discarded to make the calculations of phenolic oil yield when phenol was used as a capping agent since this compound was also collected in the phenolic oil stream.

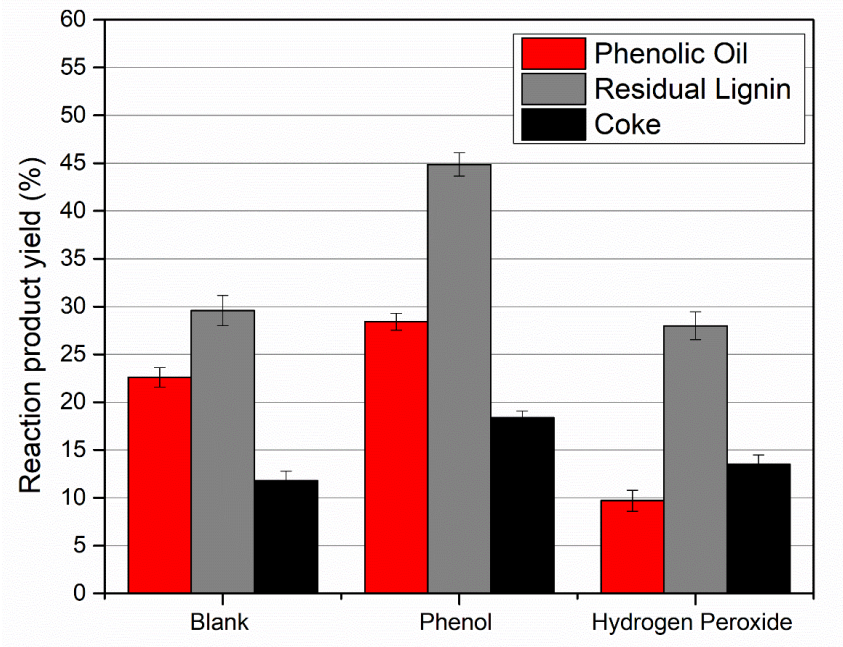

Figure 3.9. Reaction product yields of the different tested scenarios.

The blank depolymerization reaction already showed a high phenolic oil production (22.6%), remarking the harsh conditions at which the reaction was carried out. Unlike the theoretical statements from the literature [130] about the direct relationship between the β-O-4 linkages content and the phenolic oil yield. In this case, for the blank reaction, the obtained oil value was extraordinarily high for lignin with such a low percentage of ether linkages. The explanation could be based on the low M_w and M_w/M_n that the KL showed, although it is thought that the density of ether bonds is more influential on the final depolymerization yield. Other explanation could come from the medium in which the reaction was developed. The alkaline conditions were slightly softer than the ones of the soda liquor used in Section 3.3. However, the presence of HS^- ions in the black liquor, which play an important role during the biomass delignification, could enhance the depolymerization process as well. The HS^- ion can be subsequently added to the quinone methide intermediate and, as a strong nucleophile, may initiate the cleavage of an aryl-ether bound to a neighboring β-C atom. Apart from the cleavage of aryl-ether bonds, carbon-carbon bonds are also cleaved to some extent, although this depolymerization reaction competes with condensation reactions caused by internal nucleophiles, especially in the final phase of the reaction, which leads to undesirable repolymerizations [270]. Therefore, even if a BCD mechanism was proposed in this section, the different chemical agents involved in the reaction played an important role to balance the adverse initial

conditions of the KL compared to the organosolv lignin samples used in the previous section.

The importance of these competing reactions can be noticed in the undesirable product yields, residual lignin and coke, which were also high. The yield of the RL was 29.6%, whereas the coke presented a value of 11.8%. This last one presented a much higher yield than the obtained from the soda liquors. Therefore, the search of capping agents to minimize these products was totally justified.

The introduction of phenol as a capping agent led to higher phenolic oil generation (28.4%), which entails an increase of 25%. However, the residual lignin quantity was also increased to almost 45%, which involved an increment of around 60%. In the same line, coke generation was incremented in more than 50%. Therefore, the phenol not only acted as a catalytic agent to maximize the phenolic oil yield, but also favored the undesirable products as well. On the other hand, the hydrogen peroxide presented a big reduction in the phenolic oil (bigger than 50%), which was considered a serious negative effect, since the target of the reaction was maximizing this stream. The reason for this decrease was due to the strong oxidative strength of the hydrogen peroxide, which broke the aromatic rings from the initial lignin as well as from the small phenolic compounds that were transformed into alkylic acids. These acids could not be quantified by the used procedure since they would be wasted in the aqueous phase that remains after the liquid-liquid extraction of the phenolic oil. Regarding the RL, the addition of hydrogen peroxide did not influence at all, presenting similar values than the ones of the blank reactions, as well as in case of the coke generation. Therefore, the best performance was obtained by using phenol as capping agent.

Besides the performance of the reaction in terms of product yields, the chemical composition of the phenolic oil was quantified, following the same methodology as in previous sections. The analyzed compounds gathered by their representative group are detailed in Table 3.9. Yields were referred to the initial lignin submitted to the reactions, considering the lignin content measured in the liquor, as it was described in Table 3.7.

Table 3.10. Phenolic monomer yields for the different tested reactions.

Reaction Type	Yield (%)	Catechols (%)	Phenol (%)	Cresols (%)	Guaiacol (%)	Syringol (%)
Blank	1.77±0.12	1.63±0.05	0.05±0.03	0.05±0.01	0.01±0.01	0.01±0.01
Phenol	8.98±0.17	0.81±0.11	5.89±0.21	1.09±0.01	-	-
Hydrogen Peroxide	1.20±0.21	1.18±0.01	0.01±0.01	0.01±0.01	-	-

The phenolic monomer yields for the blank reaction were low in comparison with the results already presented by the solid BCD depolymerization reactions, as it can be seen in Table 3.2. Although this yield was very similar to the one obtained by the direct depolymerization of the soda black liquor (Table 3.6), or even slightly higher, which could be justified by the action of HS^- ions involved in the direct depolymerization of the Kraft black liquor. The distribution of the obtained products was very similar to those obtained from ASL and OSL liquors, with catechol derivatives as the main compounds, countersigning the similar mechanism reaction in both processes. However, the phenolic monomer yield when phenol was added as a capping agent was really high. Indeed, the highest value obtained in this chapter so far. Despite the initial quantity of phenol was discarded to make the calculations of the total yield, it was clear that the main compound in this oil was phenol. However, it can be seen that more cresols than catechol derivatives were obtained, which leads to conclude that phenol was enabling the lignin depolymerization into small phenolic compounds but also preventing the demethoxylation reactions that convert cresols into catechol compounds. In the case of hydrogen peroxide, the same tendency as in the blank reaction was found, with the obtaining of even lower total phenolic monomer yields. Catechol was almost the unique product of the reaction as well, which can be explained as the hydrogen peroxide provokes an excess of hydroxyl groups during the reaction, facilitating the pathway to form catechol derivatives.

3.5. General conclusions of lignin depolymerization reactions

In this chapter, different strategies have been proposed to obtain small phenolic compounds from lignin. At first, the isolated lignin already characterized in Chapter 2, was depolymerized by BCD. Although it was difficult to establish connections between the results and the lignin characteristics, it was found that the lignin molecular weight and the percentage of ether linkages were the only parameters that could have a clear influence on the final results.

From the liquors obtained after the delignification stage, a direct depolymerization of the lignin was approached before its isolation by the precipitation stage. The obtained phenolic

oil yields were similar to the best results obtained from isolated lignin samples. Furthermore, similar results were obtained regardless of the two different mechanisms that were addressed: BCD for the soda liquors, and solvolysis for the organosolv liquors. However, the phenolic monomer yields were lower, mostly for soda liquors, with similar values for organosolv liquors than in the case of depolymerization from solid samples. Moreover, the solvolysis mechanism generated a different distribution on the monomers found in the phenolic oil, with syringol and guaiacol units as main products instead of catechol derivatives, as in the case of the rest of BCD reactions.

Finally, several approaches focused to maximize the phenolic monomer compounds content were investigated using industrial Kraft black liquor as a lignin source. In general, the poorer characteristics of the Kraft lignin were balanced by the possible action of HS- ions that catalyzed the lignin depolymerization. In this way, the blank reaction showed similar values than the ones obtained with soda liquors. However, the inclusion of phenols presented promising results, since the phenolic oil, as well as the phenolic monomer yields were enhanced with the best results obtained in this work so far. The drawback of using phenol was the generation of bigger amounts of undesirable products. On the other hand, the hydrogen peroxide reduced the phenolic oil yield of the reaction. The extremely harsh conditions of the reaction led to the breakup of the aromatic structures of lignin, which it was not pursued in this work. Hence, the use of this compound is recommended under softer reaction conditions in terms of time and temperature.

IV) Techno-economic assessment

4.1. Motivation and scope

The lignin-based products must be competitive with their petroleum-derived counterparts. At this point, it is very important to design energetically efficient processes for the lignin extraction and purification stages. Otherwise, it would be difficult to offer a feasible alternative to the current consolidated products that are obtained from fossil resources. For this purpose, the obtaining of lignin-based products has to be approached as a section of the integrated biorefineries, where multiple products could be obtained. In this line, the economic competition in existing markets could be faced. This also brings the necessity to implement advanced synthesis methods that allow the integration and optimization of whole processes to guarantee the economic feasibility with lower environmental impact. Based on that, the techno-economic evaluation of the global process should involve both the identification of primary cost drivers as well as the feasibility to scale the designed processes to industrial level.

In this sense, after the qualitative and quantitative evaluation of the obtained laboratory experimental results accomplished in Chapter 3, deeper analyses were conducted to determine the scalability of the designed processes in the experimental sections. A commercial simulation software was used to compare the different approached scenarios to obtain small phenolic compounds. As it will be depicted below, the modeling of industrial processes by simulation software is a very useful tool to validate the economic feasibility of new scenarios without the necessity to build up the physical process.

Therefore, the scaling of lignin-based chemicals was addressed in this chapter from laboratory experiments to industrial scale by means of a virtual simulator. Specifically, the whole process of lignin extraction from a lignocellulosic stream (almond shell was the biomass selected for this study) to its final conversion into phenolic monomer compounds was compared in terms of mass balances, energetic duties, and economic costs. Several scenarios were tested to identify the most suitable route to maximize the quality and efficiency of the whole process.

4.2. Biorefinery simulation design (Publication V)

The design of chemical processes, as well as the integration and optimization of the units by advanced simulators allow the assessment of many parameters and scenarios to enhance the final product yield, quality, manufacturing cost or environmental impact, without the necessity to accomplish real tests.

Aspen Plus® software was used in this chapter, since it is the market-leading software in the optimization of chemical processes, mostly used in the bulk, fine, specialty and

biochemical industries, as well as the polymers industry for the design, operation, and optimization of safe and profitable manufacturing facilities. It is a sequential simulator, in which each unit (block) has implemented several equations. It uses simple blocks, easy to calculate, but also complex units, such as distillation, gas adsorption, etc [271].

This software has been also applied to design biomass processes, mainly in the pulp and paper industry, although it has emerged as a useful tool for the simulation of biorefinery processes too [272]. The application of this software in processes in which lignocellulosic biomass is the raw material, has the difficulty of the heterogeneity of these sources and the lack of components data bases where the components present in the biomass composition are defined with precision. In this study, the data were defined by the chemical properties of wood components, such as cellulose, lignin or hemicelluloses, which were described by the National Renewable Energy Laboratory (NREL), who created a database with the main physico-chemical parameters of these type of compounds [273].

Several works can be found in the literature about the simulation of biorefinery processes by Aspen Plus® software for the design of the manufacturing processes to obtain value-added chemicals from lignocellulosic resources. Moncada et al. [274] evaluated the production of C6 sugars from softwood and corn feedstocks, approaching two techniques: organosolv of spruce and corn wet mill. Nhien et al. [275] proposed a hybrid extraction/distillation process to produce furfural. The simulation process allowed evaluating different solvents to find the most suitable alternatives. However, only a few of them considered the whole integrated biorefinery approach. Celebi et al. [276] developed a systematic methodology to design an integrated biorefinery that utilized wood as feedstock to obtain C5 and C6 carbohydrates, lignin and syngas platforms. Nitzsche et al. [277] assessed the conversion of beech wood into different chemical products (ethylene, organosolv lignin, biomethane and hydrolysis lignin) by simulating the process. In a previous work of this research group, a deep analysis of energetic and economic analysis was already proposed from an experimental work, which consisted in the production of catechol from the olive tree pruning wastes [278]. In this section, an integrated multiproduct biorefinery approach was evaluated from the experimental processes designed at laboratory scale in the previous chapters to check the environmental and economic feasibility to implement these processes to an industrial scale.

4.3. Simulation process modeling

The experimental data presented in Chapter 3 were used in this section to evaluate the influence of the delignification method on the lignin depolymerization products as well as the effect of removing the precipitation stage of the lignin before its depolymerization. Only experimental values from one lignocellulosic raw material were selected in this section to

carry out the simulation process in order to simplify the evaluation. Almond shells were selected as raw material due to their higher lignin extraction yields obtained in the experimental section in comparison with other tested streams. The simulated scenarios were divided by the different employed delignification methods: (i) organosolv and (ii) soda; and two routes to depolymerize lignin: (i) from precipitated lignin and (ii) directly from the black liquors. In total, four different simulations were conducted, from which the obtained mass and energy balances were compared to identify the most interesting route. Both analyses were completed with an economic evaluation.

4.3.1. Flowsheet description

The process description was drawn up following the experimental approach from sections 3.2 and 3.3. The processes began with an autohydrolysis pre-treatment to increase the lignin concentration of the almond shell stream prior to the delignification stage. After this unit, the solid material was cleaned and driven to the delignification stage, where the organosolv and the soda processes were compared in terms of lignin obtaining. The generated black liquors were driven to either a precipitation stage or to the direct lignin depolymerization reaction. Both precipitated lignin and black liquors were subjected to a depolymerization reaction to obtain small phenolic compounds.

The undesirable byproduct of this reaction, the tar, which contains the RL and the coke fractions, was removed by acid precipitation and the phenolic oil was extracted by a liquid-liquid extraction using ethyl acetate as organic solvent. Finally, the solvent was recovered by distillation and further distillation stages were also designed to fractionate the phenolic monomer compounds from the rest of the phenolic oil. The whole process is depicted in Figure 4.1.

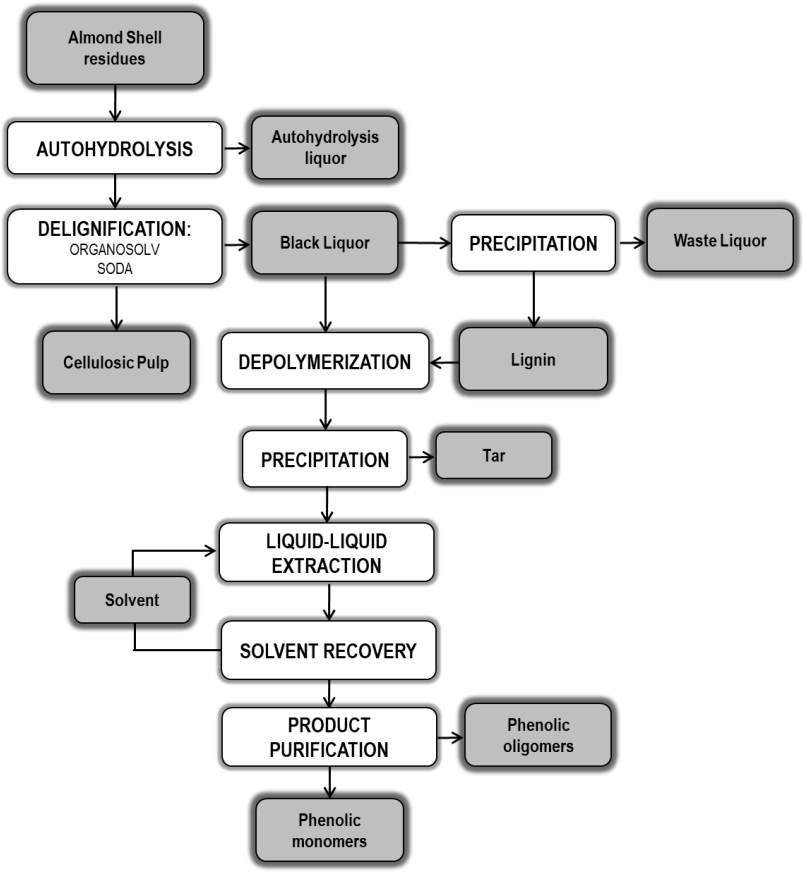

Figure 4.1. Description of the lignin extraction and conversion process to produce small phenolic compounds.

4.3.2. Modeling design

Based on the processes described above, the simulation was built up by Aspen Plus® (V10) software. The flowsheets were divided into two sections. Section 1 (S1) was composed of the initial stages to obtain and isolate lignin as powder. Section 2 (S2) was composed of the lignin depolymerization and the downstream processes to isolate and fractionate the different reaction products.

The Non-Random Two-Liquid-Redlich-Kwong (NRTL-RK) model was selected to simulate the thermodynamic properties of the streams involved in the process. This method includes the NRTL equation, obtained by Renon and Prausnitz, for the calculation of activity coefficients of liquids, the Henry's law for the dissolved gases and the RKS (Redlich-Kwong-Soave) equation of state for the vapor phase [279]. The simulation of the first

section used 100 kg/h of dry almond shell as basis for the calculations, whose composition was extracted from Figure 2.13. The cellulose, hemicelluloses, and lignin were defined by the physico-chemical properties obtained from the National Renewable Energy Laboratory (NREL) database [273], and by own chemical characterizations.

4.3.2.1. Modeling of Section 1

Almond shells were submitted to the autohydrolysis pretreatment, defined by a stoichiometric reactor, whose reaction conditions were set following the reaction parameters from the experimental section (180 ºC for 30 min, using water as reagent in a solid:liquid ratio of 1:8). The biomass dissolving reactions were defined by next reactions:

1) Cellulose (s) → Cellulose (d)
2) Cellulose (d) + H_2O → Glucose (d)
3) Xylan (s) → Xylan (d)
4) Xylan (d) + H2O → Xylose (d)
5) Lignin (s) → α Lignin1 (d) + β Lignin2 (s)
6) Extractives (s) → Extractives (d)
7) Ash (s) → Ash (d)

The solid cellulose (s) was firstly converted into dissolved cellulose (d). After that, this cellulose (d) was hydrated to form glucose (d). In a similar way, the hemicelluloses which were defined as xylan (s), were partially transformed into xylose (d). The lignin (s) contained in the biomass was converted into dissolved lignin1 (d) and other fraction remained in the pulp as lignin2 (s). The molecular formula of lignin (s) contained in the solid and lignin1 (d) were defined using a previous work developed in the BioRP group with hardwood lignin [278]. The lignin2 (s), whose composition differs with regard to the original one, was calculated to satisfy the mass balance of the reaction. The conversion index was fixed to the unit and the product yields were fixed by the stoichiometric factors (α and β). The extractives were assumed to be exclusively formed by β-sitosterol, following the same procedure as in other works [280,281]. The ash content was defined as CaO to simplify the simulation. All the yields for each reaction or stoichiometric factors were obtained from the experimental section, whose values are detailed in Table 4.1. The conversion factors for the reactions Nº2 and Nº4 were not possible to be experimentally fixed and, thus, they were arbitrarily estimated. In the case of the reaction Nº7 for the soda process, it was considered that all the ash content was dissolved to guarantee the enough ash content in the liquor to be able to adjust the final composition of the lignin sample after its precipitation.

Table 4.1. Reaction yields of autohydrolysis and delignification stage for organosolv and soda scenarios.

Reaction	Autohydrolysis	Organosolv	Soda
1	0.416	0.118	0.317
2	0.100	0.100	0.250
3	0.744	0.014	0.594
4	0.500	0.250	0.500
5(α)	0.414	0.779	0.544
5(β)	0.586	0.221	0.456
6	0.050	0.299	0.120
7	0.230	0.577	1.000

The resulting stream from the autohydrolysis pretreatment was divided by the "FILTER1" in two fractions: a solid stream with 10% of moisture content fixed by a design of specification, and a liquid one, containing the rest of the liquid fraction. The solid was washed with clean water, using a ratio of 1:2.5 solid:water, and sent to the delignification stage, whereas the liquid fraction (autohydrolysis liquor) was extracted from the circuit as an output stream. The washed solid fraction was then submitted to the delignification stage where two scenarios were proposed.

In the organosolv process, the solid fraction was mixed with a stream of ethanol:water (70/30 v/v) in a liquid:solid ratio of 6:1. The stream was heated up to 200 ºC and driven to a stoichiometric reactor. The reactions that took place in this reactor were the same that were defined for the autohydrolysis reactor, although the yields were notably different, as it can be seen in Table 4.1. The only exception was the reaction Nº 5, whose description is as follow:

5) Lignin2 (s) $\rightarrow$ α Lignin2 (d) + β Lignin3 (s)

The obtained stream was driven to a flash unit to reduce the pressure until the atmospheric level as well as to recirculate the condensed stream, which was mainly composed of ethanol (~80%). In this way, the volume of the stream that had to be cooled down after this stage was reduced, which minimized the energy duty of this cooling stage, as it will be seen in the further sections. Thus, the depressurized stream was cooled down to 25 ºC and separated in the "FILTER2", in a solid fraction of 80% of consistency, and a liquid fraction. In this case, the solid fraction was washed in two steps: (i) using the recirculated ethanol/water mixture in a solid:liquid ratio of 1:2, and (ii) a final cleaning stage using 2 volumes of water to obtain a clean "unbleached cellulosic pulp", whose composition was fixed according to the analysis reported in Figure 2.13. On the other hand, the obtained

liquid fraction from the reactor was mixed with the output stream from the "WHASER2", to collect the liquor that was removed from the solid fraction in this washing stage. The lignin contained in the stream resulting from this mixture was precipitated by adding acidified water. The composition of this acidified water was designed to obtain a stream of pH = 2 using H_2SO_4 (96 wt.%). The flow of this stream was designed to be 2 times the flow of the total black liquor stream. During the precipitation, whose simulation was defined by a stoichiometric reactor, the following reactions took place:

1) Lignin2 (d) → Lignin4 (s)
2) Xylose (d) → Xylan (s)
3) Ash (d) → Ash (s)

The conversion factor of reaction Nº1 was defined by the experimental section. However, the reactions Nº2 and Nº3 were defined by means of a design of specifications to reach the exact composition of AO2vol lignin sample that was previously reported in Table 2.8. These values are detailed in Table 4.2.

Table 4.2. Reaction yields for precipitation stage.

Reaction	Organsolv	Soda
1	0.776	0.776
2	0.094	0.121
3	0.404	0.952

The resulting stream from the precipitation stage was fractionated in the "FILTER3" in a solid fraction, which was defined with a moisture content of 1.0% and it was entitled the "Lignin" stream. The liquid fraction was submitted to a recuperation stage, where the solvent (mixture of water and ethanol) was distilled to be recirculated to the delignification stage and the "WASHER2". The reflux ratio and the number of stages were fixed to 1.5 and 5 respectively, following the methodology described in a previous work of the research group [278], whereas the distillated to feed ratio was designed by a design of specification to obtain a final condensate stream, whose composition would contain 70 wt.% of ethanol (same than solvent used in the delignification stage). In this way, ethanol consumption was reduced by 95.8%, i. e., to an almost negligible quantity.

Besides the ethanol recovery to minimize the solvent consumption, another recirculation loop was approached to reduce the water consumption of the whole process. The water stream from "WASHER1" and "WASHER3" were recirculated to "TANK3" to minimize the water consumption in the precipitation stage around a 45%. The final flowsheet of the organosolv lignin extraction section is presented in Figure 4.2.

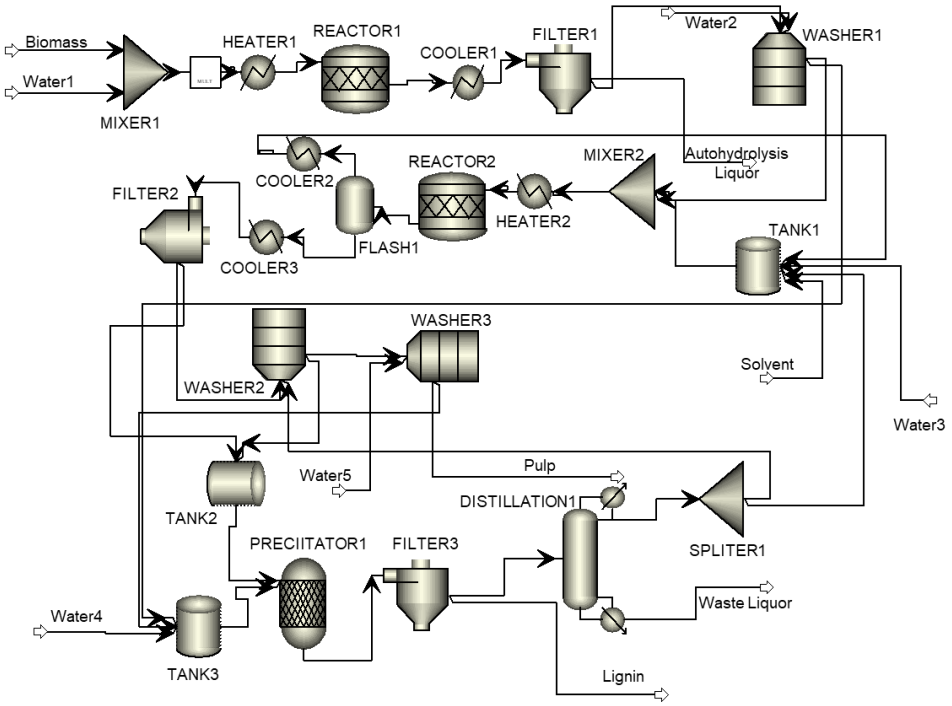

Figure 4.2. Flowsheet of S1 for the organosolv process.

In the case of the soda process, the solid fraction submitted to the delignification stage was mixed with soda (7.5 wt.%) in a liquid:solid ratio of 1:6. The reactions were introduced in the same format as in the organosolv process. The differences were based on the reaction yields that were also included in Table 4.1. However, the temperature of this reaction was noticeably lower (121 ºC).

After the delignification stage, the separation of the solid fraction and the black liquor was carried out in the "FILTER2", remaining 20% of moisture content in the solid. The cleaning stage of the solid was divided into two stages: (i) with NaOH 7.5 wt.% that was mixed with the black liquor in "TANK1", in a proportion of 1:2 to the solid stream, and (ii) with clean water in a ratio of 1:2.

The liquid streams for "FILTER2" and "WASHER2" were gathered together and driven to the unit "PRECIPITATOR1". The precipitation reactions were defined in the same procedure as in the organosolv scenario, although the yields of the reactions were different, in order to achieve the same composition of the ASpH4 lignin sample that was already reported in Table 2.8. In this stage, the precipitation of the lignin was accomplished by adding H_2SO_4 (96 wt.%) in excess to neutralize the [OH^-] ions and generate an acid

medium (pH = 4). This excess was defined by a design of specification. The new reaction (Nº4) was introduced in this unit as follow:

4) $2\ NaOH + H_2SO_4 \rightarrow Na_2SO_4 + 2\ H_2O$

In this scenario there was not a recuperation stage for the used solvent, thus the solid was uniquely separated from the liquid fraction in "FILTER3", remaining a moisture content of 1% in the "Lignin" stream. However, the recirculation of the washing water from "WASHER1" was totally re-used to reduce the water consumption in "WASHER2", where the cellulosic pulp was cleaned, as well as in "FILTER3", the stage where the precipitated lignin was cleaned and separated. A schematic representation of the soda lignin extraction process is represented in Figure 4.3.

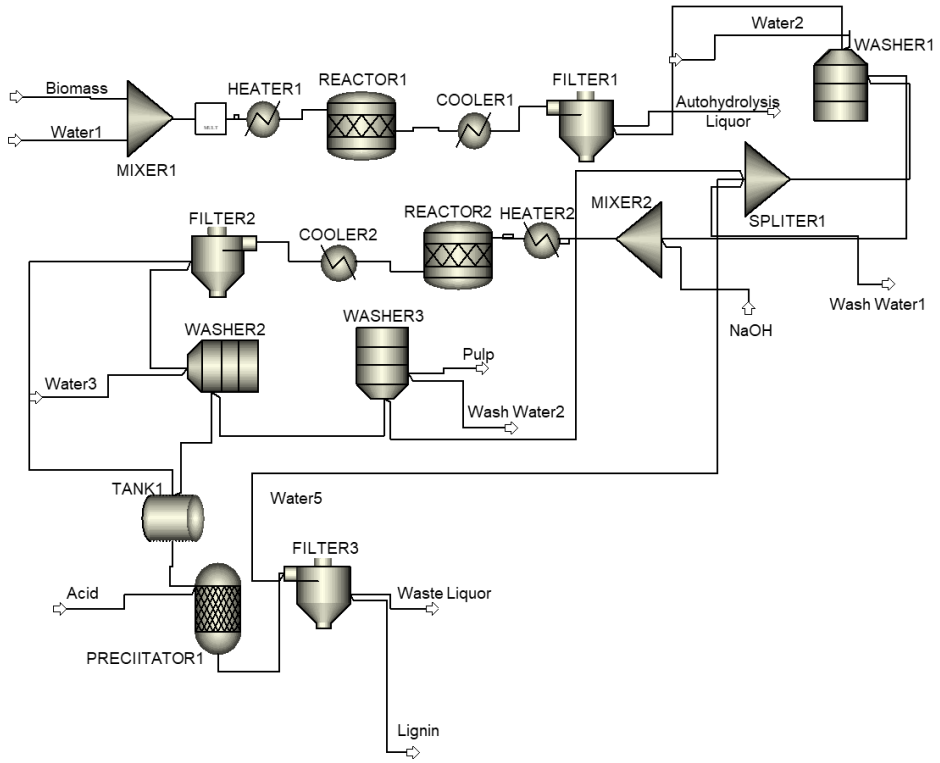

Figure 4.3. Flowsheet of S1 the soda process.

As a summary, Table 4.3 collects all the specification parameters for each unit employed in the modeling process of Section 1 for both scenarios.

Table 4.3. Designed parameters for the units involved in organosolv and soda scenarios.

Unit	Aspen Module	Organosolv	Soda
MIXER1	Mixer	1 bar	
HEATER1	Heater	180 ºC, 0 vapor fraction	
REACTOR1	RStoic	180 ºC, 0 vapor fraction	
COOLER1	Heater	25 ºC, 1 bar	
FILTER1	SSplit	Solid stream: 80 wt.% consistency	
WASHER1	SSplit	Water:solid cleaning ratio of 2.5:1, Solid stream 10% moisture content	
TANK1	Mixer	1 bar	
MIXER2	Mixer	1 bar	
HEATER2	Heater	200 ºC, 0 vapor fraction	121 ºC, 0 vapor fraction
REACTOR2	RStoic	200 ºC, 0 vapor fraction	121 ºC, 0 vapor fraction
FLASH	Flash2	1 bar, adiabatic	-
COOLER2	Heater	1 bar, 0 vapor fraction	1 bar, 25 ºC
COOLER3	Heater	1 bar, 25 ºC	-
FILTER2	SSplit	Solid stream: 80 wt.% consistency	
WASHER2	SSplit	Solvent:solid cleaning ratio of 2:1, Solid stream 20% moisture content	
WASHER3	SSplit	Water:solid cleaning ratio of 2:1, Solid stream 20% moisture content	
TANK2	Mixer	1 bar	
TANK3	Mixer	1 bar	-
PRECIPITATOR1	RStoic	1 bar, adiabatic	
FILTER3	SSplit	Solid stream dry (1% moisture content)	
DISTILLATION	RadFrac	1 bar, 5 stages, reflux ratio 1.5	-
SPLITER1	SSplit	Stream to Washer2 2:1 to solid	

4.3.2.2. Modeling of Section 2

In this section, two scenarios were approached for each lignin extraction process: (i) the depolymerization from the isolated lignin samples (AOS and ASS), and (ii) the direct lignin depolymerization from the black liquors (AOL and ASL).

In the first option, the process started with the mixture of the lignin and NaOH (4 wt.%) in a unit defined as a stoichiometric reactor, whose reactions were exactly the opposite of the ones described for "PRECIPITATOR1". In this case, since all the solid was totally dissolved in the alkaline medium, the conversion factor for all the reactions was the unit.

This mixture was submitted to the depolymerization reactor with a previous heating up to 300 ºC. "REACTOR3" was also defined as a stoichiometric reactor, where the following reaction took place:

1) Lignin4 (d) $\rightarrow$ α Phenol + β Catechol + χ Cresol + δ Guaiacol + ε Syringol + ϕ Oil + γ Tar + η Methanol
2) 0.6 Xylan (d) + 1.6 H_2O $\rightarrow$ 2 Methanol + CO_2

The phenolic oil and the tar properties were defined from similar literature works [108,278]. The vanillin compound was defined as guaiacol to simplify the simulation. The conversion for the reaction Nº1 was fixed as total and the product conversion factors were defined by the stoichiometric factors required to obtain the same yield as in the experimental sections. The methanol conversion factor was adjusted to guarantee the molar balance of the reaction. All the conversion yields or stoichiometric factors are detailed in Table 4.4.

Table 4.4. Stoichiometric factors and depolymerization reaction yield for each proposed scenario (AOS: Almond Organosolv Solid depolymerization; ASS: Almond Soda Solid depolymerization; AOL: Almond Organosolv Liquor depolymerization; and ASL: Almond Soda Liquor depolymerization).

Reaction	AOS	ASS	AOL	ASL
1α	9.38E-04	0.00E00	8.2E-04	4.29E-04
1β	2.01E-02	3.55E-03	1.12E-02	3.43E-03
1χ	3.95E-04	1.40E-04	4.40E-04	1.95E-04
1δ	4.59E-05	2.21E-05	1.90E-02	1.95E-05
1ε	0.00E00	0.00E00	3.37E-02	0.00E00
1ϕ	8.03E-02	4.09E-02	2.28E-01	3.31E-01
1γ	7.41E-01	2.64E-01	7.07E-01	6.65E-01
1η	1.02E00	1.89E00	1.00E-05	1.00E-05
2	1.00E00	1.00E00	1.00E00	1.00E00

After the reaction and before the cooling, the pressure was released using two flash separation units ("FLASH2" and "FLASH3"). In the first unit, the pressure was reduced to 50 bar and it reached 1 bar in the second one. This configuration was selected to drive the process in softer and safer conditions. In these units, two gaseous streams were generated; whose compositions were mainly water and methanol. In fact, the methanol was totally removed from the circuit by these streams. Once the pressure was set to the atmospheric level, the liquid stream was cooled down to 25 ºC and driven to a precipitator to remove the tar produced during the reaction by the acidification until pH = 2 with HCl. The "PRECIPITATOR2" was defined as a stoichiometric reactor as well, where the following reaction took place:

1) Tar (d) → Tar (s)
2) Ash (d) → Ash (s)
3) NaOH + HCl → NaCl + H_2O

The HCl quantity was fixed by a design of specification as the required amount to reach a pH = 2 in the medium after the reaction. All the conversion factors were established as the unit, e. i., a total precipitation was assumed in this stage. The solid tar was isolated by the "FILTER4", remaining a 10% of moisture content in the tar stream.

The liquid fraction, where the phenolic monomer products were contained, was driven to a liquid-liquid extraction operation in the "ABSORPTION COLUMN" unit. In this stage, the

flow of ethyl acetate was fixed as 5 times the flow of the fed stream, in order to extract the phenolic oil from the aqueous stream. Then, two distillation columns were needed to separate the phenolic oil stream, which also contained the phenolic monomers, from the ethyl acetate. Both columns, "DISTILLATION 2" and "DISTILLATION3", were defined by 5 stages with a reflux ratio of 1.5, as in the previous distillation column. However, the distillate to fed ratio parameter was set by a design of specification to reach a percentage of separation for the ethyl acetate of 99.5 wt.% and 99.9 wt.%, respectively. The collected ethyl acetate from the distillate streams was recirculated to the liquid-liquid extraction column to minimize the consumption of this component. With this recirculation, only 1.15% of the initially required quantity was necessary to be fed in the system. Finally, the separation of the phenolic oligomers and the phenolic monomers was also conducted by a distillation column ("DISTILLATION4"). In this unit, 5 stages and a reflux ratio of 1.5 were also fixed following the methodology described by Mabrouk et al. [278]. However, the distillate to fed ratio parameter was designed by a design of specification to reach a concentration in the distillate stream ("Phenolic monomers") higher than 95 wt.%. A schematic representation of the lignin depolymerization and the product separation (S2) processes is represented in Figure 4.4.

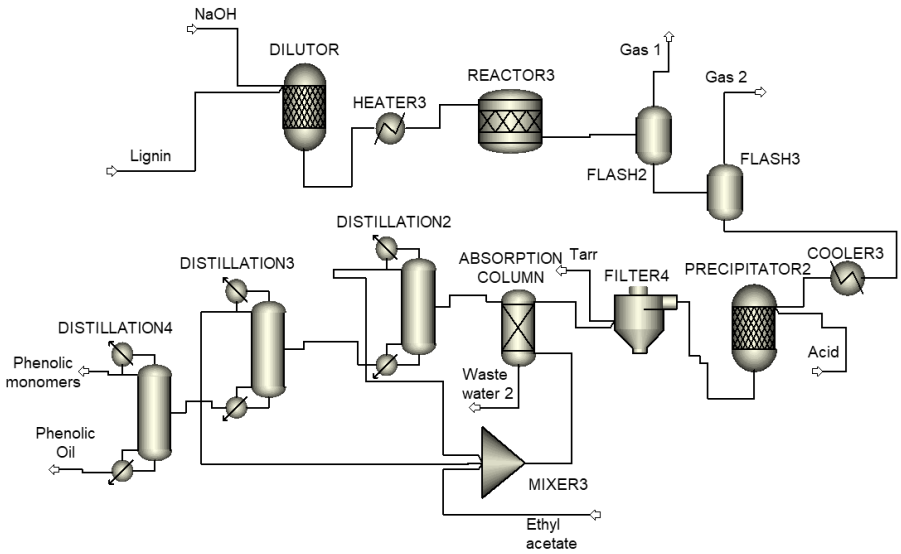

Figure 4.4. Flowsheet of the S2 for lignin depolymerization and purification of the phenolic monomer products.

For the scenarios where the depolymerization reaction was accomplished directly from the black liquors (AOL and ASL), the "DILUTOR" unit was suppressed. Hence, the liquor was directly driven to the depolymerization reactor. The reactions were defined as in the previous case, but different stoichiometric factors were established to obtain the same

yields than in the experimental section, as it was already shown in Table 4.5. Nevertheless, the rest of the units followed the same principles. All the specification parameters for each unit used in S2 are detailed in Table 4.5.

Table 4.5. Designed parameter for the units involved in S2.

Unit	Aspen Module	Parameters
DILUTOR	RStoic	25 ºC, adiabatic
HEATER3	Heater	300 ºC, 0 vapor fraction
REACTOR3	RStoic	300 ºC, 0 vapor fraction
FLASH2	Flash2	50 bars, adiabatic
FLASH3	Flash2	1 bar, adiabatic
COOLER3	Heater	25 ºC, 1 bar
PRECIPITATOR2	RStoic	1 bar, adiabatic
FILTER4	SSplit	Solid stream 95% solid content
ABSORPTION COLUMN	Extract	6 stages, adiabatic
DISTILLATION2	RadFrac	1 bar, 5 stages, reflux ratio 1.5
DISTILLATION3	RadFrac	1 bar, 5 stages, reflux ratio 1.5
DISTILLATION4	RadFrac	1 bar, 5 stages, reflux ratio 1.5
MIXER3	Mixer	1 bar

4.4. Mass balance analysis

The process efficiency was evaluated in terms of the out-put streams, the products and the waste streams, as well as the water and chemicals (ethanol or soda) consumptions. In Table 4.6, the product yields and the water and chemicals consumptions are detailed.

Table 4.6. Process efficiency in terms of product yields, water, chemicals and energy consumption as well as waste streams.

Parameter	Units	Organosolv	Soda
Lignin yield	%	4.89	10.21
Pulp yield	%	55.21	38.19
Solvent consumption	kg/h	14.65	427.3
Water consumption	kg/h	1371	946.9
Waste Streams	kg/h	1433	1391
Acid	kg/h	-	75.84

The product yields, referred to the initial biomass introduced to the system, were clearly influenced by the extraction methods. The soda process highlighted its major suitability to solubilize biomass despite its lower severity factor (121 ºC for soda process against 200 ºC for organosolv method). Consequently, the solid fraction (pulp), presented lower yield but the recovered lignin was higher, since it is the main product solubilized from the solid fraction. This difference was significant, as the lignin yield of the soda process was double than the yield obtained in the organosolv process. Regarding, the cellulosic pulp, the yield of the soda process was around 30% lower. Therefore, the delignification process could be selected in function of the product that it would want to be maximized.

The inclusion of the distillation column in the organosolv process led to an extremely lower solvent consumption. Less than 5% of ethanol was required in the organosolv process in comparison with the soda, which positioned the organosolv process as a sustainable method, with almost negligible solvent consumption. However, water consumption was greater in the organosolv method. This fact was caused by the lignin precipitation stage, where big volumes of water were consumed (double volume than the black liquor), whereas only low quantities of acid were used in the soda process. In general, 40% more water was consumed in the organosolv process. Because of the high consumption of water, greater quantities of waste streams were also produced in the organosolv process. One of the main drawbacks of using the soda method instead of the organosolv was the necessity to include high volumes of strong acids during the process, which presents safety risk in terms of chemical handling for the operators and the environment.

The evaluation of the S2 and the global process was assessed by the results shown in Table 4.7, where the yields of the obtained product streams are expressed referred to the lignin obtained in the S1, and the accumulated yield was referred to the initial biomass used from S1.

Table 4.7. Process efficiency in terms of product yields, water, chemicals, and energy consumption as well as waste streams (OS: Organosolv Solid lignin depolymerization; OL: Organosolv Liquor depolymerization; SS: Soda Solid lignin depolymerization; SL: Solid Liquor depolymerization.

	Parameter	Units	OS_1	OS_T	OL_1	OL_T	SS_1	SS_T	SL_1	SL_T
Inputs	Lignin	kg/h	100.0	4.9	100.0	5.8	100.0	10.2	100.0	11.9
	NaOH	kg/h	1894	92.6	-	-	1984	202.1	-	-
	Acid	kg/h	331.2	16.2	1404	81.0	216.9	22.1	1310	155.7
	Ethyl acetate	kg/h	108.3	5.3	147.6	8.5	62.6	6.4	139.7	16.6
Outputs	Phenolic monomers	kg/h	1.60	0.08	1.42	0.08	0.30	0.03	0.46	0.05
	Phenolic oil	kg/h	54.09	2.64	27.76	1.60	9.80	1.00	32.46	3.86
	Tar	kg/h	32.15	1.57	69.92	4.03	35.14	3.58	66.41	7.89
	Waste water	kg/h	1233	60.3	1404	81.0	1137	115.9	2648	314.7
	Gas	kg/h	981.9	48.0	5448	314.3	1050	106.9	1753	208.3

1: yields referred to lignin fed to section 2.

T: results referred to 100 kg/h biomass.

**OL tar precipitation was carried out using acidified water (2 volumes), not HCl as other reactions.*

The variations in the consumed inputs streams demonstrated the huge difference between lignin depolymerization from the precipitated lignin and the direct lignin depolymerization from the black liquors. The high soda/lignin ratio used at the experiments (20:1) provoked the great consumption of soda in the precipitated lignin depolymerization reaction. However, the precipitation of lignin prior to its depolymerization led to work with lower volumes, which had a big influence on acid and ethyl acetate consumptions in the downstream processes, showing bigger volumes of acid consumption in the OL and SL scenarios.

In the case of the phenolic monomer stream, except in the case of OL depolymerization, the main products obtained in the phenolic monomers stream were catechol and catechol derivatives (considered together to facilitate the interpretation), with a selectivity higher than 95%. In the case of OL depolymerization, a mixture of monomers was obtained, where the syringol was the most plenty product (>50%), followed by the guaiacol (<25%) and the catechol derivatives (>15%), emphasizing the different reaction mechanism experimented when a mixture ethanol/water was used for the solvolysis of the lignin, as it was seen in the experimental section. In terms of the reaction yields, the organosolv lignins, both depolymerized from the precipitated lignin or directly from the black liquor showed not only better depolymerization yields, but also higher yields referred to the original biomass. In

spite of the lower yield in the lignin extraction from biomass in S1, the global yield to depolymerize lignin was finally better for the organosolv process. This fact means that the organosolv lignin presented a more suitable structure to be depolymerized than the soda lignin. Regarding the influence of the direct depolymerization process, in the case of the organosolv process it was noticeable the fact that despite the depolymerization reaction yield for the phenolic monomers were lower than using the precipitated lignin (OL1 vs OS1), the total yield with regard to the initial biomass was higher (OLT vs OST). The reason was caused by the bigger amount of lignin fed to the depolymerization reaction when the precipitation stage was removed. The removal of this stage mainly reduced the loss of lignin, whereas, in the soda process, the removal of that stage led to an increase in the total depolymerization yield as well, probably due to the extremely low yield obtained in the SS reaction. In any case, the direct lignin depolymerization provoked clear benefits for the most interesting products: phenolic monomers plus phenolic oil. Indeed, more phenolic oil was obtained for SL than OL, the unique scenario where the soda process was more efficient than the organosolv one. The tar, a byproduct of the depolymerization reaction formed by a mixture of the RL and the coke, was produced in higher amount by direct depolymerizations, regardless the employed delignification method. In this line, the inclusion of capping agents to stabilize those compounds prior to its depolymerization would be necessary for further surveys.

Another negative impact of the direct lignin depolymerization was the higher waste water generated as output. If the lignin is not precipitated, more volume had to be treated and as a consequence, more water was finally discharged. The higher amount of waste streams was not the only drawback of using the direct depolymerization concept. As it was mentioned before, in the organosolv process it was not allowed recirculating ethanol by the inclusion of a distillation column. As a result, the increase of the solvent used for the organosolv reaction rose up from 14.65 kg/h to 245.5 kg/h. This fact was expected to hugely increase the raw material costs of this scenario.

The composition of the gas streams produced in the flash units was mainly steam that could be used for heating other streams in parallel to save energy. In the case of OL, these streams presented a bigger volume due to the evaporation of the ethanol, which led to a decrease the total flow of water disposal in comparison with the SL reaction. In further optimizations, the ethanol could be extracted from these streams to be recirculated to the system to reduce its consumption. However, such stage would be complicated to implement due to the high level of trace compounds also contained in these streams.

4.5. Energetic evaluation

The performances of the designed processes were not only evaluated in terms of mass balances and product yields. Energy plays an important role in the production cost and in the environmental impact of industrial processes. Thus, the energetic duties should be considered as well. In this section, the energetic demands of all proposed scenarios were analyzed using Aspen Energy Analyzer® software. The base simulation was defined considering that all the energetic demands were applied from utility streams. The streams data, such as flows, temperatures and enthalpies are used by the software to quantify the possibilities of energy saving by the integration of heat from different existing streams, following the methodology of the “pinch” analysis, which is considered as the most widely used technique to calculate the maximum thermodynamically feasible targets in energetic integration [282].

4.5.1. Energy balance analysis

The total utility demands, as well as the distribution of this demand by stage, were calculated to compare the developed scenarios in the previous sections. The total energetic duties for each section are detailed in Table 4.8.

Table 4.8. Energetic duties for different scenarios (S1: Section corresponding to lignin extraction; S2.1: Section corresponding to lignin depolymerization from precipitated lignin; S2.2: Section corresponding to lignin depolymerization from black liquor; T: Accumulate values for the global process).

Section	Organosolv			Soda		
	Heating (kW)	Cooling (kW)	Total (kW)	Heating (kW)	Cooling (kW)	Total (kW)
S1	479	435	914	192	196	387
S2.1	107	118	225	279	213	492
S2.1T	587	553	1140	470	409	879
S2.2	373	198	570	707	673	1380
S2.2T	606	435	1040	899	868	1767

In the case of S1, the total energetic duties were strongly influenced by the inclusion of the distillation column for the solvent recovery on the organosolv process and the higher temperature required on the delignification stage. In general, more than the double of the energetic utilities were required for the organosolv process than in the case of the soda process.

In Figure 4.5 and Table 4.9, the distributions of those duties for S1 are detailed. It can be observed that 50% of the total duties were caused by the distillation column (as sum of the reboiler and the condenser duties). The autohydrolysis reaction was the second stage with the highest energetic demand, considering the combination of “Heater1” and “Cooler1”. This influence was more notorious for the soda process (four times higher than the delignification reaction, for instance) due to lower temperature was used in the delignification stage (121 ºC) in comparison with the organosolv process (200 ºC). The influence of the flow on the energetic demands was highlighted in the organosolv process since even when the delignification reaction required a greater temperature than the autohydrolysis pretreatment, the bigger flow to be treated in the pretreatment reaction led to a higher energetic duty (more than two times).

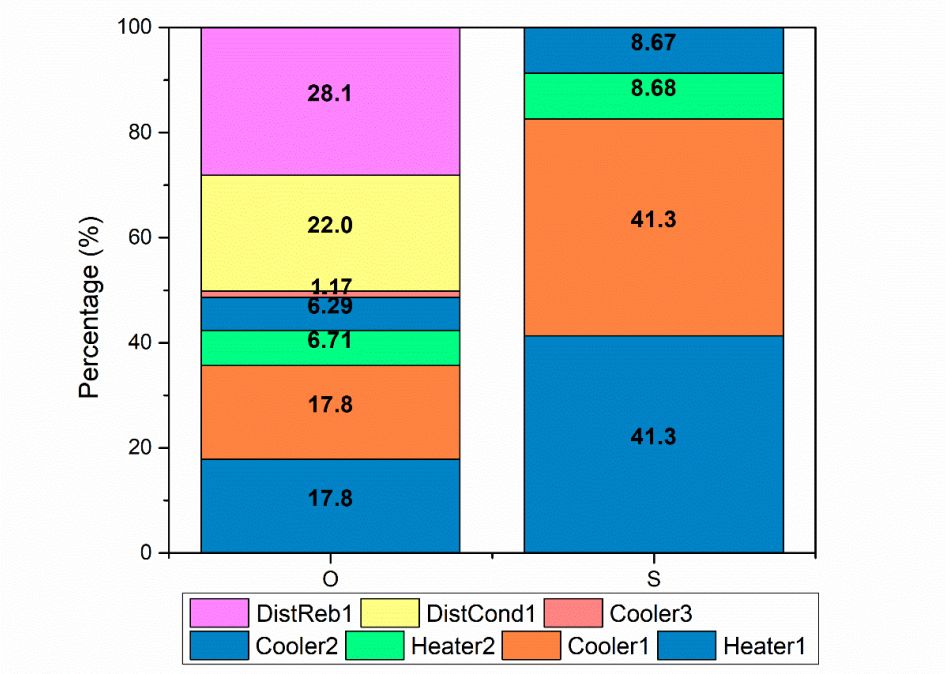

Figure 4.5. Distribution of energetic duties by unit for S1 scenarios.

Table 4.9. Energetic duties by each unit in the different S1 tested scenarios.

Stage	Units	O	S
Heater1	kW	165.9	165.9
Cooler1	kW	165.7	165.8
Heater2	kW	62.4	34.8
Cooler2	kW	58.4	34.8
Cooler3	kW	10.9	-
Dist1Con	kW	204.8	-
Dist1Reb	kW	261.3	-

In the case of S2.1, the energetic demand was clearly correlated to the flow treated as the initial stream for this section. In general, the process was the same for both precipitated lignin: organosolv and soda. However, the quantity of fed lignin to this section was greater for the soda process and, as a consequence, more material had to be heated. According to the global process, more than 20% of the energetic duties were required for the organosolv process in comparison with the soda one, which could be considered as the counterpart for the recuperation of the solvent in the case of the organosolv delignification method.

For S2.2, in the case of the organosolv liquor depolymerization process, the reduction of the total energy demand was caused by the removal of the distillation column emplaced in the S1 to recirculate the ethanol used in the organosolv reaction. However, the decrease of the energy demand was not directly correlated with the elimination of this stage because of the greater flow that had to be treated in this new scenario. This fact provoked an increase in energy consumption in S2.2, specifically more than the double of the consumption generated in S2.1. However, the results were still lower for S2.2T than in S2.1T, although the reduction was not as high as it was expected (lower than the 10% in the total energetic duties).

In Figure 4.6 and Table 4.10 the distribution of the total energetic demand by each unit for the different scenarios proposed for S2 of the flowsheet are detailed.

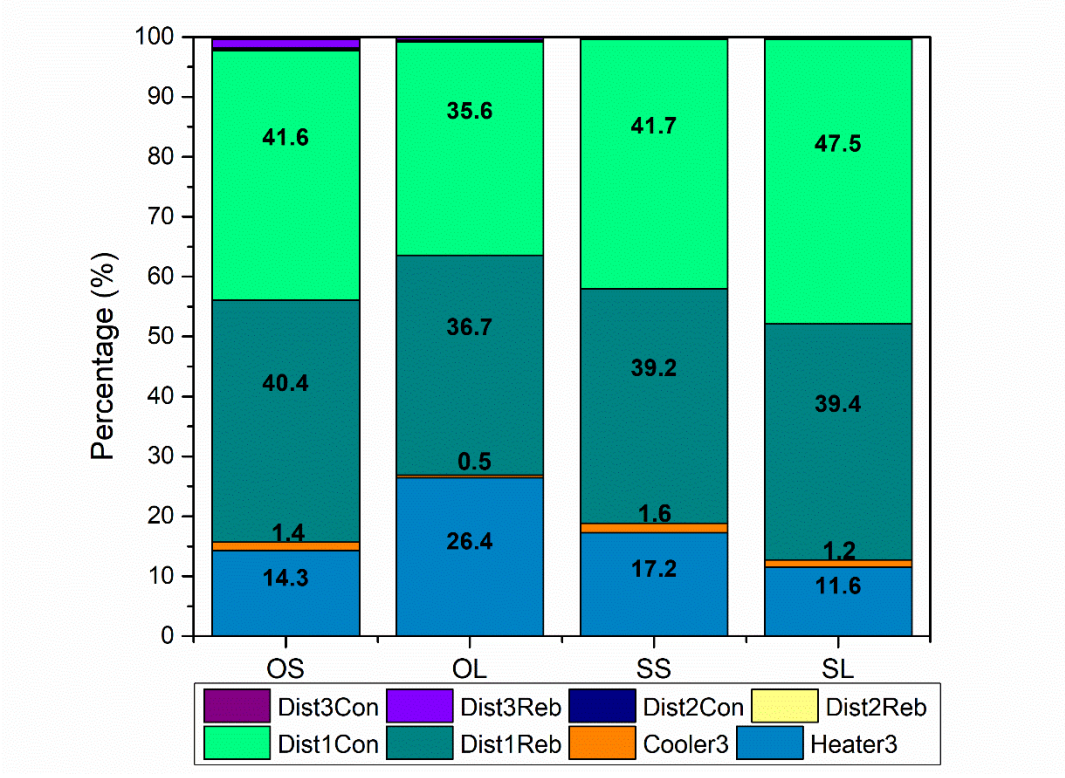

Figure 4.6. Distribution of energetic duties by each unit for S2 scenarios.

Table 4.10. Energetic duties by each unit in the different S2 tested scenarios.

Equipment	Units	OS	OL	SS	SL
Heater3	(kW)	39.0	144.2	84.8	159.5
Cooler3	(kW)	3.8	2.5	8.0	15.9
Dist2Reb	(kW)	110.7	200.1	192.5	543.8
Dist2Con	(kW)	113.8	194.3	204.9	655.8
Dist3Reb	(kW)	0.8	1.0	0.6	1.8
Dist3Con	(kW)	0.3	0.7	0.4	1.1
Dist4Reb	(kW)	4.3	2.8	0.6	2.0
Dist4Con	(kW)	0.9	0.1	0.0	0.1

Except in the case of the OL simulation, more than the 80% of the total energetic demand required in S2 was caused by the "Dist2" unit, as the sum of its corresponding reboiler ("Reb") and its condenser ("Con"), whereas in the case of the OL was around the 70%. Despite the maximum temperature that had to be reached in this unit was not relatively high (around 80 ºC), the greater volume to be treated in this stage converted this stage into the most demanding one in terms of energy consumption. Once again, it was demonstrated that the main parameter to be optimized to reduce the energy consumption would be the flows to be treated, trying to reduce as much as possible these huge volumes. The reasons of these high volumes to be treated in the first distillation column of this section was the high volume of ethyl acetate used to extract the phenolic oil from the aqueous stream, resulting after the tar precipitation (5 volumes of ethyl acetate for one of aqueous stream). Therefore, it is thought that, for further cost reductions, this stage should be optimized to minimize the volumes to be handled. The second most important unit in this section was the "Heater3", where the fed stream to the depolymerization reactor was heated until 300 ºC. Establishing a comparison between the different scenarios, it was clear the high impact of the flow to be treated, with greater demands always for the direct liquor depolymerization, where the flows of the reactions were significantly higher. The influence of this stage over the S2 was around 15% for each scenario, except in the OL, where it represented a 25%. This fact was based on the greater reduction for the further streams during the flash separations after the depolymerization reaction for the OL scenario because higher percentages were evaporated when ethanol was used as solvent. From the rest of units, the enormous reduction of the flow caused by "Dist2", minimized the influence of the rest of the distillation columns over the global process. Indeed, the energetic demand of the last two distillation columns could be considered as completely negligible. This was the main reason why such high level of product purification could be

afforded; because bearing in mind the whole picture of the global process, a fine separation did not impact on the final production cost in terms of the utility demand.

After the modeling in Aspen Plus®, Aspen Energy Analyzer® was employed to identify the most critical stages for potential energetic cost reduction.

2.5.2. Heat Integration

The Aspen Energy Analyzer® software did not only report the energetic duties calculated from the simulation developed by the Aspen Plus® software but led to calculate the maximum possibilities to reduce the energy cost using the same flowsheet by energy integration. This is accomplished by combining the existing units through heat exchangers in order to take advantage of their head load. To identify the possibilities that the current flowsheets could present regarding the integration of energy, the methodology of the "pinch" analysis was applied. As first step, the composite curves were built, where temperature vs enthalpy changes are represented. These curves represent the evolution of each stream though its initial and final temperatures. The hot and the cold curves are separated by the selected minimum temperature difference, in this case 10 ºC was the selected gap. Above this point ("pinch" point), heating utilities have to be applied whereas, below it, cooling utilities have to be applied instead. The composite curves for the four approached cases are presented in Figure 4.7.

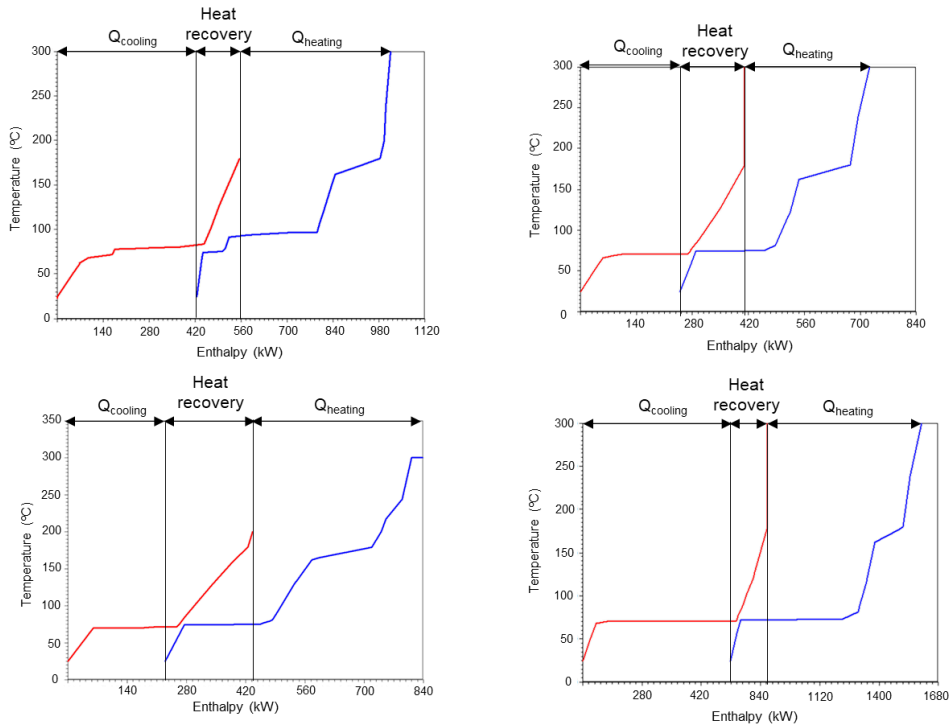

Figure 4.7. Composite curves of the proposed simulation cases. A) Solid organosolv lignin. B) Liquor organosolv lignin. C) Solid soda lignin. D) Liquor soda liquor.

From these curves, the theoretical available energy that could be used by the energy integration was calculated (section from the center of the curve). The theoretical maximum available savings from the base case simulations are detailed in Table 4.11.

Table 4.11. Potential savings in energetic duties for the global processes.

Parameter	Units	OS	OL	SS	SL
Base Simulation	kW	1140	1040	879.2	1767
Target Simulation	kW	880.5	629.7	558.1	1419
Potential Saving	%	22.8	39.5	36.5	19.7

In the case of solid lignin depolymerization, SS allowed a higher percentage of energy integration (almost 40%). However, the absolute value was bigger for the organosolv process as the energetic duties in the base case simulation were noticeably higher for the latter one. Considering the four global scenarios when lignin was depolymerized from solid samples, the SS scenario presented more possibilities to achieve higher energy savings in percentage and absolute value. Regarding the processes that used liquor as feedstock for the lignin depolymerization, the OL process showed bigger potential of energy savings in absolute values as well as the total percentage. This fact adds even more negative vision of the direct depolymerization in the soda process as it was not only the process with the highest energy demand, but also the integration possibilities are not at the level of the rest of the tested scenarios.

4.6. Economic assessment

The economic assessment was carried out to compare the different scenarios developed by the simulation process as well as the current situation in a hypothetical real market situation. The cost of purchasing and installing equipment (BMC) for the main production sections were calculated by the technique of economies of scale (Equation 2.1) described by Sadhukhan et al. [283], where the base cost of an equipment with a specific size is scaled up/down to calculate the final cost of the equipment for the desired size. Most of the equipment costs were scaled from similar previous works [284–288], and updated to the cost of the current year (2017) by the Equation 2.2, using the chemical engineering plant cost indexes (CEPCI).

$$\frac{COST_{size2}}{COST_{size1}} = \left(\frac{SIZE_2}{SIZE_1}\right)^R \quad \text{(Eq. 2.1)}$$

where SIZE1 is the capacity of the base system, $COST_{size1}$ is the cost of the base system, SIZE2 is the capacity of the system after scaling up/down, $COST_{size2}$ is the cost of the system after the scaling up/down, and R is the scaling factor.

$$C_{pr}=C_o\left(\frac{I_{pr}}{I_o}\right) \quad \text{(Eq. 2.2)}$$

Where C_{pr} is the present cost, C_o is the original cost, I_{pr} is the present index value, and I_o is the original index value.

The fixed capital invested (FCI) was estimated using the on-site costs, obtained by Guthrie's method [289], taking into account the off-site and the indirect costs, the working capital and the plant startup cost, as it is detailed in Table 4.12. The manufacturing costs (COM) were estimated considering the operating labor cost (COL), the costs of utilities (CUT), the waste treatment cost (CWT), and the cost of raw materials (CRM) [29].

Table 4.12. Description of estimated parameters calculated in this work.

Parameter	Calculation/Value	Reference
FCI	**1.3·Fixed Capital**	[290]
On-site Cost	BMC	[290]
Off-site Cost	0.45· On-site Cost	[290]
Indirect Cost	0.25·(On-site + Off-site)	[290]
Fixed Capital	On-site + Off-site + Indirect Cost	[290]
COM	**$0.28 \cdot FCI + 2.73 \cdot C_{OL} + 1.23 \cdot (C_{UT} + C_{WT} + C_{RM})$**	[290]
Operating Labor Cost		
Operators Salary	$41{,}600 \cdot (1.03)^{(\text{Current year-2003})}$	[291]
Utility Cost		
Cool water	8.67E-05 €/kg	Local mill
Low-pressure steam	1.1E-02 €/kg	Local mill
Medium-pressure steam	1.12E-02 €/kg	Local mill
High-pressure steam	1.45E-02 €/kg	Local mill
Furnace heat	2.46E-02 €/kg	Local mill
Waste treatment Cost		
Waste water treatment	0.08 €/m^3	[274]
Raw material Cost		
Biomass	0.052 €/kg	[292]
NaOH	0.4 €/kg	Local mill
Ethanol	0.61 €/kg	[276]
Ethyl acetate	0.72 €/kg	[293]
HCl	0.15 €/kg	Local mill
H2SO4	0.04 €/kg	Local mill

4.6.1. Economic results

The first step to carry out the economic evaluation was the sizing calculation to estimate the cost of the equipment needed in each scenario. The costs per group of equipment are detailed in Table 4.13.

Table 4.13. Purchased and installation costs (BMC) of the equipment needed in each scenario.

Equipment	Units	OS	OL	SS	SL
Heat Exchangers	k€	1,877	3,519.5	3,722	5,138
Reactors	k€	1,302	1,625.1	1,437	1,907
Distillation Columns	k€	1,415	749.1	752.0	1,573
Absorption Coulumn	k€	518.1	818.1	825.1	1,709
Separator units	k€	1,089	952.5	1,174	1,455
Tanks	k€	877.9	231.7	439.4	43.6
Total BMC	**k€**	**7,078**	**7,896**	**8,350**	**11,826**

Based on these estimated results, it could be established that the investment for equipment would be lower for the OS scenario. The higher costs of the soda processes with regard to organosolv ones were caused by the higher flows that had to be manipulated in the second part of the process (S2). The greater lignin extraction yield in the soda process involved much more NaOH to be used to dissolve lignin before its depolymerization, and subsequently, it increased the volume of the needed ethyl acetate to separate the phenolic oil from the aqueous phase. As a consequence of the greater flows to be treated, the size of the equipment was noticeably bigger in the SS scenario than in the OS one for instance, which made this process much more expensive (almost 20% more cost). The same situation was undergone when the direct lignin depolymerization from the liquors was approached. Not to isolate lignin prior to its depolymerization, involved an increase of the volume that had to be heated to 300 ºC at the depolymerization reactor, the stage with the highest temperature of the whole process. In the case of the OL scenario, the avoiding of the lignin precipitation stage led to an increase in the equipment cost of more than 10%, whereas in the soda process the increase to avoid that stage was more than the 40%. This fact highlighted the great sensitivity of the process regarding the solvent ratio used in the depolymerization reaction. As it can be seen, the biggest increment in the BMC costs with regard to the OS simulation was located in the heat exchangers units because the energetic duties for the depolymerization reaction had to be applied by direct-furnace equipment, a type of heater much more expensive than a common heat exchanger. There were also differences in the reactor costs, based on the higher volumes they had to be treated in the rest of the simulations. In addition, the bigger cost for the distillation column in the OS process for the ethanol recovery stage was buffered by the reduction of the flow to be fed to the depolymerization reaction in the case of the OL scenario. Thus, the inclusion of the distillation column did not involve a direct increase in equipment costs.

Hereafter, the estimations of the operational costs were calculated based on the utilities, raw materials, labors, and waste treatment costs. The cost breakdown for the utilities and the raw materials are detailed in Table 4.14 and Table 4.15 respectively.

Table 4.14. Utility costs breakdown by stream.

Stream	Units	OS	OL	SS	SL
Cooling	k€	3.0	2.3	2.2	4.7
LP Steam	k€	38.2	23.4	22.5	63.6
MP Steam	k€	0.0	0.0	4.3	3.8
HP Steam	k€	32.4	34.8	23.7	23.7
Furnace heat	k€	14.2	60.6	30.2	57.1
Total cost of utilities	**k€**	**87.8**	**121.1**	**82.9**	**152.9**

At first, it has to be mentioned that the cost of the cooling stream was almost negligible based on the current low cost of water that was considered as a reference (a paper industry in the region in which this work was proposed – the Basque Country). Consequently, the costs of the utilities were significantly reduced. Therefore, the total final costs of the utilities were mostly generated by the heating streams. Once again, the main differentiation in the cost amongst the proposed simulations was created by the energetic duties of the depolymerization stage where it was compulsory to use a furnace to reach the reaction temperature. The higher energetic duties for the direct depolymerization were caused by the bigger volume to be warmed up in this stage. This was the reason why the OL and the SL simulations presented the bigger costs. Comparing the solid lignin depolymerization simulations, the utility costs were lower for the SS scenario despite the bigger cost in the depolymerization stage. The inclusion of the distillation column in the S1 in the OS simulation to recover the ethanol provoked this higher cost.

Table 4.15. Raw materials cost breakdown for the different developed simulation processes.

Stream	Units	OS	OL	SS	SL
Biomass	k€	344.1	344.1	344.1	344.1
Ethanol	k€	38,066	637,727	0.0	0.0
NaOH	k€	8,929	0.0	60,708	41,214
Acid	k€	14,591	0.0	40,735	140,290
Ethyl Acetate	k€	18,865	30,297	22,716	59,124
Water	k€	353.8	258,321	94.5	94.5
Total	**k€**	**81,148**	**926,689**	**124,598**	**241,067**

The raw material costs also drove to identify great differences between the simulation processes as the total costs hugely varied from one simulation to others. OS scenario was the cheapest scenario based on the recovery of the solvent (mixture of ethanol/water) after the delignification stage. As the compounds with the highest costs were ethanol and ethyl acetate, the reduction of the required volume from these streams led to a significant reduction in the cost in comparison with other simulations. Specifically, with regard to the OL simulation, the non-recovery stage of the ethanol in the S1 for the OL scenario deeply increased the final cost of the raw materials more than 10 times. In addition, as it was observed before, the insertion of the distillation column for the first scenario did not mean an increment of the equipment costs and only the energetic requirement was increased, but at an acceptable level. In the case of the soda processes, the impossibility to recover the solvent after the delignification stage provoked an increase in the costs of consumed chemicals with high costs for both alkaline and acids streams. Only in the SS scenario, the raw material cost was increased by around 50% in comparison with the OS one. The cost for the SL scenario was almost double than the SS process as a consequence of the greater volume that was driven to the S2, which led to a relevant escalation in the acid and ethyl acetate expenditures to precipitate the tar and to extract the phenolic oil, respectively.

From the previous sizing and operational calculated costs, the summary of the total project is described in Table 4.16.

Table 4.16. Economic evaluation for the studied processes.

Parameter	Units	OS	OL	SS	SL
BMC	k€	7,078	7,896	8,350	11,825
FCI	**k€**	**16,678**	**18,605**	**19,675**	**27,864**
C_{OL}	k€	936.0	861.4	861.4	861.4
C_{UT}	k€	87.82	121.1	82.91	152.9
C_{WT}	k€	49.79	46.53	56.35	48.83
C_{RM}	k€	81.15	926.7	172.1	241.1
COM	**k€**	**7,494**	**8,907**	**8,244**	**10,698**

In line with the previous values, the OS scenario obtained the lowest FCI cost, which identified this process as the cheapest scenario to initially invest. In addition, the total operational costs (COM) were also lower than the rest of the approached scenarios. These facts highlighted the greatest efficiency of the OS process over the rest of the tested simulation processes. Concretely, the total FCI cost was increased by more than 10% for the OL simulation and the COM cost in almost 20% for the OL simulation, mostly based on the higher reactant costs. However, this process was behind the direct lignin depolymerization processes (OL and SL ones) in terms of the production of phenolic monomers, which is thought to have an important influence on the case of a great final price for this stream. In any case, it has to be reminded that the volume of this product was really low in comparison to the fed biomass. The soda processes were more expensive than the organosolv processes in terms of the FCI costs, being bigger for the direct depolymerization from the liquor, as well as in the organosolv processes. As it was commented before, the greater volume in the critical stages that had to be handled in these processes led to such increase in the investment costs. The same situation was experienced with the COM costs. In this case, it was caused by the high demand for chemicals that the soda processes required.

4.7. General remarks

The different scenarios studied in this chapter by process simulation were evaluated in terms of the product yields, raw material consumption, and waste streams disposal. The soda delignification method offered greater lignin yield (around the double). However, the pulp yield, an important product to be considered in a full integrated biorefinery, was poorer than in the organosolv process. The most significant difference between both processes was the possibility to recover the solvent from the delignification stage in the organosolv process, which reduced the consumption of the chemicals almost to a negligible degree.

Considering the second section of the process, where lignin was depolymerized including a previous precipitation stage or being depolymerized directly from the liquor, it was confirmed that regardless the higher lignin amount extracted in the soda process, the organosolv lignin was more suitable to be depolymerized, leading to a greater phenolic monomer yield than in the soda processes. It was also demonstrated that the direct depolymerization kept or enhanced the product yields since the avoiding of the precipitation stage reduced the lignin loss throughout the process.

Besides the mass balances, the energetic and economic assessments were accomplished. By the energetic analysis, it was established that the great impact caused in the OS simulation by the inclusion of the ethanol recovery distillation column was buffered by the reduction of the treated volume in the S2, where the most critical stage, in terms of harsh conditions, was located: the depolymerization reaction. This fact was also the reason why the energetic demand for the SL scenario was really high, as the treated flow in this stage was much bigger than in the other simulations. However, the SS simulation was the flowsheet with the minimum energetic demand.

Besides the traditional assessment of the energetic duties, a “pinch” analysis was carried out to identify potential energetic savings in the process, in order to approach optimized simulations in further investigations. In this sense, great possibilities to reduce the utility demand were found for all the proposed flowsheets with the OL scenario presenting almost 40% of utility reduction.

Finally, the economic analysis was conducted following Guthrie’s method to calculate both the FCI and the COM costs. Both costs were extremely influenced by the high volume to be treated at the most critical stage, specifically the lignin depolymerization reaction were the harsh conditions (the temperature and the pressure) were required. As a consequence, the costs of the equipment to supply the required energy were deeply incremented. Therefore, to reduce the cost for further investigations two alternatives could be proposed: (i) reducing the liquid/solid ratio for every reaction of the circuit, especially for the depolymerization reaction, and/or (ii) reducing the harsh conditions of the depolymerization stage to be capable to use more economically feasible equipment. In any case, in both alternatives, the reaction yields would be expected to be negatively impacted.

The calculation of the revenues was difficult to be addressed due to the generation of different product streams (catechol derivatives, phenolic oil, unbleached pulp, and tar streams). However, using current commercial prices indicated in Section 3.1, the profit and loss accounts were negative for all tested cases. In this sense, it was demonstrated the negative influence of the oversized flows that were handled in some stages, on the final cost of the processes, both in the investment as well as in the operational costs.

In any case, the economic evaluation has been important to identify what simulation process presented the best conditions, not as an absolute value but in a comparative way instead. The OS scenario was demonstrated to be the most feasible solution in these conditions since its cost in the FCI and the COM were the lowest of the four different tested scenarios.

V) General Conclusions

5.1. General conclusions

In this work the design of different routes to obtain high-pure lignin samples to be furtherly depolymerized by thermochemical processes was addressed. After the depolymerization, some separation stages were performed to purify the products into different streams: phenolic oil, residual lignin and coke. The quantities and composition of these streams varied with the employed methodology and sources. Finally, a techno-economic analysis of the different proposed routes to obtain phenolic monomer compounds was accomplished with the help of a simulator software to identify the most feasible strategy in terms of process efficiency, energy consumption, and costs.

5.1.1. Lignin extraction from different sources and routes

The survey started with the evaluation of different sources and processes to obtain lignin samples. In this sense, lignin from the agave bagasse and leaves were obtained from the delignification and bleaching stages. Lignin samples extracted from the organosolv process (the delignification stage) presented higher purity, less condensed structure (higher S/G ratio), lower Tg value, and higher extraction yields in comparison with the lignin samples obtained from the bleaching stages. The possibility to obtain lignin from those streams was demonstrated but with more recalcitrant properties, as well as lower extraction yields.

The difference between the lignin properties depending on the source (bagasse or leaves) showed similar properties, excepting for the higher S/G ratio for bagasse samples, but higher yields for the lignin extraction from bagasse, probably due to the higher lignin content in the feedstock.

The inclusion of a pretreatment stage, an autohydrolysis reaction, was evaluated in order to obtain purer lignin samples, based on the reduction of the hemicellulosic content in the solid fraction after this pretreatment. Although the improvement of the purity was not very high, the homogeneity of the obtained lignin samples was increased. This fact could minimize the influence of the initial feedstock on the final properties of the lignin stream, an important problem in current processes that use this type of biomass sources.

The final route to obtain lignin was performed using almond shell and olive tree pruning as lignocellulosic raw materials, comparing two delignification methods after the autohydrolysis stage: organosolv and soda processes.

The main differences were found in the delignification process, being the soda treatment the most profitable in terms of lignin extraction yields, whereas the organosolv process generated the lignin samples with the highest purity, lower Mw sizes, polydispersity

indexes, and greater relative percentages of ether linkages, which are easier to break down to furtherly convert lignin macromolecule into small phenolic compounds.

5.1.2. Lignin depolymerization by thermochemical processes

After the lignin extraction and characterization, some of the obtained samples were submitted to a depolymerization reaction to obtain a phenolic oil as aimed product.

The depolymerization reaction by homogeneous BCD was carried out using lignin samples from almond shell and olive tree pruning as feedstock. As a global trend, higher phenolic oil yields were obtained with lignin samples from the organosolv process and the lignin samples from almond shells presented higher yields than the ones from the olive tree pruning. Focusing on the composition of the phenolic oil, the most abundant monomer found in the oil was catechol and its derivatives, which demonstrated that the guaiacol and syringol compounds were degraded into more elemental products due to the harsh conditions of the reaction. In such frame, demethoxylation, demethylation and dealkylation reactions took placed, leading to the degradation of the lignin monomers into more elemental structures, such as catechol, cresol and their derivative compounds. However, regarding the used precipitation method, no clear influence was observed.

The undesirable repolymerization happened following the same mechanism, regardless the used lignin sample, since it was observed that the chemical composition of all residual lignin presented similar size and yields.

Other methodology was also approached to depolymerize lignin without its previous precipitation or isolation. In this sense, the black liquors from the delignification methods were directly submitted to thermochemical depolymerization reactions. Therefore, two different reaction mechanisms were approached: (i) solvolysis of the lignin for the organosolv black liquors, and (ii) BCD for the soda black liquors.

Similar phenolic oil yields (20-24%) were obtained for all the different tested reactions. The main difference was noticed in the quantities of the byproducts obtained during the reaction. The organosolv liquors produced much more coke (more than 30%) but lower RL (20-30%), whereas the soda liquors produced more residual lignin (40-45%) and much lower amount of coke (below 3%), almost negligible.

Regarding the phenolic monomer compositions, the BCD with the soda liquors led to complete reactions of demethoxylation, demethylation and dealkylation to obtain catechol, cresols and their derivative compounds as main products, in line with previous comments. However, the total yield of monomers generation was found to be three times lower than the ones provided by the lignin solvolysis, which allowed reaching significant high yields.

In addition, the solvolysis mechanism undergone in the case of the black liquors let to obtain unaltered guaiacol and syringol compounds as main products of the phenolic oil.

As a summary, it could be established that the most important parameters to obtain higher phenolic monomer yields were the abundancy of ether linkages and the Mw, although the S/G ratio had also an influence.

Another important conclusion extracted from this work is that, after de depolymerization, the same products were obtained regardless the used lignocellulosic raw material. This fact is considered as an important achievement since it means that it is possible to use different lignocellulosic wastes to obtain the monomers. This fact could reduce one of the most important drawbacks of the process that is the heterogeneity and seasonality of lignocellulosic streams.

Furthermore, an industrial Kraft black liquor was used for testing this approach of direct depolymerization of lignin from black liquors. In this case, the harsh conditions of the reaction, as well as the action of the HS- ions, which catalyzed the depolymerization of lignin, led to obtain similar phenolic oil yields as in the case of the soda liquors. The inclusion of phenol as capping agent worked out as catalyst to increase the product generation since all the products were maximized with values of phenolic oil around 25% higher. On the other hand, the hydrogen peroxide provoked a decrease in the phenolic oil due to the breaking of the aromatic ring of the phenolic molecules to form alkylic acids, which were not measured in the phenolic oil.

In terms of phenolic monomers, phenol also generated the higher value, even the higher in comparison with the other reactions tested before. It was remarkable the different distribution of the measured monomers since more cresols than catechol was obtained in comparison with the blank reaction.

5.1.3. Techno-economic assessment of the phenolic monomer obtaining

The experimental values to obtain phenolic oil from almond shells were used to design some global scenarios, which were developed using Aspen Plus® simulation software to evaluate the most convenience route.

From the lignin extraction section of the tested scenarios, the soda delignification method had greater lignin yield. The most significant difference between both processes was the possibility to recover the solvent from the delignification stage in the organosolv process, which reduced the consumption of chemicals to almost a negligible degree.

In the lignin depolymerization method, it was confirmed that, regardless of the higher lignin amount extracted in the soda process, the organosolv lignin was more suitable to be depolymerized, leading to greater phenolic monomers yield than in the soda processes.

The energetic analysis drove to conclude that the most important parameter to increase the energy consumption was the volume to be treated since, even when an additional distillation column was included in the organosolv delignification method, the final consumption was not much higher because of the lower volumes to be treated in the further depolymerization and purification stages.

The economic analysis was noticeable influenced by the equipment with the harsher stage of the whole process: the depolymerization reactor. Consequently, the cost of utilities and equipment was really influenced by the volume to be treated on this stage. In this sense, the direct liquor depolymerization scenarios showed higher costs because of the bigger volumes to be treated.

Although the obtained products in the tested scenarios were not found to be competitive in the current market, this analysis is compulsory to identify the most suitable strategy, as well as to identify the most important drawbacks to be addressed in further optimization studies.

As a summary, it has to be highlighted that it has been the first time in which a techno-economic assessment of a whole biorefinery process designed from experimental data has been developed. Up to now, the experimental optimizations had been developed to maximize yields of a singular stage, without considering the influence on the global process. For further optimizations, the reduction of the volume to be treated in the reactions, precipitation stages, separation, and cleaning processes will be the main initial consideration. In this sense, the economic feasibility of the global process would be hugely impacted and closer to current industrial processes.

5.2. Recommendations and future work

To continue and widen the research presented in this work, several options could be considered. Regarding the lignin source, its influence on the final lignin depolymerization yields was not observed. However, it was found a clear difference in the S/G ration for the different lignocellulosic source evaluated in this work: agave bagasse and leaves, almond shells, and olive tree pruning. It is thought that the G units are more prone to generate more condensed structures due to the steric availability in the C5 of the aromatic ring, whereas the appearance of a methoxy group in this position for the S units forms more stable molecules, which are less prone to undergo repolymerization reaction. Therefore, although in this work no clear correlation between the S/G ratio and higher phenolic

monomer yields was found, for further studies, it would be interesting to use lignocellulosic sources with higher S/G ratio.

According to the results presented before, the Mw, Mw/Mn and the percentage of ether bonds in the lignin molecule are the most important parameters to maximize the depolymerization yields. In this sense, the organosolv process was more suitable than the soda process since smaller Mw, and Mw/Mn, and higher percentage of ether bonds were found in the lignin samples obtained by this method. In future works, the optimization of the organosolv process parameters in order to improve the properties of the extracted lignin in terms of molecular weight and polydispersity would be very interesting. In addition, the inclusion of different solvents or methodologies (for example, the use of catalyst) to employ softer conditions where lignin would be less damaged is also advised.

The depolymerization of the lignin was accomplished by the routes tested in this work. The strategies to maximize the obtained results should be driven to the lignin extraction methodology as it was mentioned before. In this stage, the future works should address the optimization of this reaction in terms of: (i) the temperature, with the use of metal catalyst to reduce the temperature to cleavage the lignin linkages in order to reduce the great energetic duty of this stage; (ii) the residential time, transforming the tested batch reactions to continuous mode, to avoid repolymerization reactions, as well as minimize the energy demand of this stage; and (iii) the solid/liquid ratio, since it was demonstrated the economic unfeasibility of the experimental works with such high liquid ratios.

References

References

[1] U. Bardi, Peak oil, 20 years later: Failed prediction or useful insight?, Energy Res. Soc. Sci. 48 (2019) 257–261.

[2] A. Jäger-Waldau, Snapshot of Photovoltaics—March 2017, Sustainability. 9 (2017) 783.

[3] F. Cucchiella, I. D'Adamo, M. Gastaldi, F. Cucchiella, I. D'Adamo, M. Gastaldi, Future Trajectories of Renewable Energy Consumption in the European Union, Resources. 7 (2018) 10.

[4] P. del Río, G. Resch, A. Ortner, L. Liebmann, S. Busch, C. Panzer, A techno-economic analysis of EU renewable electricity policy pathways in 2030, Energy Policy. 104 (2017) 484–493.

[5] B. Kamm, P.R. Gruber, M. Kamm, Biorefineries - Industrial Processes and Products, in: Ullmann's Encycl. Ind. Chem., Wiley-VCH Verlag GmbH & Co. KGaA, Weinheim, Germany, 2007.

[6] M. FitzPatrick, P. Champagne, M.F. Cunningham, R.A. Whitney, A biorefinery processing perspective: Treatment of lignocellulosic materials for the production of value-added products, Bioresour. Technol. 101 (2010) 8915–8922.

[7] M. Höök, X. Tang, Depletion of fossil fuels and anthropogenic climate change—A review, Energy Policy. 52 (2013) 797–809.

[8] J.J. Bozell, G.R. Petersen, Technology development for the production of biobased products from biorefinery carbohydrates—the US Department of Energy's "Top 10" revisited, Green Chem. 12 (2010) 539.

[9] L.R. Lynd, C. Wyman, M. Laser, D. Johnson, R. Landucci, Strategic Biorefinery Analysis: Analysis of Biorefineries, 2002. http://www.osti.gov/bridge (accessed January 7, 2019).

[10] Daniel Morán, BioRefineries Blog: European advanced biorefineries at commercial scale, (2019). https://biorrefineria.blogspot.com/p/listado-de-biorrefiern.html (accessed January 13, 2019).

[11] Metsä Fibre, Metsä Group's Bioproduct mill, (2019). https://www.metsafibre.com/en/about-us/Bioproduct-mill/Pages/default.aspx (accessed January 13, 2019).

[12] R. van Ree, B. Annevelink, Status Report Biorefinery 2007, 2007. www.biorefinery.nl (accessed January 13, 2019).

[13] H. Langeveld, M. Meeusen, J. Sanders, The biobased economy: biofuels,

materials and chemicals in the post-oil era, Earthscan, 2010. https://www.osti.gov/etdeweb/biblio/21360718 (accessed January 25, 2019).

[14] D.L. Van Dyne, M.G. Blase, L. Davis Clements, A Strategy for Returning Agriculture and Rural America to Long-Term Full Employment Using Biomass Refineries, 1999. https://www.hort.purdue.edu/newcrop/proceedings1999/pdf/v4-114.pdf (accessed January 13, 2019).

[15] C. Okkerse, H. van Bekkum, From fossil to green, Green Chem. 1 (1999) 107–114.

[16] B. Kamm, M. Kamm, Biorefineries – Multi Product Processes, in: White Biotechnol., Springer Berlin Heidelberg, Berlin, Heidelberg, 2007: pp. 175–204.

[17] F.H. Isikgor, C.R. Becer, Lignocellulosic biomass: a sustainable platform for the production of bio-based chemicals and polymers, Polym. Chem. 6 (2015) 4497–4559.

[18] C.E. Wyman, Aqueous pretreatment of plant biomass for biological and chemical conversion to fuels and chemicals, 2013.

[19] S. Octave, D. Thomas, Biorefinery: Toward an industrial metabolism, Biochimie. 91 (2009) 659–664.

[20] O. Gordobil, New Products from Lignin, University of the Basque Country, 2018. http://weekly.cnbnews.com/news/article.html?no=124000.

[21] D. Fengel, G. Wegener, Wood: chemistry, ultrastructure, reactions, Walter de Gruyter, Berlin, 1989.

[22] E. Sjöström, Wood chemistry: fundamentals and applications, Academic Press, 1993.

[23] J. Fernández-Rodríguez, X. Erdocia, P.L. de Hoyos, A. Sequeiros, J. Labidi, Catalytic Cascade Transformations of Biomass into Polyols, Springer, Singapore. (2017) 187–219.

[24] A. Ebringerová, Z. Hromádková, T. Heinze, Hemicellulose, in: T. Heinze (Ed.), Polysaccharides I Struct. Charact. Use, Springer Berlin Heidelberg, Berlin, Heidelberg, 2005: pp. 1–67.

[25] L. Christopher, ed., Integrated Forest Biorefineries, Royal Society of Chemistry, Cambridge, 2012.

[26] S.C. Fry, The growing plant cell wall: chemical and metabolic analysis., Longman Group Limited, 1988.

[27] W.J. Liu, H. Jiang, H.Q. Yu, Thermochemical conversion of lignin to functional materials: a review and future directions, Green Chem. 17 (2015) 4888–4907.

[28] R.M. Rowell, R.A. Young, J.K. Rowell, Paper and composites from agro-based resources, CRC/Lewis Publishers, 1997.

[29] N. Sorek, T.H. Yeats, H. Szemenyei, H. Youngs, C.R. Somerville, The Implications of Lignocellulosic Biomass Chemical Composition for the Production of Advanced Biofuels, Bioscience. 64 (2014) 192–201.

[30] V. Bischoff, S. Nita, L. Neumetzler, D. Schindelasch, A. Urbain, R. Eshed, S. Persson, D. Delmer, W.-R. Scheible, TRICHOME BIREFRINGENCE and Its Homolog AT5G01360 Encode Plant-Specific DUF231 Proteins Required for Cellulose Biosynthesis in Arabidopsis, Plant Physiol. 153 (2010) 590 LP – 602.

[31] G.J. Seifert, K. Roberts, The Biology of Arabinogalactan Proteins, (2007).

[32] S. V. Vassilev, D. Baxter, L.K. Andersen, C.G. Vassileva, An overview of the chemical composition of biomass, Fuel. 89 (2010) 913–933.

[33] J. Werkelin, B.-J. Skrifvars, M. Hupa, Ash-forming elements in four Scandinavian wood species. Part 1: Summer harvest, Biomass and Bioenergy. 29 (2005) 451–466.

[34] J.W. Gooch, Lignin, in: J.W. Gooch (Ed.), Encycl. Dict. Polym., Springer New York, New York, NY, 2011: p. 427.

[35] N. Smolarski, High-Value Opportunities for Lignin: Unlocking its Potential, 2012. https://www.greenmaterials.fr/wp-content/uploads/2013/01/High-value-Opportunities-for-Lignin-Unlocking-its-Potential-Market-Insights.pdf (accessed January 13, 2019).

[36] J.S. Lupoi, S. Singh, R. Parthasarathi, B.A. Simmons, R.J. Henry, Recent innovations in analytical methods for the qualitative and quantitative assessment of lignin, Renew. Sustain. Energy Rev. 49 (2015) 871–906.

[37] J. Fernández-Rodríguez, X. Erdocia, F. Hernández-Ramos, M.G. Alriols, J. Labidi, Lignin Separation and Fractionation by Ultrafiltration, Sep. Funct. Mol. Food by Membr. Technol. (2019) 229–265.

[38] O. Lanzalunga, M. Bietti, Photo- and radiation chemical induced degradation of lignin model compounds, J. Photochem. Photobiol. B Biol. 56 (2000) 85–108.

[39] A.B. Wardrop, H. Harada, The Formation and Structure of the Cell Wall in Fibres and Tracheids, J. Exp. Bot. 16 (1965) 356–371.

[40] P. Azadi, O.R. Inderwildi, R. Farnood, D.A. King, Liquid fuels, hydrogen and

chemicals from lignin: A critical review, Renew. Sustain. Energy Rev. 21 (2013) 506–523.

[41] R. Parthasarathi, R.A. Romero, A. Redondo, S. Gnanakaran, Theoretical Study of the Remarkably Diverse Linkages in Lignin, J. Phys. Chem. Lett. 2 (2011) 2660–2666.

[42] T. Dutta, N.G. Isern, J. Sun, E. Wang, S. Hull, J.R. Cort, B.A. Simmons, S. Singh, Survey of Lignin-Structure Changes and Depolymerization during Ionic Liquid Pretreatment, (2017).

[43] A.L. Macfarlane, M. Mai, J.F. Kadla, Bio-based chemicals from biorefining: lignin conversion and utilisation, in: Adv. Biorefineries, Woodhead Publishing, 2014: pp. 659–692.

[44] A. Berlin, M. Balakshin, Industrial Lignins: Analysis, Properties, and Applications, Bioenergy Res. Adv. Appl. (2014) 315–336.

[45] G. Cazacu, M. Capraru, V.I. Popa, Advances Concerning Lignin Utilization in New Materials, in: Springer, Berlin, Heidelberg, 2013: pp. 255–312.

[46] A. Naseem, S. Tabasum, K.M. Zia, M. Zuber, M. Ali, A. Noreen, Lignin-derivatives based polymers, blends and composites: A review, Int. J. Biol. Macromol. 93 (2016) 296–313.

[47] W.O.S. Doherty, P. Mousavioun, C.M. Fellows, Value-adding to cellulosic ethanol: Lignin polymers, Ind. Crops Prod. 33 (2011) 259–276.

[48] H. Chung, A. Al-Khouja, N.R. Washburn, Lignin-Based Graft Copolymers via ATRP and Click Chemistry, in: Green Polym. Chem. Biocatal. Mater. II. ACS Symp. Ser. No.1144, Washington, DC, 2013: pp. 373–391.

[49] X. Dong, M. Dong, Y. Lu, A. Turley, T. Jin, C. Wu, Antimicrobial and antioxidant activities of lignin from residue of corn stover to ethanol production, Ind. Crops Prod. 34 (2011) 1629–1634.

[50] J. Lora, Industrial commercial lignins: sources, properties and applications, in: M.N. Belgacem, A. Gandini (Eds.), Monomers, Polym. Compos. from Renew. Resour., Elsevier, Amsterdam, 2008: pp. 225–241.

[51] W. Schutyser, T. Renders, S. Van den Bosch, S.-F. Koelewijn, G.T. Beckham, B.F. Sels, Chemicals from lignin: an interplay of lignocellulose fractionation, depolymerisation, and upgrading, Chem. Soc. Rev. 47 (2018) 852–908.

[52] G.A. Smook, Handbook for pulp and paper technologists, Third, Angus Wlide Publications Inc., Vancouver, 2002. http://agris.fao.org/agris-search/search.do?recordID=US201300693483 (accessed January 13, 2019).

[53] H. Sixta, ed., Handbook of Pulp, Wiley-VCH Verlag GmbH, Weinheim, Germany, 2006.

[54] H.L. Hintz, Paper: Pulping and Bleaching, Encycl. Mater. Sci. Technol. (2001) 6707–6711.

[55] T. Llano, N. García-Quevedo, N. Quijorna, J.R. Viguri, A. Coz, Evolution of Lignocellulosic Macrocomponents in the Wastewater Streams of a Sulfite Pulp Mill: A Preliminary Biorefining Approach, J. Chem. 2015 (2015) 1–10.

[56] G. Yu, B. Li, H. Wang, C. Liu, X. Mu, Preparation of Concrete Superplasticizer by Oxidation-Sulfomethylation of Sodium Lignosulfonate, BioResources. 8 (2013) 1055–1063.

[57] M. V. Galkin, J.S.M. Samec, Lignin Valorization through Catalytic Lignocellulose Fractionation: A Fundamental Platform for the Future Biorefinery, ChemSusChem. 9 (2016) 1544–1558.

[58] M. V. Galkin, J.S.M. Samec, Lignin Valorization through Catalytic Lignocellulose Fractionation: A Fundamental Platform for the Future Biorefinery, ChemSusChem. 9 (2016) 1544–1558.

[59] S. V. Patil, D.S. Argyropoulos, Stable Organic Radicals in Lignin: A Review, ChemSusChem. 10 (2017) 3284–3303.

[60] C. Li, X. Zhao, A. Wang, G.W. Huber, T. Zhang, Catalytic Transformation of Lignin for the Production of Chemicals and Fuels, Chem. Rev. 115 (2015) 11559–11624.

[61] T. Aro, P. Fatehi, Production and Application of Lignosulfonates and Sulfonated Lignin, ChemSusChem. 10 (2017) 1861–1877.

[62] A. Rahimi, A. Ulbrich, J.J. Coon, S.S. Stahl, Formic-acid-induced depolymerization of oxidized lignin to aromatics, Nature. 515 (2014) 249–252.

[63] G.F. Dahl, US296935A - Pulping cellulose-containing materials with inorganic bases or alkaline reacting compounds, e.g. sulfate processes in presence of S-containing compounds, 1884. https://patents.google.com/patent/US296935 (accessed November 17, 2019).

[64] G.H. Tomlinson, US2285876A - Waste sulphite liquor recovery, 1938. https://patents.google.com/patent/US2285876A/en (accessed November 17, 2019).

[65] M. Ragnar, G. Henriksson, M.E. Lindström, M. Wimby, J. Blechschmidt, S. Heinemann, Pulp, in: Ullmann's Encycl. Ind. Chem., Wiley-VCH Verlag GmbH & Co. KGaA, Weinheim, Germany, 2014: pp. 1–92.

[66] R. Rinaldi, R. Jastrzebski, M.T. Clough, J. Ralph, M. Kennema, P.C.A. Bruijnincx, B.M. Weckhuysen, Paving the Way for Lignin Valorisation: Recent Advances in Bioengineering, Biorefining and Catalysis, Angew. Chemie Int. Ed. 55 (2016) 8164–8215.

[67] P.C.A. Bruijnincx, R. Rinaldi, B.M. Weckhuysen, Unlocking the potential of a sleeping giant: lignins as sustainable raw materials for renewable fuels, chemicals and materials, Green Chem. 17 (2015) 4860–4861.

[68] R. Patt, O. Kordsachia, R. Suttinger, Pulp, in: Ullmann's Encycl. Ind. Chem., WILEY-VCH Verlag, Weinheim, 2012: pp. 476–539.

[69] P. Huber, A. Burnet, M. Petit-Conil, Scale deposits in kraft pulp bleach plants with reduced water consumption: A review, J. Environ. Manage. 141 (2014) 36–50.

[70] H. Tran, E.K. Vakkilainnen, The Kraft chemical recovery process, in: TAPPI Kraft Recover, 2012.

[71] K. Kuparinen, E. Vakkilainen, T. Tynjälä, Biomass-based carbon capture and utilization in kraft pulp mills, Mitig. Adapt. Strateg. Glob. Chang. (2019).

[72] S. Gillet, M. Aguedo, L. Petitjean, A.R.C. Morais, A.M. da Costa Lopes, R.M. Łukasik, P.T. Anastas, Lignin transformations for high value applications: towards targeted modifications using green chemistry, Green Chem. 19 (2017) 4200–4233.

[73] J.-P. Lange, Renewable Feedstocks: The Problem of Catalyst Deactivation and its Mitigation, Angew. Chemie Int. Ed. 54 (2015) 13186–13197.

[74] S. Laurichesse, L. Avérous, Chemical modification of lignins: Towards biobased polymers, Prog. Polym. Sci. 39 (2014) 1266–1290.

[75] M.P. Vinardell, V. Ugartondo, M. Mitjans, Potential applications of antioxidant lignins from different sources, Ind. Crops Prod. 27 (2008) 220–223.

[76] O. Gordobil, R. Herrera, M. Yahyaoui, S. İlk, M. Kaya, J. Labidi, Potential use of kraft and organosolv lignins as a natural additive for healthcare products, RSC Adv. 8 (2018) 24525–24533.

[77] F. Öhman, H. Wallmo, H. Theliander, An improved method for washing lignin precipitated from kraft black liquor - the key to a new biofuel, Filtration. 7 (2007) 309–315.

[78] H. Wallmo, H. Theliander, H. Theliander, A.-S. Jönsson, O. Wallberg, K. Lindgren, The influence of hemicelluloses during the precipitation of lignin in kraft black liquor, Nord. Pulp Pap. Res. J. 24 (2009) 165–171.

[79] P. Tomani, The LignoBoost Process, Cellul. Chem. Technol. 44 (2010) 53–58.

https://pdfs.semanticscholar.org/0812/1594360601ae6c8eab8a7616e452ad458fde.pdf (accessed January 19, 2019).

[80] L. Kouisni, A. Gagné, K. Maki, P. Holt-Hindle, M. Paleologou, LignoForce System for the Recovery of Lignin from Black Liquor: Feedstock Options, Odor Profile, and Product Characterization, (2016).

[81] V.B. Agbor, N. Cicek, R. Sparling, A. Berlin, D.B. Levin, Biomass pretreatment: Fundamentals toward application, Biotechnol. Adv. 29 (2011) 675–685.

[82] F.G. Calvo-Flores, J.A. Dobado, J. Isac-García, F.J. Martín-Martínez, Lignin and Lignans as Renewable Raw Materials, John Wiley & Sons, Ltd, Chichester, UK, 2015.

[83] P. Azadi, O.R. Inderwildi, R. Farnood, D.A. King, Liquid fuels, hydrogen and chemicals from lignin: A critical review, Renew. Sustain. Energy Rev. 21 (2013) 506–523.

[84] S. Gillet, M. Aguedo, L. Petitjean, A.R.C. Morais, A.M. da Costa Lopes, R.M. Łukasik, P.T. Anastas, Lignin transformations for high value applications: towards targeted modifications using green chemistry, Green Chem. 19 (2017) 4200–4233.

[85] A.N. Evdokimov, · Alexander, V. Kurzin, · Olesya, V. Fedorova, P. V Lukanin, V.G. Kazakov, A.D. Trifonova, Desulfurization of kraft lignin, Wood Sci Technol. 52 (2018) 1165–1174.

[86] C. Li, X. Zhao, A. Wang, G.W. Huber, T. Zhang, Catalytic Transformation of Lignin for the Production of Chemicals and Fuels, Chem. Rev. 115 (2015) 11559–11624.

[87] M.G. Alriols, A. Tejado, M. Blanco, I. Mondragon, J. Labidi, Agricultural palm oil tree residues as raw material for cellulose, lignin and hemicelluloses production by ethylene glycol pulping process, Chem. Eng. J. 148 (2009) 106–114.

[88] L. Capolupo, V. Faraco, Green methods of lignocellulose pretreatment for biorefinery development, Appl. Microbiol. Biotechnol. 100 (2016) 9451–9467.

[89] C. Løhre, G.-A.A. Laugerud, W.J.J. Huijgen, T. Barth, Lignin-to-Liquid-Solvolysis (LtL) of Organosolv Extracted Lignin, ACS Sustain. Chem. Eng. 6 (2018) 3102–3112.

[90] Z. Xu, F. Huang, Pretreatment Methods for Bioethanol Production, Appl. Biochem. Biotechnol. 174 (2014) 43–62.

[91] E. Kiran, H. Balkan, High-pressure extraction and delignification of red spruce with binary and ternary mixtures of acetic acid, water, and supercritical carbon dioxide, J. Supercrit. Fluids. 7 (1994) 75–86.

[92] M.P. Pandey, C.S. Kim, Lignin Depolymerization and Conversion: A Review of Thermochemical Methods, Chem. Eng. Technol. 34 (2011) 29–41.

[93] B.B. Hallac, Y. Pu, A.J. Ragauskas, Chemical Transformations of Buddleja davidii Lignin during Ethanol Organosolv Pretreatment, (2010).

[94] J. Zakzeski, P.C.A. Bruijnincx, A.L. Jongerius, B.M. Weckhuysen, The Catalytic Valorization of Lignin for the Production of Renewable Chemicals, Chem. Rev. 110 (2010) 3552–3599.

[95] X. Zhao, S. Li, R. Wu, D. Liu, Organosolv fractionating pre-treatment of lignocellulosic biomass for efficient enzymatic saccharification: chemistry, kinetics, and substrate structures, Biofuels, Bioprod. Biorefining. 11 (2017) 567–590.

[96] N. V. Plechkova, K.R. Seddon, Applications of ionic liquids in the chemical industry, Chem. Soc. Rev. 37 (2008) 123–150.

[97] L. Weigand, S. Mostame, A. Brandt-Talbot, T. Welton, J.P. Hallett, Effect of pretreatment severity on the cellulose and lignin isolated from Salix using ionoSolv pretreatment, Faraday Discuss. 202 (2017) 331–349.

[98] J.-L. Wen, T.-Q. Yuan, S.-L. Sun, F. Xu, R.-C. Sun, Understanding the chemical transformations of lignin during ionic liquid pretreatment, Green Chem. 16 (2014) 181–190.

[99] A. George, A. Brandt, K. Tran, S.M.S.N.S. Zahari, D. Klein-Marcuschamer, N. Sun, N. Sathitsuksanoh, J. Shi, V. Stavila, R. Parthasarathi, S. Singh, B.M. Holmes, T. Welton, B.A. Simmons, J.P. Hallett, Design of low-cost ionic liquids for lignocellulosic biomass pretreatment, Green Chem. 17 (2015) 1728–1734.

[100] Y. Dai, J. van Spronsen, G.-J. Witkamp, R. Verpoorte, Y.H. Choi, Natural deep eutectic solvents as new potential media for green technology, Anal. Chim. Acta. 766 (2013) 61–68.

[101] Z.-L. Huang, B.-P. Wu, Q. Wen, T.-X. Yang, Z. Yang, Deep eutectic solvents can be viable enzyme activators and stabilizers, J. Chem. Technol. Biotechnol. 89 (2014) 1975–1981.

[102] A.K. Kumar, B.S. Parikh, M. Pravakar, Natural deep eutectic solvent mediated pretreatment of rice straw: bioanalytical characterization of lignin extract and enzymatic hydrolysis of pretreated biomass residue, Environ. Sci. Pollut. Res. 23 (2016) 9265–9275.

[103] C. Alvarez-Vasco, R. Ma, M. Quintero, M. Guo, S. Geleynse, K.K. Ramasamy, M. Wolcott, X. Zhang, Green Chemistry Cutting-edge research for a greener sustainable future www.rsc.org/greenchem Unique low-molecular-weight lignin with high purity extracted from wood by deep eutectic solvents (DES): a source of

lignin for valorization †, Green Chem. 18 (2016) 5133.

[104] J.E. Holladay, J.F. White, J.J. Bozell, D. Johnson, Top Value-Added Chemicals from Biomass - Volume II—Results of Screening for Potential Candidates from Biorefinery Lignin, Richland, WA (United States), 2007.

[105] B. Rößiger, G. Unkelbach, D. Pufky-Heinrich, Base-Catalyzed Depolymerization of Lignin: History, Challenges and Perspectives, in: Lignin - Trends Appl., InTech, 2018.

[106] A. Rodriguez, D. Salvachúa, R. Katahira, B.A. Black, N.S. Cleveland, M. Reed, H. Smith, E.E.K. Baidoo, J.D. Keasling, B.A. Simmons, G.T. Beckham, J.M. Gladden, Base-Catalyzed Depolymerization of Solid Lignin-Rich Streams Enables Microbial Conversion, ACS Sustain. Chem. Eng. 5 (2017) 8171–8180.

[107] V.M. Roberts, V. Stein, T. Reiner, A. Lemonidou , X. Li, J.A. Lercher, Towards Quantitative Catalytic Lignin Depolymerization, Chem. - A Eur. J. 17 (2011) 5939–5948.

[108] R. Beauchet, F. Monteil-Rivera, J.M. Lavoie, Conversion of lignin to aromatic-based chemicals (L-chems) and biofuels (L-fuels), Bioresour. Technol. 121 (2012) 328–334.

[109] J. Fernández-Rodríguez, X. Erdocia, C. Sánchez, M. González Alriols, J. Labidi, Lignin depolymerization for phenolic monomers production by sustainable processes, J. Energy Chem. 26 (2017) 622–631.

[110] L. Du, Z. Wang, S. Li, W. Song, W. Lin, A Comparison of Monomeric Phenols Produced from Lignin by Fast Pyrolysis and Hydrothermal Conversions, Int. J. Chem. React. Eng. 11 (2013) 1–11.

[111] A. Toledano, L. Serrano, J. Labidi, Organosolv lignin depolymerization with different base catalysts, J. Chem. Technol. Biotechnol. 87 (2012) 1593–1599.

[112] X. Bai, K.H. Kim, R.C. Brown, E. Dalluge, C. Hutchinson, Y.J. Lee, D. Dalluge, Formation of phenolic oligomers during fast pyrolysis of lignin, Fuel. 128 (2014) 170–179.

[113] J. Long, Q. Zhang, T. Wang, X. Zhang, Y. Xu, L. Ma, An efficient and economical process for lignin depolymerization in biomass-derived solvent tetrahydrofuran, Bioresour. Technol. 154 (2014) 10–17.

[114] K.H. Kim, C.S. Kim, Recent Efforts to Prevent Undesirable Reactions From Fractionation to Depolymerization of Lignin: Toward Maximizing the Value From Lignin, Front. Energy Res. 6 (2018) 92.

[115] M.M. Hepditch, R.W. Thring, Degradation of solvolysis lignin using Lewis acid

catalysts, Can. J. Chem. Eng. 78 (2000) 226–231.

[116] B. Güvenatam, E.H.J. Heeres, E.A. Pidko, E.J.M. Hensen, Lewis-acid catalyzed depolymerization of Protobind lignin in supercritical water and ethanol, Catal. Today. 259 (2016) 460–466.

[117] R. Jastrzebski, S. Constant, C.S. Lancefield, N.J. Westwood, B.M. Weckhuysen, P.C.A. Bruijnincx, Tandem Catalytic Depolymerization of Lignin by Water-Tolerant Lewis Acids and Rhodium Complexes, ChemSusChem. 9 (2016) 2074–2079.

[118] M. Kleinert, T. Barth, Phenols from Lignin, Chem. Eng. Technol. 31 (2008) 736–745.

[119] R.J.A. Gosselink, W. Teunissen, J.E.G. van Dam, E. de Jong, G. Gellerstedt, E.L. Scott, J.P.M. Sanders, Lignin depolymerisation in supercritical carbon dioxide/acetone/water fluid for the production of aromatic chemicals, Bioresour. Technol. 106 (2012) 173–177.

[120] T. Yoshikawa, T. Yagi, S. Shinohara, T. Fukunaga, Y. Nakasaka, T. Tago, T. Masuda, Production of phenols from lignin via depolymerization and catalytic cracking, Fuel Process. Technol. 108 (2013) 69–75.

[121] A. Margellou, K. Triantafyllidis, A. Margellou, K.S. Triantafyllidis, Catalytic Transfer Hydrogenolysis Reactions for Lignin Valorization to Fuels and Chemicals, Catalysts. 9 (2019) 43.

[122] P.J. Deuss, M. Scott, F. Tran, N.J. Westwood, J.G. de Vries, K. Barta, Aromatic Monomers by in Situ Conversion of Reactive Intermediates in the Acid-Catalyzed Depolymerization of Lignin, J. Am. Chem. Soc. 137 (2015) 7456–7467.

[123] Z. Sun, B. Fridrich, A. de Santi, S. Elangovan, K. Barta, Bright Side of Lignin Depolymerization: Toward New Platform Chemicals, Chem. Rev. 118 (2018) 614–678.

[124] M. V. Galkin, S. Sawadjoon, V. Rohde, M. Dawange, J.S.M. Samec, Mild Heterogeneous Palladium-Catalyzed Cleavage of β- *O* -4'-Ether Linkages of Lignin Model Compounds and Native Lignin in Air, ChemCatChem. 6 (2014) 179–184.

[125] A. Kloekhorst, H.J. Heeres, Catalytic Hydrotreatment of Alcell Lignin Using Supported Ru, Pd, and Cu Catalysts, ACS Sustain. Chem. Eng. 3 (2015) 1905–1914.

[126] A. Narani, R.K. Chowdari, C. Cannilla, G. Bonura, F. Frusteri, H.J. Heeres, K. Barta, Efficient catalytic hydrotreatment of Kraft lignin to alkylphenolics using supported NiW and NiMo catalysts in supercritical methanol, Green Chem. 17 (2015) 5046–5057.

[127] A. Toledano, L. Serrano, J. Labidi, Improving base catalyzed lignin depolymerization by avoiding lignin repolymerization, Fuel. 116 (2014) 617–624.

[128] J. Long, Y. Xu, T. Wang, Z. Yuan, R. Shu, Q. Zhang, L. Ma, Efficient base-catalyzed decomposition and in situ hydrogenolysis process for lignin depolymerization and char elimination, Appl. Energy. 141 (2015) 70–79.

[129] A. Vigneault, D.K. Johnson, E. Chornet, Base-Catalyzed Depolymerization of Lignin: Separation of Monomers, Can. J. Chem. Eng. 85 (2008) 906–916.

[130] S. Van den Bosch, S.-F. Koelewijn, T. Renders, G. Van den Bossche, T. Vangeel, W. Schutyser, B.F. Sels, Catalytic Strategies Towards Lignin-Derived Chemicals, Top. Curr. Chem. 376 (2018) 36.

[131] C. Zhao, J.A. Lercher, Catalytic Depolymerization and Deoxygenation of Lignin, in: Role Catal. Sustain. Prod. Bio-Fuels Bio-Chemicals, Elsevier, 2013: pp. 289–320.

[132] X. Huang, T.I. Korányi, M.D. Boot, E.J.M. Hensen, Ethanol as capping agent and formaldehyde scavenger for efficient depolymerization of lignin to aromatics, Green Chem. 17 (2015) 4941–4950.

[133] E. Feghali, T. Cantat, Unprecedented organocatalytic reduction of lignin model compounds to phenols and primary alcohols using hydrosilanes, Chem. Commun. 50 (2014) 862–865.

[134] J. Fernández-Rodríguez, X. Erdocia, P.L. De Hoyos, M. González Alriols, J. Labidi, Small Phenolic Compounds Production from Kraft Black Liquor by Lignin Depolymerization with Different Catalytic Agents, in: Chem. Eng. Trans., 2017: pp. 133–138.

[135] T. Vangeel, W. Schutyser, T. Renders, B.F. Sels, Perspective on Lignin Oxidation: Advances, Challenges, and Future Directions, Top. Curr. Chem. 376 (2018) 30.

[136] P. Cerruti, S.M. Alzamora, S.L. Vidales, Vanillin as an Antimicrobial for Producing Shelf-stable Strawberry Puree, J. Food Sci. 62 (1997) 608–610.

[137] M. Fache, B. Boutevin, S. Caillol, Vanillin Production from Lignin and Its Use as a Renewable Chemical, ACS Sustain. Chem. Eng. 4 (2016) 35–46.

[138] P.C. Rodrigues Pinto, E.A. Borges da Silva, A.E. Rodrigues, Lignin as Source of Fine Chemicals: Vanillin and Syringaldehyde, in: Biomass Convers., Springer Berlin Heidelberg, Berlin, Heidelberg, 2012: pp. 381–420.

[139] J.C. Villar, A. Caperos, F. García-Ochoa, Oxidation of hardwood kraft-lignin to phenolic derivatives with oxygen as oxidant, Wood Sci. Technol. 35 (2001) 245–255.

[140] A.L. Mathias, A.E. Rodrigues, Production of Vanillin by Oxidation of Pine Kraft Lignins with Oxygen, Holzforschung. 49 (1995) 273–278.

[141] H. Werhan, J.M. Mir, T. Voitl, P. Rudolf von Rohr, Acidic oxidation of kraft lignin into aromatic monomers catalyzed by transition metal salts, Holzforschung. 65 (2011) 703–709.

[142] H. Werhan, N. Assmann, P. Rudolf von Rohr, Lignin oxidation studies in a continuous two-phase flow microreactor, Chem. Eng. Process. Process Intensif. 73 (2013) 29–37.

[143] R. Ma, M. Guo, X. Zhang, Selective Conversion of Biorefinery Lignin into Dicarboxylic Acids, ChemSusChem. 7 (2014) 412–415.

[144] E. Dorrestijn, M. Kranenburg, D. Poinsot, P. Mulder, Lignin Depolymerization in Hydrogen-Donor Solvents, Holzforschung. 53 (1999) 611–616.

[145] T.L.-K. Yong, Y. Matsumura, Kinetic Analysis of Lignin Hydrothermal Conversion in Sub- and Supercritical Water, Ind. Eng. Chem. Res. 52 (2013) 5626–5639.

[146] H. Pińkowska, P. Wolak, A. Złocińska, Hydrothermal decomposition of alkali lignin in sub- and supercritical water, Chem. Eng. J. 187 (2012) 410–414.

[147] Y. Ye, J. Fan, J. Chang, Effect of reaction conditions on hydrothermal degradation of cornstalk lignin, J. Anal. Appl. Pyrolysis. 94 (2012) 190–195.

[148] H. Lee, J. Jae, J.-M. Ha, D.J. Suh, Hydro- and solvothermolysis of kraft lignin for maximizing production of monomeric aromatic chemicals, Bioresour. Technol. 203 (2016) 142–149.

[149] Wahyudiono, M. Sasaki, M. Goto, Recovery of phenolic compounds through the decomposition of lignin in near and supercritical water, Chem. Eng. Process. Process Intensif. 47 (2008) 1609–1619.

[150] R. Lou, S. Wu, G. Lyu, Quantified monophenols in the bio-oil derived from lignin fast pyrolysis, J. Anal. Appl. Pyrolysis. 111 (2015) 27–32.

[151] L. Fan, Y. Zhang, S. Liu, N. Zhou, P. Chen, Y. Cheng, M. Addy, Q. Lu, M.M. Omar, Y. Liu, Y. Wang, L. Dai, E. Anderson, P. Peng, H. Lei, R. Ruan, Bio-oil from fast pyrolysis of lignin: Effects of process and upgrading parameters, Bioresour. Technol. 241 (2017) 1118–1126.

[152] P.R. Patwardhan, R.C. Brown, B.H. Shanks, Understanding the Fast Pyrolysis of Lignin, ChemSusChem. 4 (2011) 1629–1636.

[153] O. Faix, D. Meier, Pyrolytic and hydrogenolytic degradation studies on lignocellulosics, pulps and lignins, Holz Als Roh- Und Werkst. 47 (1989) 67–72.

[154] D.J. Nowakowski, A.V. Bridgwater, D.C. Elliott, D. Meier, P. de Wild, Lignin fast pyrolysis: Results from an international collaboration, J. Anal. Appl. Pyrolysis. 88 (2010) 53–72.

[155] S. Zhou, R.C. Brown, X. Bai, The use of calcium hydroxide pretreatment to overcome agglomeration of technical lignin during fast pyrolysis, Green Chem. 17 (2015) 4748–4759.

[156] S. Zhou, Y. Xue, A. Sharma, X. Bai, Lignin Valorization through Thermochemical Conversion: Comparison of Hardwood, Softwood and Herbaceous Lignin, ACS Sustain. Chem. Eng. 4 (2016) 6608–6617.

[157] L. Zhang, Z. Bao, S. Xia, Q. Lu, K. Walters, L. Zhang, Z. Bao, S. Xia, Q. Lu, K.B. Walters, Catalytic Pyrolysis of Biomass and Polymer Wastes, Catalysts. 8 (2018) 659.

[158] Z. Ma, E. Troussard, J.A. van Bokhoven, Controlling the selectivity to chemicals from lignin via catalytic fast pyrolysis, Appl. Catal. A Gen. 423–424 (2012) 130–136.

[159] Y. Zhao, L. Deng, B. Liao, Y. Fu, Q.-X. Guo, Aromatics Production via Catalytic Pyrolysis of Pyrolytic Lignins from Bio-Oil, Energy & Fuels. 24 (2010) 5735–5740.

[160] N. Scarlat, M. Martinov, J.-F. Dallemand, Assessment of the availability of agricultural crop residues in the European Union: Potential and limitations for bioenergy use, Waste Manag. 30 (2010) 1889–1897.

[161] Ence, Resumen Plan Estratégico 2019-2023, (2018). https://ence.es/wp-content/uploads/pdf/Resumen_Plan_Estrategico_2019_2023.pdf (accessed March 18, 2019).

[162] X. Wang, L. Meng, F. Wu, Y. Jiang, L. Wang, X. Mu, Efficient conversion of microcrystalline cellulose to 1,2-alkanediols over supported Ni catalysts, Green Chem. 14 (2012) 758.

[163] K.L. Galindo-Hernández, A. Tapia-Rodríguez, F. Alatriste-Mondragón, L.B. Celis, J. Arreola-Vargas, E. Razo-Flores, Enhancing saccharification of Agave tequilana bagasse by oxidative delignification and enzymatic synergism for the production of hydrogen and methane, Int. J. Hydrogen Energy. 43 (2018) 22116–22125.

[164] Consejo Regulador del Téquila, CRT, (2019). https://www.crt.org.mx/EstadisticasCRTweb/ (accessed March 18, 2019).

[165] G. Iñíguez-Covarrubias, R. Díaz-Teres, R. Sanjuan-Duenas, J. Anzaldo-Hernández, R.M. Rowell, Utilization of by-products from the tequila industry. Part 2: Potential value of Agave tequilana Weber azul leaves, Bioresour. Technol. 77 (2001) 101–108.

[166] J.R. Rubio-Ríos, R.A. Guzmán-Plazola, V. Ayala-Escobar, R. Rubio-Cortés, Spatial and temporal dynamics of blue agave (Agave tequilana Weber var. azul) wilt in Jalisco Mexico, J. Phytopathol. 167 (2019) 299–311.

[167] G. Campos-Rivero, L.F. Sánchez-Teyer, E.A. De la Cruz-Arguijo, M.S. Ramírez-González, C.P. Larralde-Corona, J.A. Narváez-Zapata, Bioprospecting for fungi with potential pathogenic activity on leaves of Agave tequilana Weber var. Azul, J. Phytopathol. 167 (2019) 283–294.

[168] E. Robles, I. Urruzola, J. Labidi, L. Serrano, Surface-modified nano-cellulose as reinforcement in poly(lactic acid) to conform new composites, Ind. Crops Prod. 71 (2015) 44–53.

[169] E. Robles, A.M. Salaberria, R. Herrera, S.C.M. Fernandes, J. Labidi, Self-bonded composite films based on cellulose nanofibers and chitin nanocrystals as antifungal materials, Carbohydr. Polym. 144 (2016) 41–49.

[170] V. Akubude, K.N. Nwaigwe, Economic Importance of edible and non-edible almond fruit as bionergy material: a review, Am. J. Energy Sci. 3 (2016) 31–39.

[171] P. y A. Ministerio de Agricultura, Encuesta sobre superficies y rendimientos de consumo, 2018. https://cpage.mpr.gob.es (accessed March 13, 2019).

[172] E. Toklu, Biomass energy potential and utilization in Turkey, Renew. Energy. 107 (2017) 235–244.

[173] P.L. de Hoyos-Martínez, X. Erdocia, F. Charrier-El Bouhtoury, R. Prado, J. Labidi, Multistage treatment of almonds waste biomass: Characterization and assessment of the potential applications of raw material and products, Waste Manag. 80 (2018) 40–50.

[174] M.S. İzgi, C. Saka, O. Baytar, G. Saraçoğlu, Ö. Şahin, Preparation and Characterization of Activated Carbon from Microwave and Conventional Heated Almond Shells Using Phosphoric Acid Activation, Anal. Lett. 52 (2019) 772–789.

[175] D. Nabarlatz, A. Ebringerová, D. Montané, Autohydrolysis of agricultural by-products for the production of xylo-oligosaccharides, Carbohydr. Polym. 69 (2007) 20–28.

[176] A.M. García, A.I. García, M.Á.L. Cabezas, A.S. Reche, Study of the Influence of the Almond Variety in the Properties of Injected Parts with Biodegradable Almond Shell Based Masterbatches, Waste and Biomass Valorization. 6 (2015) 363–370.

[177] Junta de Andalucía, The Spanish Olive Tree and OLive oil production (Olea Europeae) Andalucia.com, (2019). http://www.andalucia.com/environment/olivetrees.htm (accessed March 18, 2019).

[178] E. Rugini, C. Silvestri, Somatic Embryogenesis in Olive (Olea europaea L. subsp. europaea var. sativa and var. sylvestris), in: Humana Press, New York, NY, 2016: pp. 341–349.

[179] D. Zohary, M. Hopf, Domestication of plants in the Old World: the origin and spread of cultivated plants in West Asia, Europe and the Nile Valley., Domest. Plants Old World Orig. Spread Cultiv. Plants West Asia, Eur. Nile Val. (2000). https://www.cabdirect.org/cabdirect/abstract/20013014838 (accessed March 18, 2019).

[180] J.D. Rejón García, C. Suárez, J. de D. Alché Ramírez, A.J. Castro, M.I.R. García, Evaluación de diferentes métodos para estimar la calidad del polen en distintos cultivares de olivo (Olea Europaea L.), Polen. 20 (2012) 60–72.

[181] J.C. Martínez-Patiño, E. Ruiz, I. Romero, C. Cara, J.C. López-Linares, E. Castro, Combined acid/alkaline-peroxide pretreatment of olive tree biomass for bioethanol production, Bioresour. Technol. 239 (2017) 326–335.

[182] M.J. Negro, P. Manzanares, E. Castro, M. Ballesteros, J.C. López-Linares, E. Ruiz, F.J. Gallego, Residual biomass potential in olive tree cultivation and olive oil industry in Spain: valorization proposal in a biorefinery context, Spanish J. Agric. Res. 15 (2017) e0206.

[183] A. Ashori, W.D. Raverty, J. Harun, Effect of Totally Chlorine Free and Elemental Chlorine Free Sequences on Whole Stem Kenaf (*Hibiscus cannabinus*) Pulp Characteristics, Polym. Plast. Technol. Eng. 45 (2006) 205–211.

[184] M.B. Roncero, A.L. Torres, J.F. Colom, T. Vidal, Effect of xylanase on ozone bleaching kinetics and properties of Eucalyptus kraft pulp, J. Chem. Technol. Biotechnol. 78 (2003) 1023–1031.

[185] N. Rehman, M.I.G. de Miranda, S.M.L. Rosa, D.M. Pimentel, S.M.B. Nachtigall, C.I.D. Bica, Cellulose and Nanocellulose from Maize Straw: An Insight on the Crystal Properties, J. Polym. Environ. 22 (2013) 252–259.

[186] K.R. Solomon, M. Hanson, Reducing Ecotoxicity, in: Handb. Green Chem., Wiley-VCH Verlag GmbH & Co. KGaA, Weinheim, Germany, 2012: pp. 407–452.

[187] D. Stewart, Lignin as a base material for materials applications: Chemistry, application and economics, Ind. Crops Prod. 27 (2008) 202–207.

[188] E. Robles, J. Fernández-Rodríguez, A.M. Barbosa, O. Gordobil, N.L.V. Carreño, J. Labidi, Production of cellulose nanoparticles from blue agave waste treated with environmentally friendly processes, Carbohydr. Polym. (2018).

[189] M. Karimi Alavijeh, S. Yaghmaei, Biochemical production of bioenergy from agricultural crops and residue in Iran, Waste Manag. 52 (2016) 375–394.

[190] J. Fernández-Rodríguez, O. Gordobil, E. Robles, M. González-Alriols, J. Labidi, Lignin valorization from side-streams produced during agricultural waste pulping and total chlorine free bleaching, J. Clean. Prod. 142 (2017) 2609–2617.

[191] O. Gordobil, I. Egüés, R. Llano-Ponte, J. Labidi, Physicochemical properties of PLA lignin blends, Polym. Degrad. Stab. 108 (2014) 330–338.

[192] A. Sequeiros, D.A. Gatto, J. Labidi, L. Serrano, Different Extraction Methods to Obtain Lignin from Almond Shell, J. Biobased Mater. Bioenergy. 8 (2014) 370–376.

[193] T.-Q. Yuan, S.-N. Sun, F. Xu, R.-C. Sun, Characterization of lignin structures and LCC linkages by quantitative 13C and 2D HSQC NMR spectroscopy., J. Agric. Food Chem. (2011) 174–178.

[194] M. Lawoko, G. Henriksson, G. Gellerstedt, Characterisation of lignin-carbohydrate complexes (LCCs) of spruce wood (Picea abies L.) isolated with two methods, Holzforschung. 60 (2006) 156–161.

[195] N. Cachet, S. Camy, B. Benjelloun-Mlayah, J.-S. Condoret, M. Delmas, Esterification of organosolv lignin under supercritical conditions, Ind. Crops Prod. 58 (2014) 287–297.

[196] S.N. Sun, M.F. Li, T.Q. Yuan, F. Xu, R.C. Sun, Sequential extractions and structural characterization of lignin with ethanol and alkali from bamboo (Neosinocalamus affinis), Ind. Crops Prod. 37 (2012) 51–60.

[197] N.-E. El Mansouri, J. Salvadó, Structural characterization of technical lignins for the production of adhesives: Application to lignosulfonate, kraft, soda-anthraquinone, organosolv and ethanol process lignins, Ind. Crops Prod. 24 (2006) 8–16.

[198] J. Rencoret, G. Marques, A. Gutiérrez, L. Nieto, J.I. Santos, J. Jiménez-Barbero, Á.T. Martínez, J.C. Del Río, HSQC-NMR analysis of lignin in woody (Eucalyptus globulus and Picea abies) and non-woody (Agave sisalana) ball-milled plant materials at the gel state, Holzforschung. 63 (2009) 691–698.

[199] F. Xu, J.-X. Sun, R. Sun, P. Fowler, M.S. Baird, Comparative study of organosolv lignins from wheat straw, Ind. Crops Prod. 23 (2006) 180–193.

[200] J. Hu, R. Xiao, D. Shen, H. Zhang, Structural analysis of lignin residue from black liquor and its thermal performance in thermogravimetric-Fourier transform infrared spectroscopy, Bioresour. Technol. 128 (2013) 633–639.

[201] M.S. Jahan, D.A.N. Chowdhury, M.K. Islam, S.M.I. Moeiz, Characterization of lignin isolated from some nonwood available in Bangladesh, Bioresour. Technol. 98 (2007) 465–469.

[202] Kevin M. Holtman, A. Hou-min Chang, J.F. Kadla, Solution-State Nuclear Magnetic Resonance Study of the Similarities between Milled Wood Lignin and Cellulolytic Enzyme Lignin, (2004).

[203] S. Wang, B. Ru, H. Lin, W. Sun, Z. Luo, Pyrolysis behaviors of four lignin polymers isolated from the same pine wood, Bioresour. Technol. 182 (2015) 120–127.

[204] Z. Ma, Q. Sun, J. Ye, Q. Yao, C. Zhao, Study on the thermal degradation behaviors and kinetics of alkali lignin for production of phenolic-rich bio-oil using TGA–FTIR and Py–GC/MS, J. Anal. Appl. Pyrolysis. 117 (2016) 116–124.

[205] D. Shen, G. Liu, J. Zhao, J. Xue, S. Guan, R. Xiao, Thermo-chemical conversion of lignin to aromatic compounds: Effect of lignin source and reaction temperature, J. Anal. Appl. Pyrolysis. 112 (2015) 56–65.

[206] O. Gordobil, R. Delucis, I. Egüés, J. Labidi, Kraft lignin as filler in PLA to improve ductility and thermal properties, Ind. Crops Prod. 72 (2015) 46–53.

[207] A. Awal, M. Sain, Characterization of soda hardwood lignin and the formation of lignin fibers by melt spinning, J. Appl. Polym. Sci. 129 (2013) 2765–2771.

[208] C. Crestini, F. Melone, M. Sette, R. Saladino, Milled Wood Lignin: A Linear Oligomer, Biomacromolecules. 12 (2011) 3928–3935.

[209] H. Hatakeyama, T. Hatakeyama, Lignin Structure, Properties, and Applications, in: Springer, Berlin, Heidelberg, 2009: pp. 1–63.

[210] F. Monteil-Rivera, M. Phuong, M. Ye, A. Halasz, J. Hawari, Isolation and characterization of herbaceous lignins for applications in biomaterials, Ind. Crops Prod. 41 (2013) 356–364.

[211] J. Zhao, W. Xiuwen, J. Hu, Q. Liu, D. Shen, R. Xiao, Thermal degradation of softwood lignin and hardwood lignin by TG-FTIR and Py-GC/MS, Polym. Degrad. Stab. 108 (2014) 133–138.

[212] C. Sánchez, L. Serrano, M.A. Andres, J. Labidi, Furfural production from corn cobs autohydrolysis liquors by microwave technology, Ind. Crops Prod. 42 (2013) 513–519.

[213] M. Nagy, M. Kosa, H. Theliander, A.J. Ragauskas, Characterization of CO_2 precipitated Kraft lignin to promote its utilization, Green Chem. 12 (2010) 31–34.

[214] J. Ponomarenko, T. Dizhbite, M. Lauberts, A. Viksna, G. Dobele, O. Bikovens, G. Telysheva, Characterization of softwood and hardwood lignoboost kraft lignins with emphasis on their antioxidant activity, BioResources. 9 (2014) 2051–2068.

[215] T.-Q. Yuan, J. He, F. Xu, R.-C. Sun, Fractionation and physico-chemical analysis

of degraded lignins from the black liquor of Eucalyptus pellita KP-AQ pulping, Polym. Degrad. Stab. 94 (2009) 1142–1150.

[216] W.J.J. Huijgen, J.H. Reith, H. den Uil, Pretreatment and Fractionation of Wheat Straw by an Acetone-Based Organosolv Process, Ind. Eng. Chem. Res. 49 (2010) 10132–10140.

[217] A. Toledano, L. Serrano, J. Labidi, Enhancement of Lignin Production from Olive Tree Pruning Integrated in a Green Biorefinery, Ind. Eng. Chem. Res. 50 (2011) 6573–6579.

[218] I. Urruzola, E. Robles, L. Serrano, J. Labidi, Nanopaper from almond (Prunus dulcis) shell, Cellulose. 21 (2014) 1619–1629.

[219] A. Toledano, I. Alegría, J. Labidi, Biorefining of olive tree (Olea europea) pruning, Biomass and Bioenergy. 59 (2013) 503–511.

[220] R.J.A. Gosselink, A. Abächerli, H. Semke, R. Malherbe, P. Käuper, A. Nadif, J.E.G. van Dam, Analytical protocols for characterisation of sulphur-free lignin, Ind. Crops Prod. 19 (2004) 271–281.

[221] A. Toledano, X. Erdocia, L. Serrano, J. Labidi, Influence of extraction treatment on olive tree (Olea europaea) pruning lignin structure, Environ. Prog. Sustain. Energy. 32 (2013) 1187–1194.

[222] A. Vishtal, A. Kraslawski, Challenges in industrial applications of technical lignins, BioResources. 6 (2011) 3547–3568.

[223] G.H. Van Der Klashorst, H.F. Strauss, Polymerization of lignin model compounds with formaldehyde in acidic aqueous medium, J. Polym. Sci. Part A Polym. Chem. 24 (1986) 2143–2169.

[224] C. Heitner, D. Dimmel, J. Schmidt, D. Dimmel, J. Schmidt, Lignin and Lignans, CRC Press, 2010.

[225] J.L. Wen, S.L. Sun, B.L. Xue, R.C. Sun, Recent advances in characterization of lignin polymer by solution-state nuclear magnetic resonance (NMR) methodology, Materials (Basel). 6 (2013) 359–391.

[226] M. Jablonsky, S. Andrea, H. Ľudmila, J. Michal, Š. Andrea, H. Aleš, Lignin, potential products and their market value, Wood Res. 60 (2015) 973–986. https://www.researchgate.net/publication/286449542 (accessed April 9, 2019).

[227] Government of Gujarat, Chemicals and Petrochemicals Government of Gujarat, in: Connect. India to World. 8th Glob. Summit, Gujarat, 2017. http://www.ineos.com/businesses/ineos-phenol/markets (accessed April 9, 2019).

[228] F.W. Ago, Phenol Europe, (2017) 3–5.

[229] M. Weber, M. Weber, Phenols, in: Phenolic Resins A Century Prog., Springer Berlin Heidelberg, Berlin, Heidelberg, 2010: pp. 9–23.

[230] M. Weber, M. Weber, M. Kleine-Boymann, Phenol, in: Ullmann's Encycl. Ind. Chem., Wiley-VCH Verlag GmbH & Co. KGaA, Weinheim, Germany, 2004.

[231] H. Fiege, H.-W. Voges, H.-J. Buysch, D. Garbe, Phenol Derivatives; in: Ullmann's Encyclopedia of Industrial Chemistry, (n.d.).

[232] P.W. Hart, Cost Estimation of Specialty Chemicals From Laboratory-Scale Prices, Cost Eng. 39 (2015) 1–6.

[233] L. Krumenacker, M. Constantini, P. Pontal, J. Sentenac, Hydroquinone, resorcinol, and catechol, in: Kirk-Othmer Encycl. Chem. Technol., n.d. https://onlinelibrary.wiley.com/doi/pdf/10.1002/0471238961.0825041811182113.a01 (accessed April 7, 2019).

[234] H. Fiege, Cresols and Xylenols, in: Ullmann's Encycl. Ind. Chem., Wiley-VCH Verlag GmbH & Co. KGaA, Weinheim, 2012: pp. 420–462.

[235] Cresol Market Size Projected To Reach $795.7 Million By 2024, (n.d.). https://www.grandviewresearch.com/press-release/global-cresol-market (accessed April 17, 2019).

[236] S. Buddoo, Process for the preparation of vanillin from a mixed m-cresol/p-cresol stream, Port Elizabeth Technikon, 2003. https://core.ac.uk/download/pdf/145050730.pdf (accessed April 9, 2019).

[237] P. Feng, H. Wang, H. Lin, Y. Zheng, Selective production of guaiacol from black liquor: Effect of solvents, Carbon Resour. Convers. 2 (2019) 1–12.

[238] C. Srinivasulu, M. Ramgopal, G. Ramanjaneyulu, C.M. Anuradha, C. Suresh Kumar, Syringic acid (SA) – A Review of Its Occurrence, Biosynthesis, Pharmacological and Industrial Importance, Biomed. Pharmacother. 108 (2018) 547–557.

[239] P. Varanasi, P. Singh, M. Auer, P.D. Adams, B.A. Simmons, S. Singh, Survey of renewable chemicals produced from lignocellulosic biomass during ionic liquid pretreatment, 2013.

[240] X. Erdocia, R. Prado, M.Á. Corcuera, J. Labidi, Base catalyzed depolymerization of lignin: Influence of organosolv lignin nature, Biomass and Bioenergy. 66 (2014) 379–386.

[241] C. Zhao, J.A. Lercher, Catalytic Depolymerization and Deoxygenation of Lignin,

Role Catal. Sustain. Prod. Bio-Fuels Bio-Chemicals. (2013) 289–320.

[242] J.E. Miller, L.R. Evans, J.E. Mudd, K.A. Brown, Batch Microreactor Studies of Lignin Depolymerization by Bases. 2. Aqueous Solvents, 2002. http://www.doe.gov/bridge (accessed April 17, 2019).

[243] A. Toledano, L. Serrano, J. Labidi, Extraction and revalorization of olive tree (Olea europea) pruning lignin, J. Taiwan Inst. Chem. Eng. 44 (2013) 552–559.

[244] A. Toledano, L. Serrano, J. Labidi, A. Pineda, A.M. Balu, R. Luque, Heterogeneously Catalysed Mild Hydrogenolytic Depolymerisation of Lignin Under Microwave Irradiation with Hydrogen-Donating Solvents, ChemCatChem. 5 (2013) 977–985.

[245] A. Toledano, L. Serrano, A.M. Balu, R. Luque, A. Pineda, J. Labidi, Fractionation of organosolv lignin from olive tree clippings and its valorization to simple phenolic compounds, ChemSusChem. 6 (2013) 529–536.

[246] A. Toledano, L. Serrano, A. Pineda, A.A. Romero, R. Luque, J. Labidi, Microwave-assisted depolymerisation of organosolv lignin via mild hydrogen-free hydrogenolysis: Catalyst screening, Appl. Catal. B Environ. 145 (2014) 43–55.

[247] R. Prado, X. Erdocia, J. Labidi, Effect of the photocatalytic activity of TiO2 on lignin depolymerization, Chemosphere. 91 (2013) 1355–1361.

[248] R. Prado, X. Erdocia, G.F. De Gregorio, J. Labidi, T. Welton, Willow Lignin Oxidation and Depolymerization under Low Cost Ionic Liquid, ACS Sustain. Chem. Eng. 4 (2016) 5277–5288.

[249] R. Prado, A. Brandt, X. Erdocia, J. Hallet, T. Welton, J. Labidi, Lignin oxidation and depolymerisation in ionic liquids, Green Chem. 18 (2016) 834–841.

[250] X. Erdocia, R. Prado, M.A. Corcuera, J. Labidi, Influence of Reaction Conditions on Lignin Hydrothermal Treatment, Front. Energy Res. 2 (2014) 13.

[251] X. Erdocia, R. Prado, J. Fernández-Rodríguez, J. Labidi, Depolymerization of Different Organosolv Lignins in Supercritical Methanol, Ethanol, and Acetone to Produce Phenolic Monomers, ACS Sustain. Chem. Eng. 4 (2016).

[252] P.S.B. Dos Santos, X. Erdocia, D.A. Gatto, J. Labidi, Bio-oil from base-catalyzed depolymerization of organosolv lignin as an antifungal agent for wood, Wood Sci. Technol. 50 (2016) 599–615.

[253] X. Erdocia, M.Á. Corcuera, J. Labidi, Novel method for the depolymerisation of lignin, US20160289256 A1, 2016. https://encrypted.google.com/patents/US20160289256?cl=un (accessed March 18, 2018).

[254] N. Mahmood, Z. Yuan, J. Schmidt, C. (Charles) Xu, Preparation of bio-based rigid polyurethane foam using hydrolytically depolymerized Kraft lignin via direct replacement or oxypropylation, Eur. Polym. J. 68 (2015) 1–9.

[255] S. Nenkova, T. Vasileva, K. Stanulov, Production of phenol compounds by alkaline treatment of technical hydrolysis lignin and wood biomass, Chem. Nat. Compd. 44 (2008) 182–185.

[256] S. Mukundan, L. Atanda, J. Beltramini, Thermocatalytic cleavage of C–C and C–O bonds in model compounds and kraft lignin by $NiMoS_2$ /C nanocatalysts, Sustain. Energy Fuels. 3 (2019) 1317–1328.

[257] S.O. Limarta, J.-M. Ha, Y.-K. Park, H. Lee, D.J. Suh, J. Jae, Efficient depolymerization of lignin in supercritical ethanol by a combination of metal and base catalysts, J. Ind. Eng. Chem. 57 (2018) 45–54.

[258] S. Dabral, J. Engel, J. Mottweiler, S.S.M. Spoehrle, C.W. Lahive, C. Bolm, Mechanistic studies of base-catalysed lignin depolymerisation in dimethyl carbonate, Green Chem. 20 (2018) 170–182.

[259] J. Long, Q. Zhang, T. Wang, X. Zhang, Y. Xu, L. Ma, An efficient and economical process for lignin depolymerization in biomass-derived solvent tetrahydrofuran, Bioresour. Technol. 154 (2014) 10–17.

[260] R. Chaudhary, P.L. Dhepe, Solid base catalyzed depolymerization of lignin into low molecular weight products, Green Chem. 19 (2017) 778–788.

[261] X. Erdocia, A. Toledano, M.Á. Corcuera, J. Labidi, Organosolv black liquor hydrolysis to obtain low molecular weight phenolic compounds, Chem. Eng. Trans. 29 (2012) 535–540.

[262] N. Abatzoglou, E. Chornet, K. Belkacemi, R.P. Overend, Phenomenological kinetics of complex systems: the development of a generalized severity parameter and its application to lignocellulosics fractionation, Chem. Eng. Sci. 47 (1992) 1109–1122.

[263] A. Svärd, E. Brännvall, U. Edlund, Rapeseed straw polymeric hemicelluloses obtained by extraction methods based on severity factor, Ind. Crops Prod. 95 (2017) 305–315.

[264] A. Toledano, L. Serrano, J. Labidi, Organosolv lignin depolymerization with different base catalysts, J. Chem. Technol. Biotechnol. 87 (2012) 1593–1599.

[265] M. Kumar, A. Olajire Oyedun, A. Kumar, A review on the current status of various hydrothermal technologies on biomass feedstock, Renew. Sustain. Energy Rev. 81 (2018) 1742–1770.

[266] K. Okuda, M. Umetsu, S. Takami, T. Adschiri, Disassembly of lignin and chemical recovery—rapid depolymerization of lignin without char formation in water–phenol mixtures, Fuel Process. Technol. 85 (2004) 803–813.

[267] C. Guizani, D. Lachenal, C. Guizani, D. Lachenal, Controlling the Molecular Weight of Lignosulfonates by an Alkaline Oxidative Treatment at Moderate Temperatures and Atmospheric Pressure: A Size-Exclusion and Reverse-Phase Chromatography Study, Int. J. Mol. Sci. 18 (2017) 2520.

[268] M. Haddad, R. Labrecque, L. Bazinet, O. Savadogo, J. Paris, Effect of process variables on the performance of electrochemical acidification of Kraft black liquor by electrodialysis with bipolar membrane, Chem. Eng. J. 304 (2016) 977–985.

[269] O. Gordobil, A. Oberemko, G. Saulis, V. Baublys, J. Labidi, In vitro cytotoxicity studies of industrial Eucalyptus kraft lignins on mouse hepatoma, melanoma and Chinese hamster ovary cells, Int. J. Biol. Macromol. 135 (2019) 353–361.

[270] R. Patt, O. Kordsachia, R. Süttinger, Y. Ohtani, J.F. Hoesch, P. Ehrler, R. Eichinger, H. Holik, U. Hamm, M.E. Rohmann, P. Mummenhoff, E. Petermann, R.F. Miller, D. Frank, R. Wilken, H.L. Baumgarten, G.-H. Rentrop, Paper and Pulp, in: Ullmann's Encycl. Ind. Chem., Wiley-VCH Verlag GmbH & Co. KGaA, Weinheim, Germany, 2000.

[271] G. Towler, R. Sinnott, CHEMICAL ENGINEERING DESIGN Principles, Practice and Economics of Plant and Process Design, 2008. http://elsevier.com (accessed June 15, 2019).

[272] H.-J. Huang, W. Lin, S. Ramaswamy, U. Tschirner, Process Modeling of Comprehensive Integrated Forest Biorefinery—An Integrated Approach, Appl. Biochem. Biotechnol. 154 (2009) 26–37.

[273] R.J. Wooley, V. Putsche, Development of an ASPEN PLUS Physical Property Database for Biofuels Components, 1996. https://www.nrel.gov/docs/legosti/old/20685.pdf.

[274] J. Moncada, I. Vural Gursel, W.J.J. Huijgen, J.W. Dijkstra, A. Ramírez, Techno-economic and ex-ante environmental assessment of C6 sugars production from spruce and corn. Comparison of organosolv and wet milling technologies, J. Clean. Prod. 170 (2018) 610–624.

[275] L.C. Nhien, N.V.D. Long, S. Kim, M. Lee, Techno-economic assessment of hybrid extraction and distillation processes for furfural production from lignocellulosic biomass, Biotechnol. Biofuels. 10 (2017) 81.

[276] A.D. Celebi, A.V. Ensinas, S. Sharma, F. Maréchal, Early-stage decision making approach for the selection of optimally integrated biorefinery processes, Energy.

137 (2017) 908–916.

[277] R. Nitzsche, M. Budzinski, A. Gröngröft, Techno-economic assessment of a wood-based biorefinery concept for the production of polymer-grade ethylene, organosolv lignin and fuel, Bioresour. Technol. 200 (2016) 928–939.

[278] A. Mabrouk, X. Erdocia, M.G. Alriols, J. Labidi, Economic analysis of a biorefinery process for catechol production from lignin, J. Clean. Prod. 198 (2018) 133–142.

[279] P. Cozma, W. Wukovits, I. Mămăligă, A. Friedl, M. Gavrilescu, Modeling and simulation of high pressure water scrubbing technology applied for biogas upgrading, Clean Technol. Environ. Policy. 17 (2014).

[280] A. Gutiérrez, J.C. del Río, F.J. González-Vila, F. Martín, Analysis of lipophilic extractives from wood and pitch deposits by solid-phase extraction and gas chromatography, J. Chromatogr. A. 823 (1998) 449–455.

[281] C.S.R. Freire, P.C.R. Pinto, A.S. Santiago, A.J.D. Silvestre, V. Evtuguin, C.P. Neto, Comparative study of lipophilic extractives of hardwoods and corresponding ECF bleached Kraft pulps, BioResources. 1 (2006) 3–17.

[282] I.C. Kemp, Pinch analysis and process integration: a user guide on process integration for the efficient use of energy, Butterworth-Heinemann, 2007.

[283] J. Sadhukhan, K.S. Ng, E.M. Hernandez, Biorefineries and Chemical Processes, John Wiley & Sons, Ltd, Chichester, UK, 2014.

[284] K.S. Ng, J. Sadhukhan, Techno-economic performance analysis of bio-oil based Fischer-Tropsch and CHP synthesis platform, Biomass and Bioenergy. 35 (2011) 3218–3234.

[285] K.S. Ng, J. Sadhukhan, Process integration and economic analysis of bio-oil platform for the production of methanol and combined heat and power, Biomass and Bioenergy. 35 (2011) 1153–1169.

[286] H.P. Loh, J. Lyons, C.W. White, Process Equipment Cost Estimation, Final Report, Pittsburgh, PA, and Morgantown, WV (United States), 2002.

[287] C.N. Hamelinck, A.P.. Faaij, Future prospects for production of methanol and hydrogen from biomass, J. Power Sources. 111 (2002) 1–22.

[288] S.B. Jones, C. Valkenburg, C.W. Walton, D.C. Elliott, J.E. Holladay, D.J. Stevens, C. Kinchin, S. Czernik, Production of Gasoline and Diesel from Biomass via Fast Pyrolysis, Hydrotreating and Hydrocracking: A Design Case, Richland, WA, 2009.

[289] L.T. Biegler, I.E. Grossmann, A.W. Westerberg, Systematic methods for chemical process design, (1997). https://www.osti.gov/biblio/293030 (accessed February

16, 2019).

[290] L.T. Biegler, I.E. Grossmann, A.W. Westerberg, Systematic methods of chemical process design, Prentice Hall PTR, 1997.

[291] M.S. Peters, K.D. Timmerhaus, R.E. West, Plant Design and Economics for Chemical Engineers, 5th Editio, McGrawHill, New York, 2011.

[292] M. Sharifzadeh, N. Shah, Comparative studies of CO2 capture solvents for gas-fired power plants: Integrated modelling and pilot plant assessments, Int. J. Greenh. Gas Control. 43 (2015) 124–132.

[293] A.J.J. Straathof, A. Bampouli, Potential of commodity chemicals to become bio-based according to maximum yields and petrochemical prices, Biofuels, Bioprod. Biorefining. 11 (2017) 798–810.

[294] C.G. Boeriu, D. Bravo, R.J.A. Gosselink, J.E.G. van Dam, Characterisation of structure-dependent functional properties of lignin with infrared spectroscopy, Ind. Crops Prod. 20 (2004) 205–218.

[295] R. Herrera, X. Erdocia, R. Llano-Ponte, J. Labidi, Characterization of hydrothermally treated wood in relation to changes on its chemical composition and physical properties, J. Anal. Appl. Pyrolysis. 107 (2014) 256–266.

[296] L. Chen, X. Wang, H. Yang, Q. Lu, D. Li, Q. Yang, H. Chen, Study on pyrolysis behaviors of non-woody lignins with TG-FTIR and Py-GC/MS, J. Anal. Appl. Pyrolysis. 113 (2015) 499–507.

[297] H. Li, A.G. McDonald, Fractionation and characterization of industrial lignins, Ind. Crops Prod. 62 (2014) 67–76.

[298] D. Schorr, P.N. Diouf, T. Stevanovic, Evaluation of industrial lignins for biocomposites production, Ind. Crops Prod. 52 (2014) 65–73.

[299] C.H. Vane, The molecular composition of lignin in spruce decayed by white-rot fungi (Phanerochaete chrysosporium and Trametes versicolor) using pyrolysis-GC-MS and thermochemolysis with tetramethylammonium hydroxide, Int. Biodeterior. Biodegrad. 51 (2003) 67–75.

Appendix

Appendix A: Materials

Blue agave (*agave tequilana Weber var. azul*) bagasse and leaves were provided by Finca Santiago Neuhtitán from Amatitán, Jalisco, Mexico. Bagasse is obtained from tequila industry in which the succulent core of the blue agave plant (pinapple) is subjected to an autohydrolysis, after these cooked cores are shredded or mashed; leaves (or stalk) are trimmed from the core and depithed with an industrial depither.

Almond shells, obtained from *prunus amygdalus* tree and olive tree pruning, from *olea europaea* species, were kindly supplied by local farmers. Both materials were conditioned and grounded to obtain size particles between 0.25–0.40 cm before their use.

Kraft black liquor was supplied by "Papelera Guipuzcoana de Zicuñaga" (Spain), whose raw material used for pulp manufacturing is eucalyptus hardwood.

The rest of reagents were provided by Sigma-Aldrich.

Appendix B: Reactors

Autohydrolysis, soda and organosolv reactions were carried out in a 4 L batch reactor (EL0723 Iberfluid) equipped with a pressure and temperature PC-controller.

The depolymerization reactions were conducted in a batch reactor (5500 Parr reactor) with a 4848 Reactor controller.

Appendix C: Analytical methods

Lignocellulosic biomass streams were characterized in terms of their macro-component content using TAPPI standard methods. Moisture (TAPPI T264 cm-07), inorganic content (TAPPI T211 om-12), ethanol-toluene extractives (TAPPI T204 cm-07), Klason lignin (TAPPI T222 om-11), holocellulose (Wise et al. 1946), cellulose (Rowell 1984) and hemicelluloses, as difference between hollocellulose and cellulose; were the list of methods followed to accomplish such characterization.

Black liquors were characterized by its density, measuring the weight in a known volume previously weighed. Total dissolved solids (TDS) were determined using a method based on TAPPI T264 cm-97 to determinate furtherly the moisture content. Inorganic matter was determined after combustion of the sample at 525 ºC using a method based on TAPPI T211 om-93 to calculate the ash content. Organic matter was determined by the difference between total dissolved solids and inorganic matter. Lignin content was estimated by its precipitation, considering that all lignin was isolated by this technique. The precipitation

step was carried out by the acidification of the liquor by adding H_2SO_4 until pH = 2. To separate the solid, a filtration through a 0.45 mm nylon filter was performed. Finally, the precipitated lignin was washed twice with acidified water (pH = 2) and then dried at 50 ºC. Lignin content was gravimetrically calculated.

Solid lignin samples were physico-chemically characterized by different methods. Acid Insoluble Lignin (AIL) as well as Acid Soluble Lignin (ASL) were measured following the method used by Gosselink et al. [294]. The sugar content that represents impurities in lignin samples was determined by means of High-Performance Liquid Chromatography (HPLC) Jasco LC-Net II/ADC equipped with a Rezex ROA-Organic Acid H^+ (8%) column, photodiade array detector and refractive index detector over the liquid fraction obtained during the AIL experiment. Samples were analyzed with a 0.005 N H_2SO_4 dissolution with 100% deionized and degassed HPLC water at 30ºC, 0.35 mL·min^{-1} flow and 40 µL as injection volume. For the calibration, high purity standards of arabinose, xylose, and glucose (≥ 99%) were used. The inorganic content of the lignin samples was measured using a Mettler Toledo TGA/SDTA RSI analyzer through a thermogravimetric analysis (TGA). Around 6-7 mg of the lignin samples were heated from 25 up to 800 ºC at a rate of 10ºC·min^{-1} using air atmosphere with constant flow.

The comparison of the molecular size of the different samples collected along the process for both agave sources was developed determining the molecular weight average (M_w), and polydispersity index (M_w/M_n) by Gel Permeation Chromatography (GPC). A Jasco LC-Net II/ADC device, equipped with a reflex index detector, PolarGel-M column (300 mm 7.5 mm) and PolarGel-M guard (50 mm 7.5 mm), was used for this purpose. Samples were analyzed with dimethylformamide as mobile phase with 0.1% of lithium bromide, with a 0.7 mL min^{-1} flow at 40 ºC. The calibration method was carried out using polystyrene standards ranging from 266 to 70,000 g·mol^{-1}.

Functional groups of the lignin samples were analyzed by Fourier Transform Infrared (FT-IR) technique. The spectra were recorded on a PerkinElmer Spectrum Two Spectrometer, equipped with a Universal Attenuated Total Reflectance (ATR) accessory with internal reflection diamond crystal lens. The defined range was from 800 to 4,000 cm^{-1} and the resolution 8 cm^{-1}. For each sample 10 scans were recorded.

The ^{1}H NMR analysis was carried out using 100 mg of lignin samples, acetylated in 1 mL of anhydrous pyridine and 1 mL of acetic anhydride. After 24 h at room temperature, 10 mL diethyl ether was added to precipitate the lignin. The lignin was washed three times with about 5 mL of diethyl ether to remove pyridine. The acetylated lignin was dried and ^{1}H NMR spectra were recorded with 20 mg acetylated lignin dissolved in 0.5 mL of $CDCl_3$

using a Bruker 400 MHz spectrometer at 400 MHz. Tetramethylsilane (5 mg) was used as internal standard.

For the 2D HSQC NMR, around 50 mg of lignin was dissolved in 0.5 mL of DMSO-d_6. 2D HSQC NMR spectra were recorded at 25 ºC in a Bruker AVANCE 500 MHz equipped with a z-gradient double resonance probe. The spectral widths for the HSQC were 5000 and 12,300 Hz for the ^{1}H and ^{13}C dimensions, respectively. The number of collected complex points was 1024 for the ^{1}H dimension with a recycle delay of 1.5 s. The number of transients was 64, and 256 times increments were always recorded in the ^{13}C dimension. The 1JCH used was 145 Hz. Prior to Fourier transformation, the data matrices were zero filled to 2048 points in the ^{13}C dimension. Data processing was performed using MestReNova software. The central solvent (DMSO) peak was used as an internal chemical shift reference point (δC/δH 39.5/2.49).

The Py–GC–MS was carried out using a 5150 Pyroprobe pyrolyzer (CDS Analytical Inc., Oxford, PA). The identification of the pyrolysis products was accomplished using a GC-MS instrument (Agilent Techs. Inc. 6890 GC/5973 MSD). The Py-GC-MS was carried out following the method described by Herrera and co-workers [295]. A quantity between 400-800 mg was pyrolyzed in a quartz boat at 600 ºC for 15 s with a heating rate of 20 ºC/ms (ramp-off) with the interface kept at 260 ºC. The pyrolyzates were purged from the pyrolysis interface into the GC injector under inert conditions using helium gas. The fused-silica capillary column used was an Equity-1701(30 m x 0.20 mm x 0.25 μm). The GC oven program started at 50 ºC and was held for 2 min. Then it was raised to 120 ºC at 10 ºC·min^{-1} and was held for 5 min after that raised to 280 ºC at 10 ºC·min^{-1}. was held for 8 min and finally raised to 300 ºC at 10 ºC·min^{-1} and was held for 10 min. The compounds were identified by comparing their mass spectra with the National Institute of Standards Library (NIST) and with compounds reported in the literature [190,296–299].

The thermal behavior of the lignin samples was studied by Differential Scanning Calorimetry (DSC) and Thermogravimetric Analysis (TGA). The TGA analyses were carried out with the same equipment mentioned above for ash content quantification in lignin samples. Samples about 5-10 mg were tested under nitrogen atmosphere at a heating rate of 10 ºC·min^{-1} from 25 ºC to 800 ºC. The glass transition temperature of lignins was determined with a METTLER TOLEDO DSC 822 differential scanning calorimeter. Samples of ~5-10 mg were tested under nitrogen atmosphere at a heating rate of 10 ºC·min^{-1}. The isolated lignins were heated from 25 ºC to 200 ºC. Each sample was first run from 25 to 100 ºC (10 min) and cooled down to 25 ºC to eliminate any interference of water.

Phenolic oil was characterized based on the monomeric phenolic compounds that constituted this stream. The oil was dissolved in ethyl acetate (HPLC grade) in a metric

flask. The solution was injected in a GC (7890A)-MS (5975C inert MSD with Triple-Axis Detector) Agilent equipped with a capillary column HP-5MS ((5%-Phenyl)-methylpolysiloxane, 30 m x 0.25 mm). The temperature program started at 50 ºC; then, the temperature was raised to 120 ºC at 10 ºC·min^{-1}, held at this temperature for 5 min, raised to 280 ºC at 10 C·min^{-1}, held at this temperature for 8 min, raised to 300 ºC at 10 ºC·min^{-1} and held at this temperature for 2 min. Helium was used as carrier gas. Calibration was done using pure compounds (Sigma-Aldrich) phenol, *o*-cresol, *m*-cresol, *p*-cresol, guaiacol, catechol, 3-methylcatechol, 4-methylcatechol, 4-ethylcatechol, 3-methoxycatechol, syringol, 4-hydroxybenzaldehyde, acetovanillone, veratrol, 4-hydroxybenzoic acid, 4-hydroxy-3-methoxyphenylacetone, vanillin, vanillic acid, syringaldehyde, 3,5-dimethoxy-4-hydroxyacetophenone and syringic acid.

The measurement of the organic acids contained in the aqueous phase collected after the liquid-liquid extraction with ethyl acetate was analyzed by High Performance Liquid Chromatography (HPLC) with a Jasco LC Net II/ADC chromatographequipped with a refractive index detector and a photodiode arraydetector. A sample of the liquid phase was used for the analysis of acetic acid, furfural and hydroxymethylfurfural using a PhenomenexRezex ROA column; the mobile phase (0.005 N H_2SO_4) was eluted at a flow rate of 0.35 mL/min at 60°C.

Appendix D: List of Publications

Publication I:

Lignin valorization from side-streams produced during agricultural waste pulping and total chlorine free bleaching. **J. Fernández-Rodríguez**, O. Gordobil, E. Robles, M. González Alriols, and J. Labidi. Journal of Cleaner Production. 142 (2017) 2609-2617.

Publication II

Lignin depolymerization for phenolic monomers production by sustainable processes. **J. Fernández-Rodríguez**, X. Erdocia, C. Sánchez, M. González Alriols, J. Labidi. Journal of Energy Chemistry. 26 (2017) 622-631.

Publication III

Direct lignin depolymerization process from sulfur-free black liquors. **J. Fernández-Rodríguez**, X. Erdocia, F. Hernández-Ramos, O. Gordobil, M. González Alriols, J. Labidi. Fuel Processing Technology. 197 (2020) 106201.

Publication IV

Small phenolic compounds production from Kraft black liquor by lignin depolymerization with different catalytic agents. **J. Fernández-Rodríguez**, X. Erdocia, P. L. de Hoyos, M. González Alriols, J. Labidi. Chemical Engineering Transactions. 57 (2017).

Publication V

Techno-economic analysis of different integrated biorefinery scenarios using lignocellulosic waste streams as source for phenolic alcohols production. **J. Fernández-Rodríguez**, X. Erdocia, M. González Alriols, J. Labidi. Journal of Industrial and Engineering Chemistry (*Under revision*).

Appendix D: List of Figures

Appendix E: List of Tables

Agradecimientos

Sin querer desmerecer la ayuda recibida por otros compañeros, creo que esta tesis puede ser considerada como uno de los trabajos donde las ayudas, no externas sino colaterales, han tenido una mayor relevancia. Es por ello que no puedo cerrar esta etapa sin hacer mención especial a aquellas personas que han sido profundamente importantes en la consecución de este trabajo, ya haya sido directa o indirectamente.

Comenzando de manera políticamente correcta, quisiera agradecer a mis directores de tesis. A Jalel, por haberme dado la oportunidad cuando no era la opción más sencilla, por haber sido comprensivo con mis circunstancias y por los consejos en momentos complicados. A María, por haber soportado tan estoicamente mis "aspenaicas" frustraciones, así como hacer mis trabajos sencillamente mejores.

Quisiera proseguir con todos aquellos compañeros que he tenido la oportunidad de conocer en el Departamento de Ingeniería Química y del Medio Ambiente del Campus de Gipuzkoa. No sólo en BioRP, pero también con el resto de compañeros del departamento, he podido vivir muchas y muy buenas vivencias todo este tiempo. Porque en los comienzos no me sentí un foráneo, por los cafés, por vuestras preguntas sobre la industria privada, por las cenas y post-cenas.

No obstante, debo y quiero destacar a los miembros de BioRP con los que he coincidido durante todos estos años. Desde mis comienzos en el máster, cuando era un voluntarioso trabajador hasta mis días finales, donde principalmente iba a pediros auxilio. Algunos explícitamente, otros de forma más implícita, pero vuestra influencia es incalculablemente notable en mi forma de trabajo. Muchas gracias por haberme enriquecido tanto durante estos años, siempre estaré eternamente agradecido e intentando seguir aprendiendo de vosotros. Mención especial quisiera hacer a Xabi, pues sin ninguna duda esta tesis tendría que llevar su nombre más allá que en el apartado de las referencias (aunque ya he incluido unas cuantas). Su constante ayuda ha posibilitado y mejorado este trabajo. Siempre me sentiré un afortunado de haber caído en el denominado "Proyecto del Ministerio".

A los "kaiku-ak", quienes hacen mi día a día más llevadero, además de haber sido unos profesores increíbles, tanto en mi desarrollo personal como profesional.

A mi familia ñoñostiarra. A Aritz, por las que hemos hecho y las que nos quedan. Y por haberme enseñado tanto de psicología, sobre todo en terrenos bastante ignorados por mí en su día. A Edu, a quien no sabría bien si emplazarlo en la zona profesional o personal de los agradecimientos. Eres un profesional de lo personal. Incansable amigo, en cualquier ambiente. Sólo puedo desearte lo mejor en el futuro y decirte que siempre serás familia, carnal. Siempre estaré abierto a charlas intra o extra-lignocelulósicas.

No olvido los orígenes donde comenzó esta aventura científica. A Cris, quien empezó a inculcarme la curiosidad y rigor científicos cuando no sabía que era ni siquiera la lignina. A mis amigos del "Valle" (sólo hay uno y verdadero), los quiero y echo de menos un montón allí donde estén. Jamás

podré agradecerles la paz que me da una breve charla con ellos, aunque a veces se alarguen en demasía… afortunadamente.

A mi familia de sangre. Mis hermanos, mis padres, mis sobrinos, mis primos, tíos y abuelos. En especial, lógicamente a los más cercanos, porque es tan sumamente sencillo como que, seamos lo diferente que seamos, vivamos a la distancia que vivamos, los unos somos parte de los otros, y los otros son parte de uno, en lo bueno y en lo malo. Gran parte de lo que soy es vuestro. Pazca donde pazca siempre llevaré vuestra influencia orgullosamente conmigo.

A todos ellos, mil gracias, eskerrik asko!

Finalmente, y a pesar de que este es un apartado de agradecimientos, quisiera pedir disculpas a aquellas personas que he fallado y no prestado la atención suficiente por haber querido culminar este capricho, muchos de ellos ya mencionados anteriormente. No creo que haya merecido la pena haberme perdido tantas cosas, pero la forma en la que he encarado este trabajo no es otra que la que sé: con la responsabilidad y pasión que pretendo dar en cada paso que doy en mi vida.

Donostia-San Sebastián, enero de 2020

Javier